UNIVERSITY OF NAIROBI

FACULTY OF ENGINEERING

DEPARTMENT OF ENVIRONMENTAL AND BIOSYSTEMS ENGINEERING

HYDROLOGICAL MODELING FOR FLOOD RISK ANALYSIS IN MATHARE, KAMUKUNJI AND MAKADARA SUB-COUNTIES IN NAIROBI, KENYA.

BY:

MULUNGO MAUREEN ADHIAMBO

REGISTRATION NO: F56/37667/2020

B.Sc. Biosystems Engineering – University of Nairobi

A Thesis submitted in partial fulfillment of the requirements for the award of the degree of Master of Science Degree in Environmental and Biosystems Engineering.

August 2023

DECLARATION

I, Maureen Adhiambo Mulungo, do declare that this research is my original work and has not been submitted for a degree or any other academic award in any other Institution or University.

Signature: Date: 30th July 2023

Maureen Adhiambo Mulungo.

This thesis has been submitted for examination with our approval as University Supervisors.

1. Signature. Date 1st August 2023

   Dr. John P.O Obiero.

2. Signature Date 1st August 2023

   Dr. Christian T. Omuto.

DEDICATION

I dedicate this thesis to my dad, Mr. Janes Mulungo, my mom, Mrs. Alice Mulungo and all my siblings for their great support.

In a special way, I dedicate this thesis to my husband, Mr. Joseph Omollo, Geospatial Engineer, for his unwavering support and for ensuring that I got access to every information and materials required for this research.

ACKNOWLEDGEMENT

I would like to thank the Almighty God for the gift of life and good health, for without Him nothing would be possible.

Special acknowledgement goes to my supervisors, Dr. JPO Obiero and Dr. CT Omuto for their tireless and diligent work in ensuring that this research is thoroughly completed. I am grateful for their constructive criticisms and input.

I greatly appreciate the University of Nairobi for the award of the Scholarship that has helped me through my Master's degree.

Members of staff in the Department of Environmental and Biosystems Engineering who assisted in one way or another in shaping this work, are hereby acknowledged.

Mr. Joseph Omollo, Geospatial Engineer, who assisted me with all the details of mapping and ensured that I got easy access to the data needed to actualize the research, is highly appreciated and acknowledged.

ABSTRACT

The objective of this study is to utilize Geographic Information System (GIS)-based hydrological model with remote sensing to analyze the risk of floods in the residential areas of Mathare, Kamukunji and Makadara sub-counties in Kenya. Data obtained from Copernicus Open Access Hub was used to obtain Sentinel data. Synthetic Aperture Radar (SAR) data was obtained from Sentinel Mission 1. Corrected data of SAR was used to create a 10m resolution Digital Elevation Model (DEM). Multispectral Satellite Imagery was used to obtain Land-use/Land-cover (LULC) using object-based classification. 10 classes of LULC were created. Several factors affecting flood risk were identified and mapped, among them were LULC and channel flow length, which mainly affected floods in the study area. The hydrological tools found in ArcGIS Software were used to divide the area of study into 4 catchments. The Hydrological Soil group of the 4 catchments was used to further sub-divide the study area into 17 sub-catchments in order to obtain accurate Curve Number (CN) values. HEC-GeoHMS (Hydrological Engineering Center's Geospatial Hydrological Model System) which is an extension in ArcGIS software was used to obtain channel slope and flow length that were used in calculating the time of concentration for peak discharge and runoff. U.S Soil Conservation Service Technique Release 55 (SCS TR-55) model helped in predicting rainfall-induced floods. This model predicted peak discharge and runoff in the sub-catchments. Runoff was determined using equations in the model and the peak discharge was computed by the model's graphical method. The overall Flood Hazard Map was produced in QGIS by overlaying the factor maps while the Flood Depth Risk Map was produced using ArcGIS software by summing up the values obtained from runoff. The results indicated that rainfall-induced flood is a serious problem with flood depth of 13-19.5cm, making the whole study area to be prone to floods especially the southern part occupied by Makadara sub county. Decrease in catchment's flow length and increase in the number of impervious areas due to growth of urbanization increased flood risk in the area. The results of this study will be useful in coming up with solutions for flood risk control which include drainage systems that will improve the infiltration capacity of runoff, appropriate infrastructure e.g. green infrastructure and early warning systems such as sensors on rivers, drainage systems etc. The models used in this study helped predict floods in the study area. The use of remote sensing techniques helped update climatic factors such as rainfall, thereby solving the shortage issue on updated information on climatic conditions in the study area and also infrastructure for accurate prediction of floods.

Table of Contents

LIST OF FIGURES

LIST OF TABLES

ABBREVIATIONS AND ACRONYMS

AHP	- Analytical Hierarchy Process
CBD	- Central Business District
CN	- Curve Number
DEM	- Digital Elevation Model
EIA	- Environmental Impact Assessment
GIS	- Geographic Information Systems
HEC GeoHMS	- Hydrological Engineering Center's Geospatial Hydrological Model System
HSG	- Hydrological Soil Group
LULC	- Land Use/ Land Cover
MCEA	- Multi Criteria Evaluation Analysis
NDVI	- Normalized Difference Vegetation Index
RS	- Remote Sensing
SAR	- Synthetic Aperture Radar
SCS TR-55	- Soil Conservation Service Technical Release – 55
SNAP	- SeNtinel Application Platform
TWI	- Topographic Wetness Index

CHAPTER 1

1.0. INTRODUCTION

1.1. Background Information

Rapid growth of urban areas, unplanned urbanization and climate change have aggravated flood risks causing loss of property, human life and major economic loss in the world. Flood has been labeled as one of the hazards causing adverse impact on human beings (Bayazıt et.al., 2021). Annually, floods have claimed the lives of over 20,000 people and also severely affected close to 75 million people globally (Smith, 2001). The risk of flooding is aggravated by the rapid growth of urban areas, unplanned urbanization and climate change. In the 1970's, approximately 37% of the population in the world lived in the urban areas (UN Habitat, 2004). The number almost doubled in 2018. By 2030, this figure is projected to rise to 60% and 70% by 2050(United Nation Publisher, 2018). 1 billion people in the world are estimated to be living in informal settlements in the urban areas (UN Habitat, 2004). This has led to rural-urban migration as people seek for cheap housing making it strenuous to provide the basic service, therefore decreasing the sustainability of the areas in question making them vulnerable to flooding especially though the construction of infrastructures and impervious paved surfaces.

Human life loss, property loss, material loss and worst still, economic loss for all, has been the norm during a flood event. Most people living in floodplain areas, especially in developing counties, are poor and cannot afford to buy legal lands therefore most of them occupy riparian lands along the river banks. Therefore, during flood event, the people living in the flood plains plus those that are neighboring them are affected by floods causing serious damages.

Most of the available maps associated with floods in African Countries lack spatial variability for local scale risk analysis. Kenya, a country in East Africa with a population of approximately 42 million people, has experienced floods and drought among other natural hazards. Kenya covers approximately 591,140 km^2 and is divided into 47 counties. Mathare, Kamukunji and Makadara constituencies are three sub-counties in Nairobi which is one of the counties in Kenya. Flooding has been declared as the most common natural disaster and is mostly due to the high average rainfall of 630mm in a year (Nairobi Climate Profile 2017).

Nairobi floods lead in the hazard map as shown in figure 1.1. The floods are prone in the highly populated areas due to poor settlement scheme. Even with the knowledge of floods as the main hazard in Kenya, very little measures have been taken to analyze the risks associated with floods. Very few scholars have done research on the risks caused by floods in Kenya especially in slums where thousands of people move to those areas due to unemployment and urbanization. The research on flood risk done for the study area include;

i. Flood risk analysis using curves in Mathare, Nairobi Kenya done by Kinyua, (2018). He developed risk curves using water-runoff data, River Mathare discharge rate data, rainfall data, field survey data and questionnaire survey. He found out that the most vulnerable buildings to flooding are those whose structures are made of mud floor and mud wall.
ii. Flood risk analysis for physical vulnerability in Mathare, Nairobi Kenya done by Kinyua and Toshio, (2018). The findings were same as those for flood risk analysis using curves.

Mathare, Makadara and Kamukunji sub-counties are occupied by low-income earners who live below a dollar per day. In future, the rapid growth of these residential areas and increase in population, with most of the residents having low socio-economic status, will definitely raise the environmental, social and economic effects caused by floods.

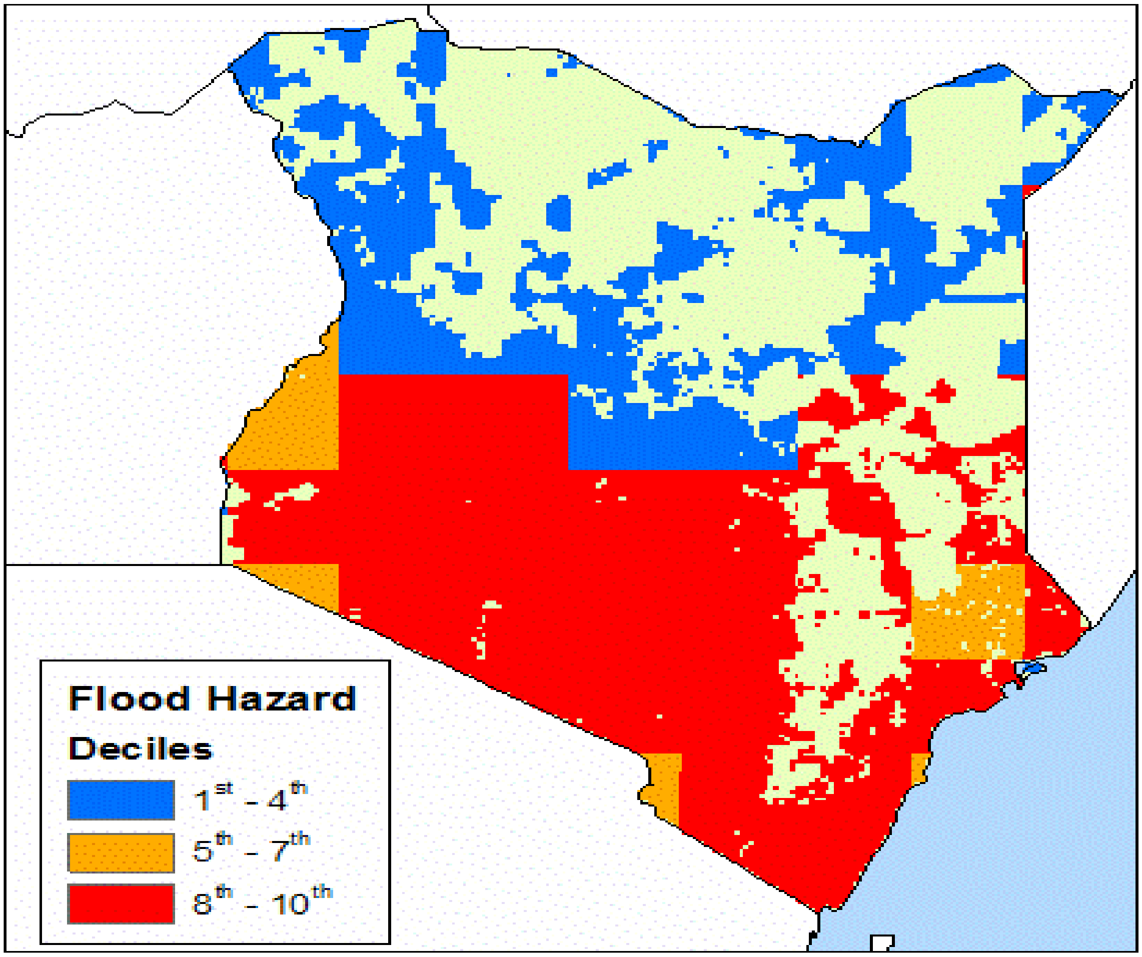

Figure 1.1: Flood hazard map (Kenya Natural Disaster Profile)

1.2. Study Site

The study area covers three sub-counties described as follows;

1.2.1. Mathare Sub- County

Mathare is a residential area occupied by low-income earners and is located in the North East of Nairobi County. It is 1650 m to 1606 m above the sea level. It has a population ranging from five hundred thousand to eight hundred thousand people living in an area of 7.25 km^2. It has a population density of 68,941 people per km^2 (Kenya Bureau of Statistics, 2019).

Mathare area receives an average annual rainfall of 900mm, with the months of April and November having the highest magnitude of 150mm and 219mm respectively. February being the hottest month in a year with maximum average daily temperatures ranging between 22^{O}C to 28^{O}C and June being the coldest month, with minimum daily temperatures ranging between $14^{O}C$ to $21^{O}C$ (NCC et.al, 2014).

The relative humidity in Nairobi County ranges from less than 40% to over 80% between morning and afternoon while sunshine duration varies from 4 to 9 hours per day. Analysis of information about the weather in Mathare (from the Moi Air force Base East Leigh Station) showed an increase in average annual temperature from $2^{o}C$ to $4.5^{o}C$ over a period of 1981 to 1999. This shows that there is the development of urban heat island in the study area and is an effect that results from modification of the minimum temperatures (Kinyua, 2018).

Among the various land uses in the area, the most dominant land use is the residential land. The land is characterized by structures that are haphazardly laid without structural spatial planning. Mathare informal residential area is a floodplain located along Mathare River, is one of the tributaries of Nairobi River basin, and connects the study area to Kiambu County. The river is adversely polluted (World Health Organization, 2011). About 30% of Mathare valley falls within 30-meter riparian reserve. The landscape slopes west to east and towards the river channel. The soils in the area are a mixture of red clay, black cotton and alluvium soil which makes most sections of the area slightly unstable in regard to the bearing capacity of the soil (Chesoto, 2013) making the area prone to waterlogging.

1.2.2. Kamukunji Sub- County

The sub-county consists of Central to Eastern area of Nairobi County. It borders Starehe constituency on the west and on the north. It borders Makadara on the Southern and Eastern part and Embakasi to the East. It has an area of $11.7km^2$; Moi Airbase occupies half of the area, $5.8km^2$ has Human occupation and the rest has commercial center and other social amenities.

The elevation of the area is 1,661 meters above the sea level. Nairobi River cuts across the sub-county. There is high competition for space for business and constructions in order to meet the growing population, this has led to the interference with vegetation and increased dumping of chemical waste into Nairobi River and its tributaries leading to pollution.

Most people live in clustered estates with structures laid haphazardly and without uniform patterns making the area more prone to flooding.

1.2.3. Makadara Sub- County

The sub-county consists of Central and southern of central areas of Nairobi.

It has an area totaling to 13km^2 and a population density of 3079 people per km^2.

The sub-county is both a residential and business center for the occupants of the area. The constituency has housing estate with high-level rate of unemployment. Nairobi River cuts across the sub-county.

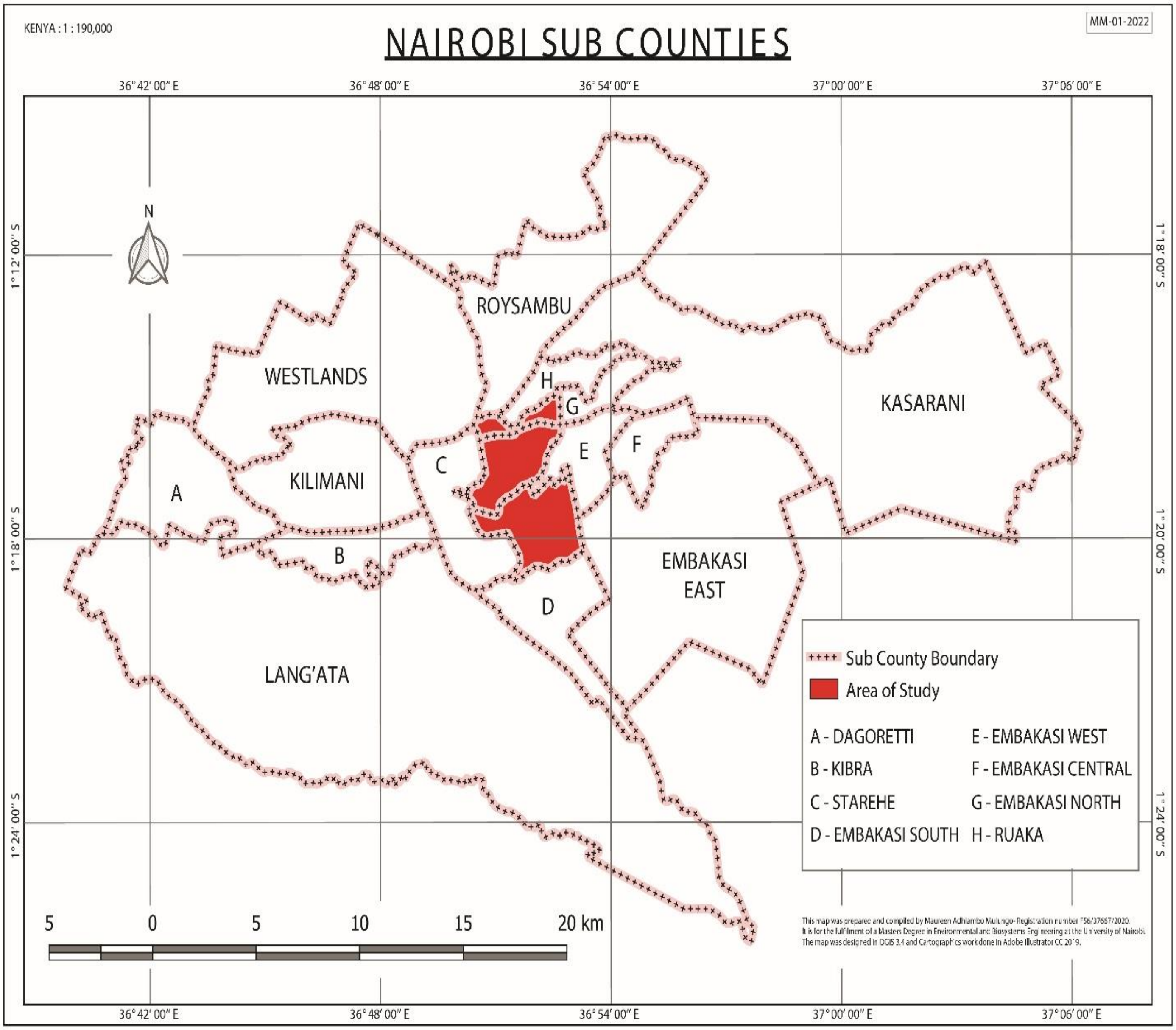

Figure 1.2: Sub-Counties in Nairobi County

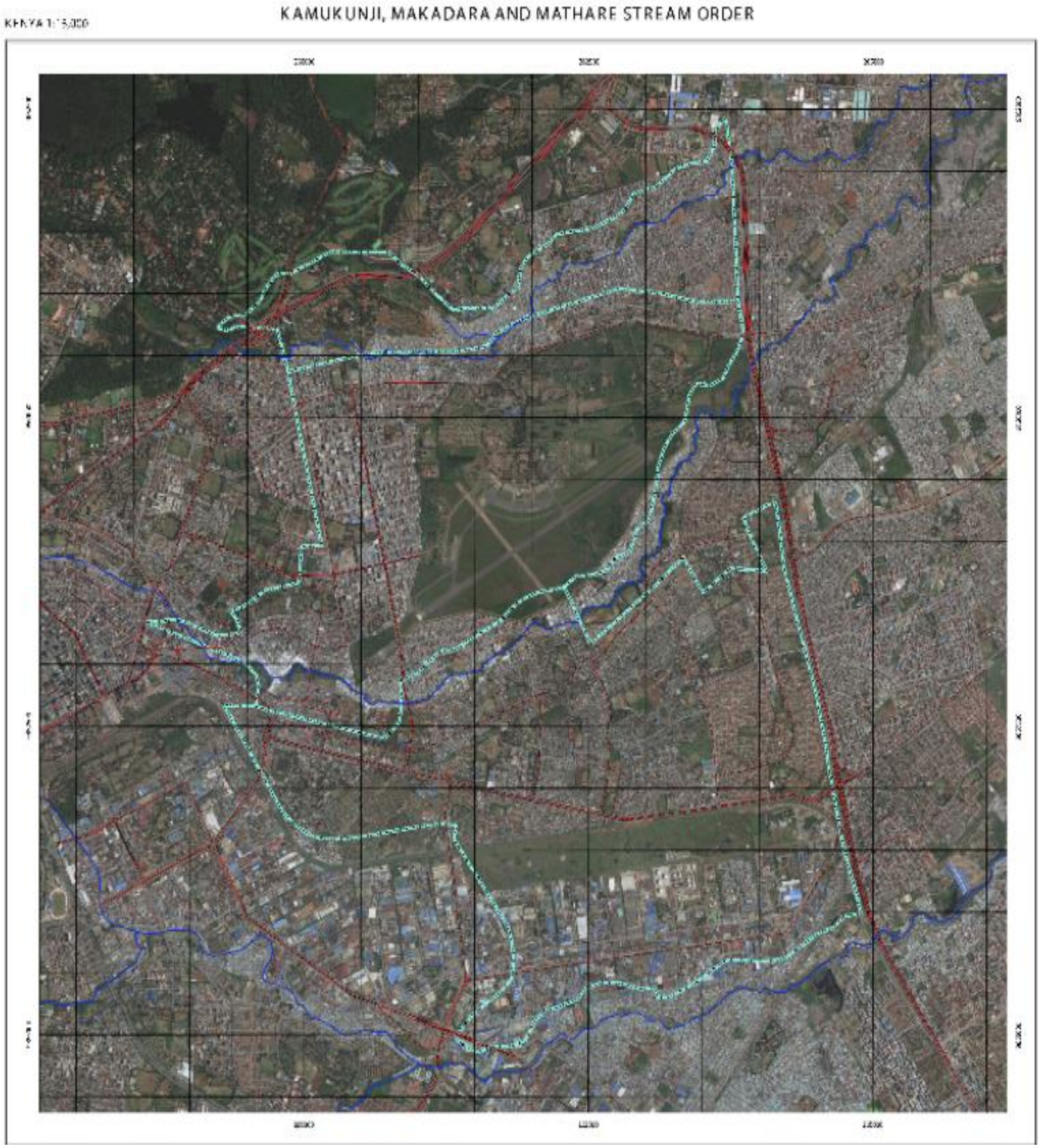

Figure 1.3: Google earth image of the Study Area

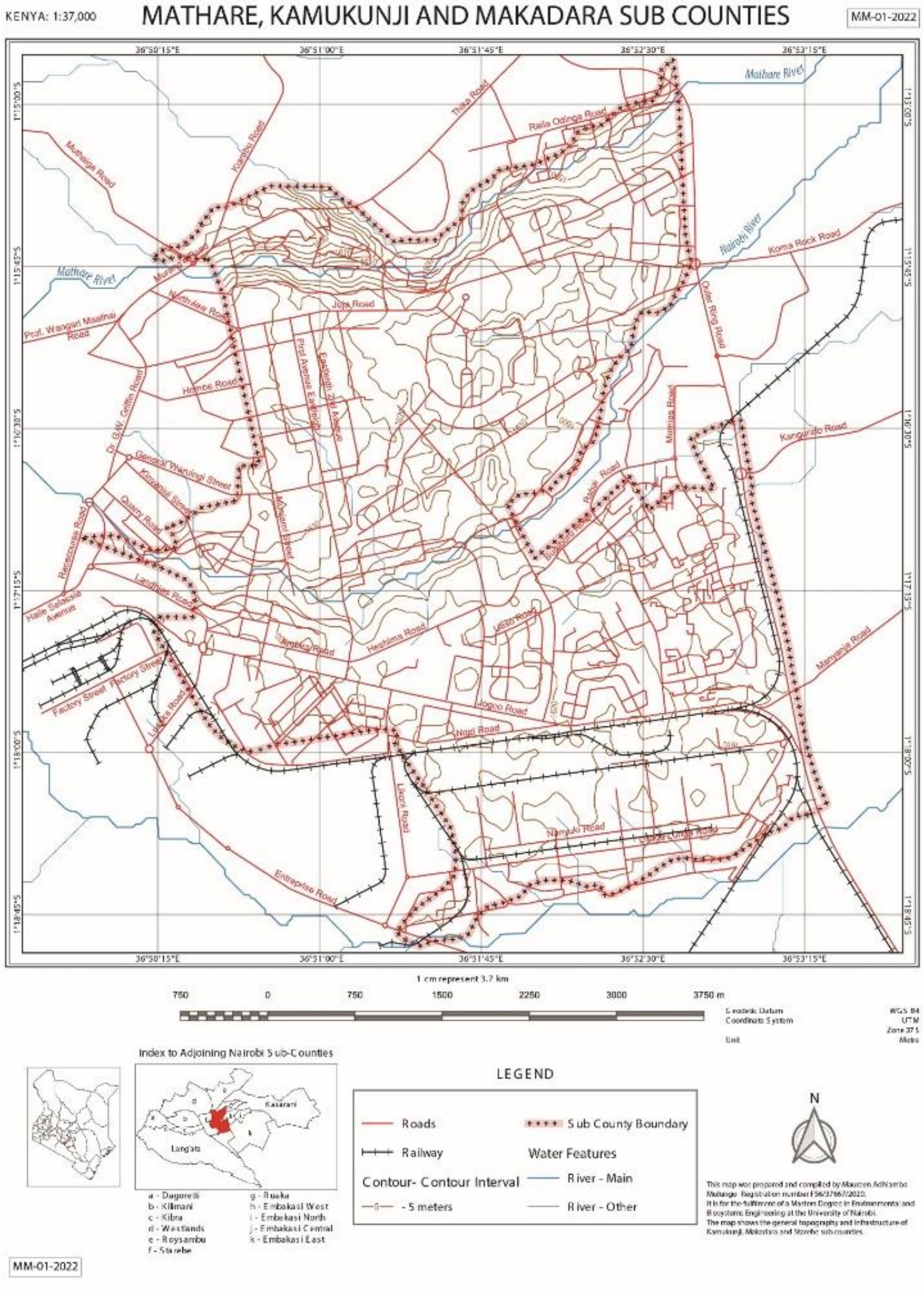

Figure 1.4: Administrative Map of the Study area

1.3. Problem statement

Figure 1.5: Mathare River, Nairobi Kenya. (Alamy Stock Photo)

Poor drainage systems combined with poor and improper maintenance of the drainage systems in Mathare, Makadara and Kamukunji is main cause of urban flooding. During rainy seasons, the drainage systems get blocked and clogged by debris and sediments causing accumulation of storm-water thereby causing floods in the area. The study area is also characterized by increased number of industries with structures like roads, buildings and paved surfaces that make most of the surfaces have impervious layers. During flood event, the impervious surfaces forces water to run off into sewer systems. This is due to decreased rate of infiltration of the rainwater, which cause runoff thereby promoting floods. Mathare sub-county has areas that have landscape which are fragile such as very steep slopes, riverbanks and floodplains. This increases the exposure of the area to floods.

Vulnerability to floods owing to lack of information on expected floods for planning early warning systems and inadequate information on flood magnitudes for use in flood management and control, have led to flood damage on the area of study. This has posed livelihood safety challenge and climate hazards such as flooding and landslides to the residents in the selected areas. (UN Habitat ,2004). The existing meteorological station (Moi Air Force Base East Leigh Station) in the study area lacks up to date data on climate. In addition, infrastructure data is not up to date and the water department lacks up to date data on some variables like bankful discharge.

These factors led to the development of this research study, which is on analysis of flood risk using GIS-based models with remote sensing techniques. The combination of the two tools help acquire spatial information such as land-use/land-cover and soil type variable, in digital form. These variables are important for flood risk analysis and hydrological modeling. The research also takes into consideration the catchment properties such as channel flow length and slope, which are some of the underlying factors causing floods.

1.4. Justification

The use of GIS based hydrological model with Remote sensing offers the three sub-counties a chance to reduce the rate of flooding in their areas. The use of the two techniques in this research is justified since remote sensing will ensure less labor is used and time is saved, and the GIS-based hydrological model will ensure accurate results. GIS is an important data analysis framework used for modeling and is a critical tool that helps project quantitative and qualitative effects of floods. GIS help in hydrological modeling to construct flood projection models in watersheds and catchments and also to prepare and analyze multi-source and multi-scale spatial data. Digital Elevation Model (DEM) helps in acquiring the necessary topographical variables such as flow directions, catchment geometry, stream networks and catchment slope from raster data on elevation, which gives effective results in the prediction and analysis of floods in the urban areas.

1.5. Research Question

What is the effectiveness of GIS-based modeling incorporating remote sensing data for flood risk analysis in Mathare, Kamukunji and Makadara sub-counties in Nairobi, Kenya?

1.6. Objectives

1.6.1. Broad Objective

Flood prediction using GIS-based hydrological models and remote sensing for flood mapping in Mathare, Kamukunji and Makadara Sub-Counties, Nairobi, Kenya.

1.6.2. Specific Objectives

i. To identify and map the factors affecting floods in the study area.

ii. To characterize the flood prone areas for flood hazard mapping using Geographic Information Systems (GIS) and Remote Sensing (RS).

iii. To model the flood magnitudes in the flood prone areas of the study catchment.

iv. To develop a flood hazard map showing flood depths in the area of study.

CHAPTER 2

2.0. LITERATURE REVIEW

2.1. Floods causes and types

Floods are the recurrent type of natural disaster caused by heavy rainfall. They occur when an overflow of water submerges a dry land. They are caused by rapid snowmelt or a storm surge from a tropical cyclone or tsunami in coastal areas. They cause damage, which results in loss of both human and animal life, personal property and critical infrastructure. In 1998-2017, floods affected two billion people in the world. The most vulnerable people are those that live in non-resistant buildings or along the floodplains. It is even worse when the people living in these areas lack warning systems and awareness of flooding hazard (World Health Organization, 2011).

2.1.1. Categories of Floods

Floods categorized depending on the cause include;

i. Regional floods
ii. Flash floods
iii. Estuarine floods
iv. Coastal flood storm surge
v. Floods caused by dam collapse

A. Regional floods

These types of floods are also known as downstream floods. They are long duration floods that usually occur over a large region, mostly in the downstream part of a stream system. An example of a downstream flood is the flood that occurred in the great Mississippi river basin in 1993, which exceeded the 100 years' level of flood (Nelson, 2012). Also, in Kenya, is the Nyando river sub basin in Nyanza.

B. Flash floods

These types of floods are also known as upstream floods. They are rapid flooding caused by heavy rains and they occur in geomorphic low- lying areas such as basins, rivers, washes and dry lakes. They are floods of a short duration that usually result in a stream system at the upper reaches. The effect of the floods is noticeable in streams that drain basins associated with high rainfall intensity, which is short term and often with a thunderstorm. Moreover, the stream is normally not capable of handling the flow, which exceeds its capacity hence floods occur. These floods come with little warning, therefore, posing great danger to human lives. They are also very common in the urban areas of County of Nairobi and its environs. This is an effect caused by non-existence of drainage system and poor drainage systems, which are to drain away all the storm water when it rains. A good example of upstream floods is the Venezuela flash flood that occurred in Merida in 2010 and 2017, Aragua in 2011, Caracas in 2010 and Vargas in 1999. The floods were triggered by intense rainfall which damaged roads, bridges and buildings resulting loss of life and displacement of residents.

In 2012, in Kenya, a flash flood occurred in Mathare. This was caused by heavy rainfall that triggered upstream of Nairobi River in Kiambu leading to flooding of the Mathare River that passes through Mathare slums. The flood event rendered one person dead and over three hundred people left homeless. (Reliefweb, 2012).

2.2. Factors Affecting Floods

2.2.1. Physical Factors

The physical factors affecting floods includes; the topography (slope, elevation etc.), drainage density, soil type and its permeability etc.

Slope and elevation variations influence the flow of water and accumulation of runoff. Steep slopes can accelerate runoff leading to increased flood risk.

Drainage density significantly affects the concentration time and therefore the peak flow magnitude. Increase in drainage density leads to increase in flood peaks.

Soil composition affects the rate of infiltration and surface runoff. Impermeable soils like clay can cause waterlogging of the soil thereby increasing surface runoff and reducing water absorption.

2.2.2. Human Factors

The main human factor affecting floods is Land Use and Land Cover. Urbanization and extensive pavements reduce natural infiltration of water thus increasing surface runoff. Rapid urbanization and inadequate urban planning can lead to increased impervious surfaces and reduced green spaces. Deforestation and clearing of vegetation decrease the ability of the land to absorb water thereby increasing flood risk. Also, unauthorized landfill and unregulated sand harvesting can alter the natural landscape and impede water flow.

2.2.3. Meteorological/Climatic Factors

The main climatic factors include rainfall and climate change. Intensity, duration and spatial distribution of rainfall events influence flood occurrence. Heavy rainfall events and prolonged precipitation can overwhelm the natural drainage system thereby causing floods.

Climate change is the change in the average weather patterns that defines the earth's climate. Huge amounts of CO_2 and other greenhouse gasses released into the atmosphere due to human activities since industrial revolution, has greatly changed the earth's climate. The human activities i.e. deforestation, agriculture and road construction, changes the reflectivity of the earth leading to local cooling or warming. This effect manifests in urban centers where there are roofs, buildings and pavements that reflect less sunlight than the natural surfaces. The change in the earth's climate causes extremely heavy precipitation events producing heavy rainfall and the trend is expected to continue as the planet continues to warm since the warm air can hold more water vapour. For each degree of warming, the air's capacity for water vapour goes up by about 7%. An atmosphere with more moisture can produce more intense precipitation event which causes flooding, which is a risk in urban areas surfaces, which forces water to run into the sewer systems. Flooding degrades water quality harming human health and the ecosystem at large.

2.3. Cases of urban flooding

2.3.1. Floods in India.

The recent floods in India occurred in July and August 2019, and it affected over thirteen states in the country. The most affected states were Karnataka and Maharashtra. This was due to heavy rainfall and severe waterlogging causing flooding of hospitals and the residential areas leaving the people and their government surprised due to the damage caused in the said regions. The floods left at least two hundred people dead and one million people displaced. This untimely heavy rainfall which causes flooding are attributed to climate change and unplanned urbanization in the cities. Urban floods in these cities are more of man-made disaster because most of the drainages are overburdened, constructions are unregulated and buildings are constructed without taking into consideration the topography and the hydro-geomorphology of the areas.

Figure 2.1: Flooding in low-lying areas near Yamuna River (Rai H.).

2.3.2. Floods in Madagascar.

The recent floods in Madagascar occurred in January 2020 and the most affected regions were Alaotro Mangoro, Betsiboka and the urban areas of Antananarivo. During this flood event, the causalities registered were; 9 reported as missing people, 31 reported dead people, 106,846 affected people and 16,031 displaced people. The flooding in the area is aggravated by urbanization caused by demographic changes, which are caused by natural increase, migration to the cities and demand for housing especially in the flood-zone areas. The floods are also caused by poor planning, construction of buildings in the flood-zone regions and poor infrastructures e.g., drainage systems.

Figure 2.2: Floodwaters in Antananarivo after heavy rainfall in January 2020(Getty images)

2.3.3. Floods in Kenya

Most of the parts in Kenya experience heavy rainfall in mid-April, which occurs unexpectedly and continues to the end of May (the long rains) and the short rains are experienced from September to November. Areas which are prone to floods are; Lake Victoria Basin which comprises of the Bundalang'i floods in the Western regions of Kenya, the Nzoia River where floodwaters arise from the Chelangani Hills and the Kano Plain Floods along the Nyando River with the flood waters arising from the Nandi Hills, the Tana River floods along the downstream areas of the river with flood waters originating from the Aberdares and Mt. Kenya catchments. Most of the existing literature on flood management in Kenya has greatly explored the physical aspects of their occurrence and nature (Mbaria, 2004).

In addition, areas in Nairobi like Nairobi Central Business District (CBD), Mathare, Kamukunji, Makadara, South C, Eastleigh, Lang'ata Road, Kayole, Ruai, Muthaiga among others are also identified as flood vulnerable areas. However, there is rapid growth in literature, which analyses and examines this issue from a social perspective with calls for more research into the social responses to flood management (Ongor, 2007). In 1997, El Nino rains were experienced in most parts of Kenya. It led to disastrous floods all over the country. Property was destroyed, people were displaced, utility facilities disrupted, transport network destroyed as well as deaths as a result of these floods. In 2015, El Nino rainfall was also experienced in some parts of the country. According to the National Disaster Operations Centre, the El Nino in 2015 was not as disastrous as El Nino of 1997/1998. However, it led to deaths, displacement of persons, disruption of transport network and destruction of public utilities among other adverse effects.

2.3.4. Floods in Nairobi County and its environs.

Flooding in the city of Nairobi is not a new occurrence. It has been experienced for a long time, however, the trend of the flooding events in the city has been rampant with the risks increasing every year.

Floods in Mathare, Kamukunji and Makadara sub-counties has led to traffic jams, transport routes destruction, interference with day-to-day activities in the areas as well as destruction of property. Sometimes, heavy rains in these areas carry along with them vehicles on the road thus leading to deaths and destruction of such vehicles. In April and May 2015, Nairobi Central Business District (CBD) experienced flash floods because of heavy rainfall. Water covered almost everywhere in the CBD. Roads were impassable, office entries inaccessible and parking lots totally flooded during some of the days in that period.

The City County of Nairobi even gave hotline numbers to the members of public to report any emergency because of these floods. The Governor of Nairobi County announced a 50 million budget to unclog the city's drainage system, which is the major contributor to floods in Nairobi. This project is still underway. Because of the experience in April/ May floods in Nairobi including the CBD, the Nairobi City County took various precautions to curb floods. This was especially after the announcement by Kenya's Meteorological Department of the likelihood of El Nino rains experienced in the months of October, November and December all over the country. Such precautions include the announcement by the County's Executive in charge of Environment on the measures to be taken by Nairobi County Government in curbing floods in the city. As it is a norm in Kenya, most of those measures were not put in place. The expected rains came though at a lesser magnitude than expected. Roads, parking lots, office entries and other buildings' entries in the city were flooded thus distracting daily activities in the Central Business District (CBD).

2.4. Multi Criteria Evaluation (MCE)

This method can be used in GIS to scuitinize the location of land to fit a specific purpose based on a variety of attributes that the selected areas have.

It makes it possible to generate compromised alternatives and ranking of alternatives depending on how appealing it is. There are two common procedures for MCE.

i. Boolen Overlay- all creteria are evaluted by threshhold of suitability to produce map.
ii. Weighted linear combination- when there are more that one cattributes that need to be considered to find the most suitable allocation, each of them are assigned a weight based on its importance. The higher the score, the more suitable is the area.

2.4.1. Analytical Hierarchy Process (AHP)

Analytical hyerachy process is a technique that is structured for analysing complex decisions based on psychology and mathematics. Its has been refined and it presents accurate ways of quantifying the weights of decision criteria. it is a method of MCE (Multi Criteria Evaluation).

This process is used in the following areas;

i. Environmental Impact Assessment (EIA) - Analytical hyerachy process is used in EIA to assess the potential impacts of a proposed development project on environment.
ii. Land Use Planning – The process is used to assess the environmental implications of alternative land use scenario.
iii. Natural Resource Management – The process is applied to support decision-making related to allocation and sustainable use of natural resources.
iv. Climate Change Adaptation and Mitigation – The process is applied to evaluate and prioritize adaptation and mitigation options.

2.5. Hydrological modeling analysis of flood risk

Hydrological modeling characterizes the real hydrologic systems and features by use of computer simulations, mathematical analogues and small-scale physical models (Allaby, 1999). It's a software used in modeling wastewater, storm water and floods. Hydrological modeling is used to answer questions pertaining to environmental transport where water scarcity, excess, dissolved or solid content is of importance (Burges, 1986). Due to the nature of environmental predictions, there is no better model; rather, there are many plausible solutions depending on purpose and needed complexity (Yu, 2015). This has made the study of hydrological modeling to include too much reliance on mathematics at the expense of true knowledge therefore suffering from the need for more rigorous evaluation of appropriateness (Klemes, 1997). There are different types of hydrological models, which are falsifiable.

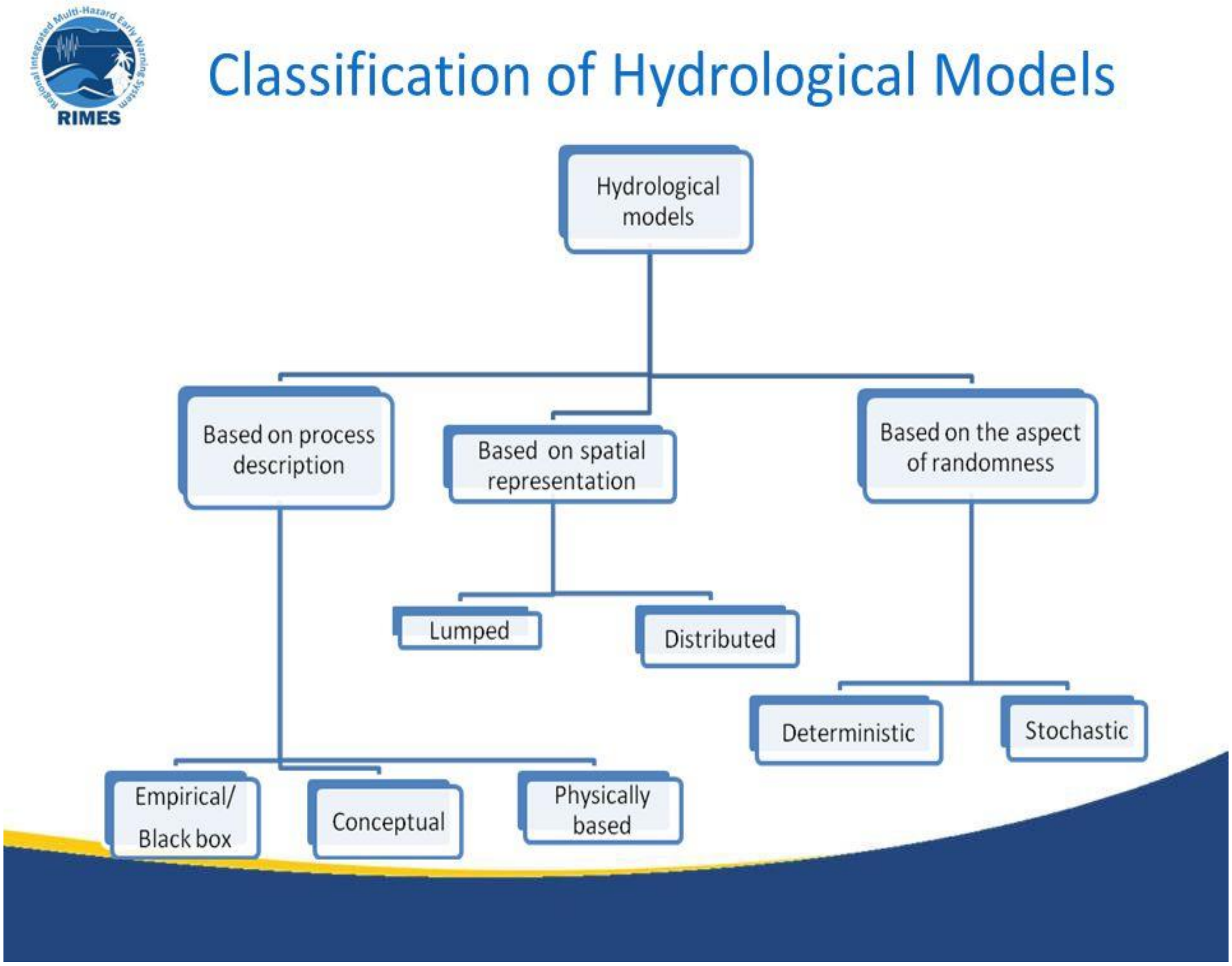

Figure 2.3: Classification of Hydrological Models (Dr. Dilip K. Gautam)

The most commonly used hydrological models are those based on spatial representation i.e.

i. Lumped- these hydrological models treat the watershed as a single homogeneous element or unit with average rainfall input.

ii. Distributed- these models use spatially varying input data for the process.

2.5.1. Significance of hydrological models

i. They help predict the effects of motion of water, especially liquid water on or under the surface of the earth.

ii. They can generate stream flow estimates and trends over a long period. With the long-term records, neither extreme floods nor droughts influence statistical analysis done over a period.

iii. They help forecast seasonal stream flow records used for future analysis of risk of floods. These records are valuable to water managers and users since they help inform their decisions pertaining to planning and management the available water resources and ensure that there is security of supply.

2.5.2. Areas where hydrological modeling has been used in flood risk assessment

River basins: hydrological models simulate the flow of water in river basins and predict flood events. The models help identify flood risk areas and assess the impact of floods on communities, infrastructure and environment.

Urban area: hydrological models simulate the behavior of storm water runoff in urban areas where high number of impervious areas can increase flood risk.

Coastal areas: hydrological models simulate storm surge and tidal flood. They help predict the extent of coastal flooding event.

Watershed: by simulating the movement of water through the watershed, the hydrological models can help identify areas prone to flooding and inform land use planning and flood management strategies.

Dams and reservoirs: the models help predict the inflow and outflows of water from the reservoir, evaluate the capacity of the dam to handle flood events and inform emergency response plan.

Climate change impact assessment: the hydrological models help assess the potential impact of climate change by incorporating climate projections into the models. The researchers can then evaluate how changes in precipitation patterns, temperature and other climate variables may affect future flood intensities and frequencies.

2.5.3. GIS-based Hydrological modeling

Geographical Information System (GIS) is an information system that enables the input, manipulation, storage, processing, output and dissemination of spatially referenced land related data at all scales (Anees, Abdullah and Nawawi, 2016). GIS is an important data analysis framework used for modeling. It is a critical tool that helps project quantitative and qualitative effects of floods (Siverturn and Prangle 2003). It helps in hydrological modeling to construct flooding projection models in watersheds and catchments and also to prepare and analyze multi-source and multi-scale spatial data (Gallegos et. al 2009).

Digital Elevation Models are used when coming up with hydrological models as GIS background, in order to acquire the necessary topographical variables such as flow directions, catchment geometry, stream networks and catchment slope from raster data on elevation. Hydrological models which are GIS based have been utilized successfully for the prediction of floods, worldwide, in most urban areas (Sarker and Siverturn, 2011).

GIS-based Hydrological models combined with Remote Sensing is an effective tool that helps in analysis of floods by identifying flood risk zones and flood impacts in undated regions. Remote sensing provides primary source of data saving the research time and labor during data collection and data analysis in the geomorphological and topographical catchment (Nicandrou, 2011). The combination help acquires spatial information such as land-use/land-cover and soil type variable, in digital form. These variables are important for flood analysis and hydrological modeling

(Samarasingheat et. al 2010). Remote sensing technique is helpful in analyzing satellite imagery and it ensures a more accurate classification of land-use/land-cover (Nicandrou, 2011). This parameter was used as an input in a GIS-based hydrological model known as SCS TR 55 model for analysis of risks pertaining to floods. Another model that was used was HECGeoHMS model.

2.5.4. SCS TR-55 model

This is a widely used hydrological model developed by the United States Department of Agriculture's Natural Resources Conservation Service. It is designed to estimate runoff and peak flows from small watersheds or urban areas. The model utilizes a simple approach to estimate runoff volume and peak flow rates based on the characteristics of the watershed and the rainfall inputs. It considers various factors such as soil type, land use and land cover, slope and rainfall intensity to estimate excess rainfall that contributes to runoff. The model assumes that excess rainfall is generated from portions of rainfall that exceeds the soil's infiltration capacity.

The model follows a step by step procedure to estimate runoff. Curve Number used in SCS method roughly calculates direct runoff from a storm water rainfall. It calculates Curve Number values by analyzing the cover conditions and catchment soil. Direct runoff is estimated from the Curve Number values obtained from the procedure. TR-55 is mostly used in hydrological models and makes use runoff-depth data, as an input, that is acquired from the modeling process to estimate the catchment's peak discharge. It also enables the model to efficiently simulate peak discharge and runoff, in order to identify a flooding event in an urban area (Ramana, 2014).

This model provides straight forward and practical approach for estimating runoff and peak flows in urban areas. It is commonly used by engineers, hydrologist and land managers to assess the impact of land development, storm water management and erosion control practices on hydrologic processes.

2.5.5. HEC GeoHMS

This is a software package for use with ArcGIS and it provides the user with procedures, tools and utilities for preparation of GIS data. Analyzing the digital terrain information, HECGeoHMS transforms the drainage paths and watershed boundaries into hydrological data structure that represent the watershed response to precipitation. With an openness to share spatial information via the internet from government agencies, commercial venders and private companies with spatial algorithm, the integration of GIS with hydrological models holds the promise of a cost-effective alternative for studying catchments. This saves time, effort and improves accuracy over traditional methods.

This model was developed as a geospatial hydrology tool kit for engineers and hydrologist with limited GIS. It allows users to visualize spatial information, document catchment characteristics, perform spatial analysis, delineate sub-basin and streams, construct inputs to hydrological model and assist with report preparation.

2.5.6. Role of GIS-based hydrological model with remote sensing technique

Despite the effort to identify and investigate the problem of flood and come up with methods that would help reduce the effects of floods in the three sub-counties, there are still severe floods occurring in the areas and therefore the need for an effective analytical tool, which is the GIS-based hydrological model (SCS TR-55), combined with remote sensing. The combination is an effective tool for analysis, identification of zones that at risk of flooding. It helps with acquisition of spatial information in digital form i.e., soil type and LULC variables. SCS (TR-55) model is effective for prediction of floods in urban areas. It will consider catchment properties and climate change, which are the underlying causes of floods. It will increase the efficiency of flood forecast by providing realistic data based on current infrastructure andclimatic factors.

2.6. Current International Research on Hydrological modeling for flood risk analysis.

Studies on analysis of floods using hydrological models have proven that SCS method is the most appropriate method to be used in determining peak discharge and runoff volume. Some of the authors include Kim (2010), Soulis and Valiant (2011), Dawod (2011), Gajbhiye and Mishra (2012) and Shadeed and Almasri (2010).

Seeni and Mansor (2000), used GIS tools with SCS TR 55 model to estimate floods in urban areas, for a small watershed and the results were effective such that they promoted the use of remote sensing technique with hydrological models for the prediction of flood risks in the urban areas.

Dang and Kumar (2017), applied RS technique and a hydrological modeling which was GIS-based the analysis of flood risk in a city in Vietnam. The results showed that the RS techniques used to identify flood risk are effective when combined with hydrological models especially the SCS TR 55 model though there is need for calibrating the model and validating the results.

2.7. Current Research on flood risk in Mathare, Kamukunji and Makadara

2.7.1. Flood risk analysis using curves in Mathare, Nairobi Kenya

Kinyua (2018), did flood risk analysis using curves in Mathare residential area. He developed risk curves using water-runoff data, River Mathare discharge rate data, rainfall data, field survey data and questionnaire survey. He found out that the most vulnerable buildings to flooding are those whose structures are made of mud floor and mud wall. He concluded that in order to reduce the damage to builds and reduce the number of deaths due to floods, there is need for incorporation of warnings, building codes and flood awareness in the study area.

2.7.2. Flood risk analysis for physical vulnerability in Mathare, Nairobi Kenya.

Kinyua and Toshio (2018), did this research. The results and conclusions were same as those of flood risk analysis using curves.

2.7.3. Gaps in the current Research

There are no studies or research done for Makadara and Kamukunji on flood risk analysis.

The current studies in Mathare Sub- County are not taking into consideration the catchment properties such as channel flow length and channel slope. The studies ignore the underlying causes of floods which has been proven to be the leading cause of floods in the region.

This research study takes into consideration the underlying factors causing floods i.e. the catchment properties, by determining and analyzing them, using models' equations and graphs.

CHAPTER 3

3.0. MATERIALS AND METHODS

3.1. Description of the Study area

The study area consists of three sub-counties; Mathare, Kamukunji and Makadara.

Mathare is located in the North East of Nairobi County with an elevation of 1650m to 1606m above the sea level. It is a residential area occupied by low-income earners and has a population ranging from five hundred thousand to eight hundred thousand people living in an area of 7.25km^2. It has a population density of 68,941km^2.

Kamukunji is located in the Central to Eastern area of Nairobi County. It borders Starehe constituency on the west and on the north and also borders Makadara on the Southern and Eastern part and Embakasi to the East. It has an area of 11.7km^2; half of the area is occupied by Moi Airbase, 5.8km^2 is occupied by residents and the rest has commercial center and other social amenities.

Makadara is located in the Central and southern of central areas of Nairobi. It has an area totaling to 13km^2 and a population density of 3079 people per km^2. The sub-county is both a residential and business center for the occupants of the area.

The sub-counties have slums and housing estate with high level rate of unemployment. Nairobi River and Mathare River cut across the sub-counties.

The soils in the area are a mixture of red clay, black cotton and alluvium soil which makes most sections of the area slightly unstable in regard to the bearing capacity of the soil (Chesoto, 2013) making the area prone to waterlogging.

3.2. Conceptual Framework

Flood risk is a function of hazard, exposure and vulnerability. The research represents methods and procedures used in analyzing flood risk in the study area. The procedures are supported by GIS- based hydrological model and other necessary and supportive software.

Flood disaster is the greatest natural disaster risks in highly populated areas throughout the world. Natural disaster indicates that a disaster has exceeded a standardized level therefore resulting to damage on social and human economies. This research used the principal of natural disaster to assess the risk caused by floods in the three sub-counties. Emergency response and recovery capability were used. This principle is as shown below;

Natural disaster risk= f (hazard, exposure, vulnerability, restorability)

Hazard describes the extreme climatic conditions that threatens and destroys the society especially by causing climate change. It is affected by topography, meteorology, hydrology and vegetation conditions. High rainfalls are mainly the cause of flood disasters.

Exposure normally describes the economic, social and ecosystem affected by floods.

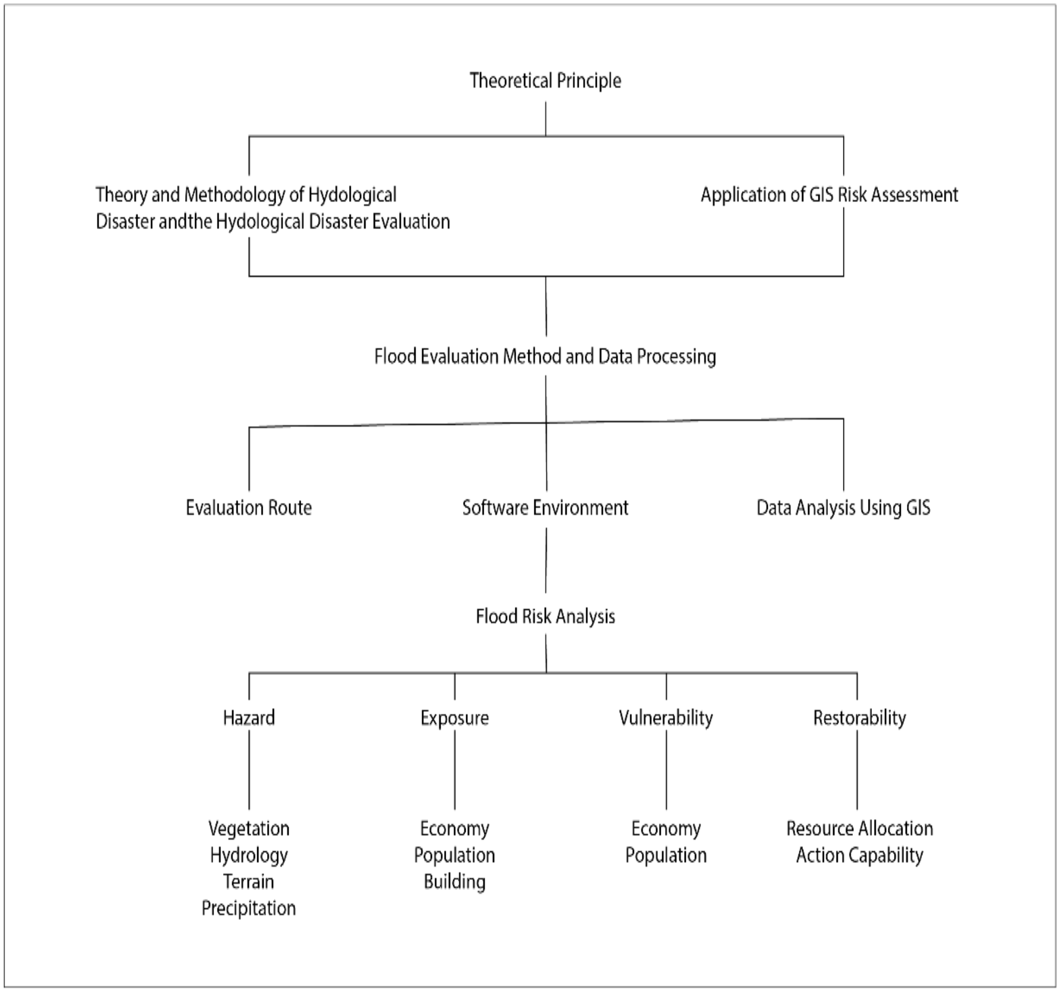

Figure 3.1: Conceptual framework for flood risk analysis

Vulnerability elaborates on the degree of damage which causes loss in the ecosystem and the population at large.

Restorability elaborates on the ability to recover from the effects of flood disaster in a short time.

The table below shows how we settled on using the hydrological models with remote sensing for the flood risk analysis in the three sub-counties. We had 3 options to use in each category. The categories included the method for flood risk analysis, the type of hydrological models to use, the type of GIS software to used, the method of modeling and the type of satellite image to use. Justification for each selection was given.

Table 3.1: Concept Generation table

	CATEGORY	**OPTION 1**	**OPTION 2**	**OPTION 3**	**SELECTION**	**JUSTIFICATION**
1	Flood risk analysis method	Estimation of design discharge	Hydrological models (rainfall-runoff models)	Both	Hydrological models (rainfall-runoff models)	Calculations are done using simplified spatial process
2.	Hydrological models	Lumped	Distributed	Both	Both	The combination gives accurate data
3.	GIS Software	QGIS	Arc-GIS	Both	Both	Flexibility and accuracy
4.	Hydrological modeling	1-Dimensional	2-Dimensional	Both	1-Dimensional	They are simplified models and are easy to use in areas with simple topography
5.	1-Dimensional	SCS-CN TR-55	HEC-GeoHMS	Both	Both	The combination gives accurate data
6.	Satellite Imagery	Landsat 8	SAR	Both	SAR	Has high resolution

3.3. Data acquisition and processing

3.3.1. Acquisition of Spatial data

Sentinel data was obtained from Copernicus Open Access Hub using SNAP (SeNtinel Application Platform).

The procedure for obtaining data is presented as follows;

i. Sentinel imagery, from multispectral satellite image, was created from sentinel mission 2. The image bands from the multispectral satellite image were classified using object classification to obtain LULC (Land Use/Land Cover) which was then used to determine the impervious layers in the study area. LULC was extracted so as to be used as input parameter for hydrological modeling in the study.

ii. SAR data (Synthetic Aperture Radar) obtained from Sentinel mission 1, was used to create 10 m resolution DEM, which was then processed in HEC GeoHMS to create drainage lines used as streams or rivers for the study. The drainage lines were used to process the drainage densities and stream access in ArcMap. Elevation, slope and Total Wetness Index are also created using DEM in ArcMap.

iii. Topographical data base e.g. LULC, administrative borders, elevation, buildings and construction, water systems etc. This data helped in mapping the different factors affecting floods. The factor maps were then overlaid in QGIS to give the flood hazard map.

iv. Soil type data, from Kenya Soils Survey, was collected in order to be used in hydrological modeling in calculating peak discharge and runoff volume.

v. Rainfall data which was used in the TR 55 model was obtained from worldclim.org and climate-data org. The data was used to create meteorological map for flood hazard mapping and also used to calculate peak discharge and runoff volume.

vi. Rivers, roads and railway data was obtained from Humanitarian OpenStreetMap Team. The data was used to create human factor map for flood hazard mapping.

3.4. Reconnaissance

The objective of the pre-visit was to investigate the site and check on the feasibility of the study and also to establish the pre-existing conditions e.g., the climate of the area, soil characteristics, the existing natural resources etc. Our main emphasis was on climate, terrain and the soil characteristics of the area.

In preparation for the site visit, we gathered the available information such as topographic maps to check the catchment area, accessibility to roads, the residential and industrial areas.

We surveyed the site by assessing the population, situation of the rivers and streams in the area, the existing residential and industrial areas etc.

3.5. Criteria for Site and Model Selection

Different factors were considered in selecting the three sub-counties. Mathare sub-county is one of the most flood prone areas in Nairobi county since it is characterized by steep slopes and poor drainage infrastructure. It has experienced frequent flooding especially in the low-lying areas and informal settlements. It was difficult getting the desired data resolution required for flood risk analysis in the sub-county and so, we extended our study area to include Makadara and Kamukunji sub-counties which are also prone to floods.

The model's selection process is shown in Table 3.1. The concept of research on analysis of flood risk came as a result of a discussion on urban flooding and the most affected urban areas in Nairobi, Kenya. We found gaps in the research and projects carried out in the sub-counties through the knowledge obtained in participating in projects, field research and linking theories with practice.

We decided to use GIS based hydrological model (SCS TR 55 and HEC GeoHMS) with remote sensing since they offer the three sub-counties a chance to reduce the rate of flooding in their areas. Remote sensing will ensure less manpower is used and time is saved, and the GIS based hydrological model will ensure accurate results by determining and analyzing the underlying causes of floods in the study area by use of equations and graphs provided by the model.

3.6. Identification and mapping of the different factors affecting floods

Three factors that affect floods in the area of study were identified through documented literature. Data was collected from Copernicus Open Access Hub using SNAP (SeNtinel Application Platform) and then mapped in QGIS and ArcGIS using spatial analyst tools. The flood factors identified included; Meteorological factors, Physical factors and Human factors.

3.6.1. Meteorological factor

This factor included rainfall distribution. Data was obtained from worldclim.org. and climate-data.org. The data was for the month of June year 2021, which is ideal for flood mapping. The 24-hour period was chosen because of the availability of daily rainfall data.

3.6.2. Physical Factors

The physical factors identified through literature review included: Drainage density, elevation, Natural Differential Vegetation Index (NDVI), slope, soil topographic wetness and drainage density.

a) Drainage Density

Drainage density is the quotient of the total length of a channel in a basin and the basin’s total area. It was created using drainage lines of the area of interest and using Line Density spatial analyst tool in ArcGIS. DEM was processed in HEC GeoHMS to create the drainage lines which were used as streams and rivers. The tool calculates magnitude per unit area of a polyline data.

b) Elevation

Elevation is the altitude of a given geographical location.

Synthetic Aperture Radar (SAR) was obtained from Sentinel's Mission 1. It has a resolution of 10 meters. Range Doppler Terrain Correction was performed on the SAR data to correct the distortion on the data caused sensor and platform characteristics of the acquiring satellite. The corrected data contained elevation data that was eventually processed into Digital Elevation Model (DEM).

C) Normalized Difference Vegetation Index (NDVI)

NDVI is an index that defines the difference in vegetation reflectance of both near infrared and visible spectra.

The formula of NDVI is:

$$\mathrm{NDVI} = \frac{\text{Near Infrared} - \text{Red}}{\text{Near Infrared} + \text{Red}}$$

NDVI for this study was created using Sentinel imagery, with the following formula:

$$\mathrm{NDVI} = \frac{\text{Band 8} - \text{Band 4}}{\text{Band 8} + \text{Band 4}}$$

Where;

Near Infrared (Band 8) is the portion of electromagnetic spectrum with wavelength just beyond visible red light, ranging from 700-1400 nanometers. Near Infrared is not visible to human eye but is strongly reflected by healthy vegetation.

Red (Band 4) is visible red lights with wavelengths ranging from 620 to 750 nanometers. It is also absorbed by vegetation but its reflectance is relatively lower compared to Near Infrared.

c) Slope

Slope is the measure of steepness of the ground given in percentage or degrees.

Slope in degrees was created using the slope spatial analyst tool in ArcGIS.

d) Soil

Soil data obtained from Kenya Soils Survey was in raster form. The soil data for Kenya was clipped to the area of study in order to get the soil map for the three sub counties. The area of study had three classes: clay (heavy), clay (light) and the urbanized area; all which were classified under HSG D (Hydrological Soil Group D).

e) Topographic Wetness Index (TWI)

TWI is the quantification of topographical control on hydrology; a function of slope and upstream contributing area per unit width perpendicular to the direction of flow of the stream.

The formula of calculating TWI is:

$$\mathrm{TWI} = \frac{\ln(\text{Local upslope area})}{\text{slope in radians}}$$

TWI was created in ArcGIS using the following procedure:

Generating a fill for DEM

Creating flow direction

Creating flow accumulation

Creating slope in degrees

Creating slope in radians using the following formula:

$$\text{Slope in radians} = \frac{\text{Slope in degrees} * 1.570796}{90}$$

Determining tan of slope using raster calculator using the formula below:

Tan slope = Con (Slope in radians > 0, tan (Slope in radians, 0.001)

Scaled flow accumulation was then calculated using:

Flow accumulation scaled = (Flow accumulation + 1) * Cell size

The cell size from the sentinel imagery (10 m resolution) is 8.931528e-5.

TWI is then given by:

$$\text{TWI} = \frac{\text{Flow Accumulation Scaled}}{\text{Tan slope}}$$

3.6.3. Human factors

a) Land use/ Land cover

Land use/ Land cover map was created from Sentinel Imagery using object-based classification. Band composites were created for more in-depth analysis of the area of interest. Band combinations included; Bands 4, 3 and 2 for the true color and bands 8, 3 and 2 for false color where vegetation appear red.

The classes of land use/ land cover that were created include: Bare ground, Concrete surfaces, High density vegetation, Industrial and commercial areas, Low density vegetation, Medium density vegetation, Residential- Permanent, Residential- Slums, Tarmac and Water body.

b) Proximity to river/ stream

Closeness to rivers and streams within the area of study was determined by calculating Euclidean distances from the centerlines of the rivers and streams. The data was obtained from Humanitarian OpenStreetMap Team.

c) Proximity to roads and railway

Closeness to roads and railway within the area of study was determined by calculating Euclidean distances from the centerlines of the roads and railway lines. The data was also obtained from Humanitarian OpenStreetMap Team.

Channel slope, flow length, Land use/land cover etc. are the parameters used as input for the hydrological model.

3.7. Data Analysis

Data collection and processing was done mainly by using remote sensing i.e. Synthetic Aperture Radar (SAR). SAR with a resolution of 10m was obtained from sentinel mission 1. The sentinel image was clipped to the area of interest extents and reflectance made. Band composites were created for more in-depth analysis of the area of interest. Band combinations included; Bands 4, 3 and 2 for the true color and bands 8, 3 and 2 for false color where vegetation appear red. This helped in coming up with LULC that was used as input in the TR 55 model.

3.7.1. Determination of impervious surfaces

The impervious surfaces were determined from the sentinel imagery in order to help analyze the water infiltration rate, not only into the aquifers but also, on the surfaces in order to aid in the reduction of vulnerability of flooding in the area of study. This is shown in the LULC map in figure 4.11 and table 4.1.

3.7.2. Characterization of the flood prone areas.

A. Delineation of the sub-catchment

Hydrological tools in ArcGIS was used to subdivide the area into sub-catchments, DEM was used as the input in order to give sufficient information for use in model.

The four catchment areas within the area of study were created from drainage outlet points, which were created using preprocessing tool of HEC GeoHMS in ArcGIS. The Catchment areas were then clipped to the area of study and then clipped again using soil data to obtain 17 sub catchment areas. Land use/land cover data of the area of study was then clipped into each of the sub-catchment zones. This helped in determining the area of each land use/ land cover in each sub-catchment.

The sub-catchments were demarcated from the Digital Elevation Model by estimating the flow accumulation grid and flow direction with the help of the flow accumulation and flow direction tools from ArcGIS. In order to divide the area of study into sub-catchments, the pour points for the sub-catchment were added depending on the flow accumulation grid, to the junction of the network of the stream divided from the flow accumulation.

Table 3.2: Catchment Delineation

Catchment	**Area (m^2)**	**%**
Catchment A	3630675	15
Catchment B	11681175	48
Catchment C	4876175	20
Catchment D	4288150	17
Total	**24476175**	

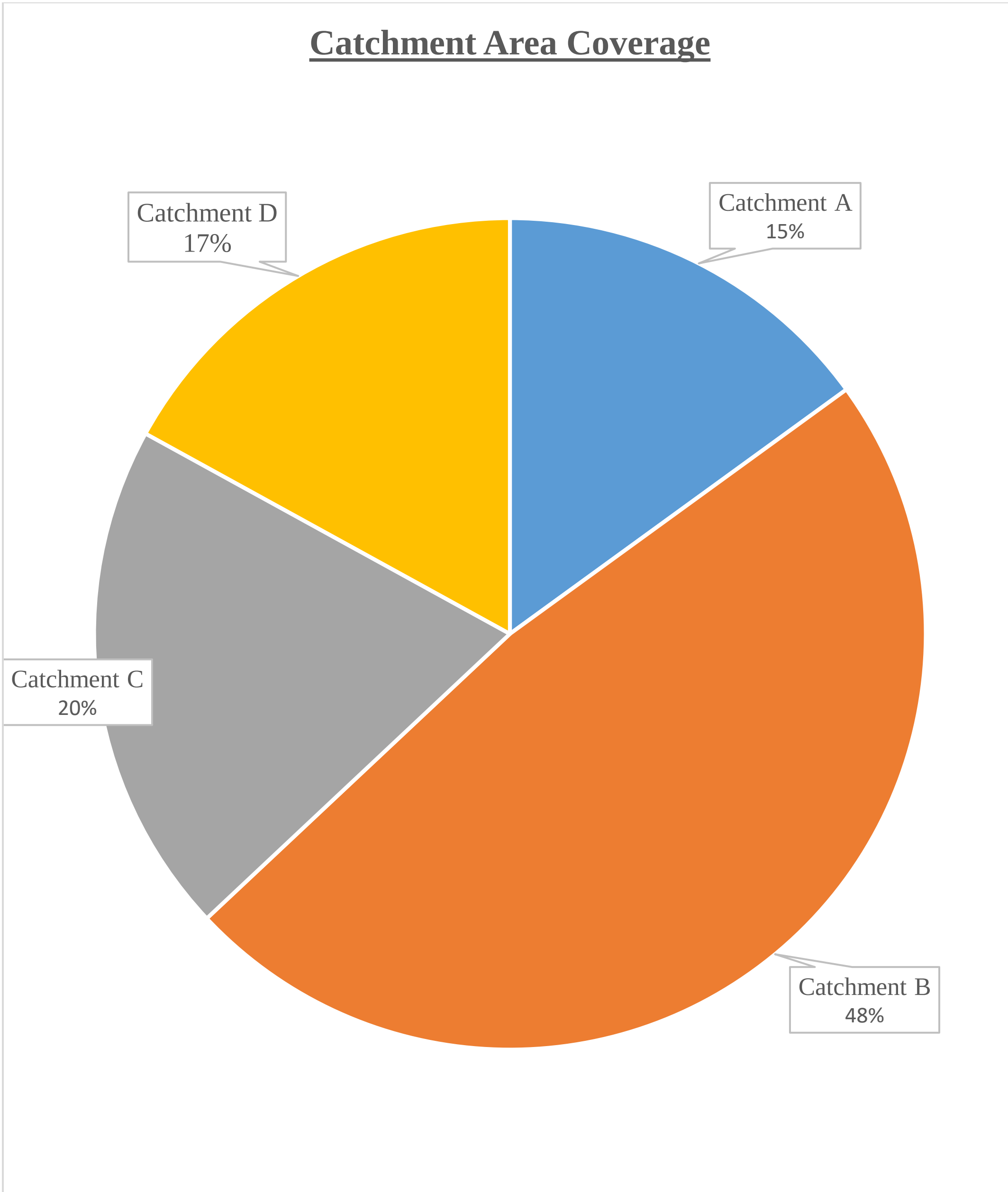

Figure 3.2: Visual presentation of Catchment Area Coverage

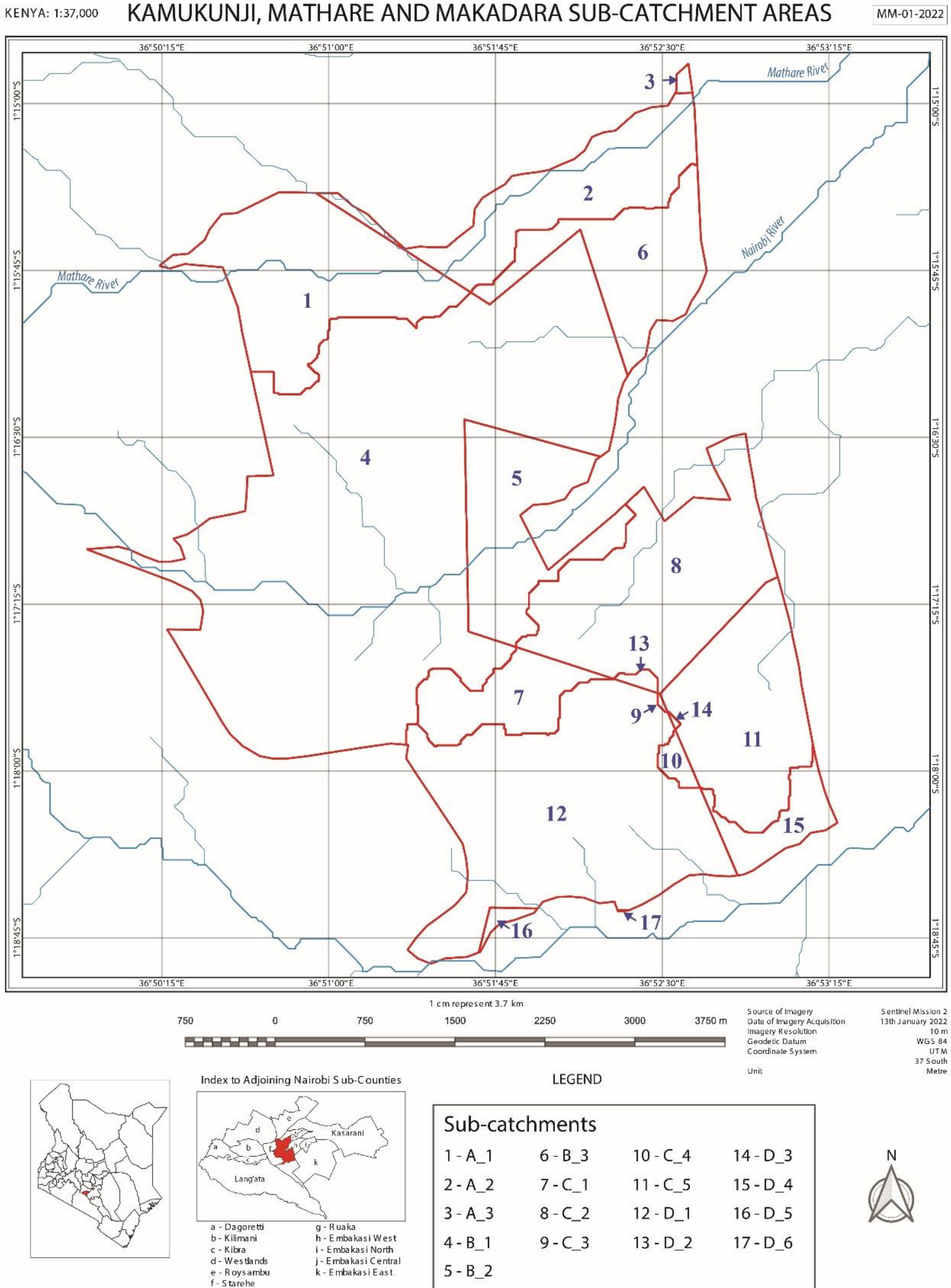

Figure 3.3: Map of sub-catchment areas in the area of study

B. Parameterization of the sub-catchment

The parameters of the sub-catchments i.e., flow length, land use/ land cover type and channel slope were calculated using ArcGIS software and then used as input into the hydrological model.

Land use/ land cover types within the sub-catchments were used to estimate the Curve Number values for the various sub-catchment as shown in table 4.1. Flow length and Channel slope parameters were calculated using HEC-GEOHMS (Hydrological Engineering Center's Geospatial Hydrological Model System), which is an extension of ArcGIS software (Flemming and Doan, 2009). The parameters were used to estimate the concentration time for the peak discharge and runoff for each sub-catchment.

3.7.3. Modeling of flood magnitude

A. Application of SCS TR-55 Model

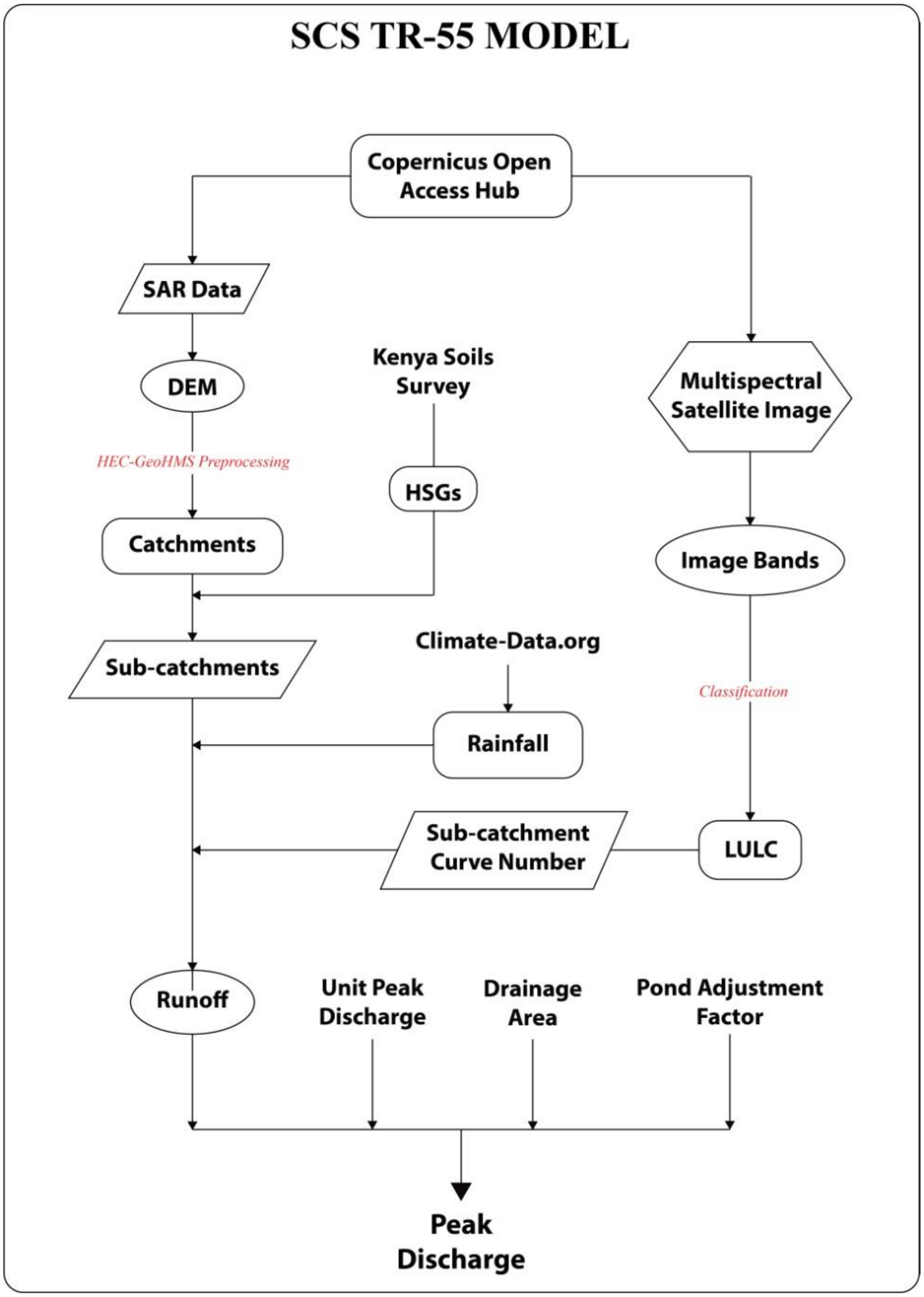

Figure 3.4: SCS TR 55 Model Flow Chart

This model was applied in the prediction of run-off and peak discharge in 17 sub-catchments. Runoff and peak discharge were determined using equations that are for the model.

Synthetic Aperture Radar (SAR) data and Multispectral satellite image were obtained from Copernicus Open Access Hub. SAR data was used to create a 10m resolution DEM which was used to delineate the catchment into sub-catchments. Classification of Multispectral satellite image created LULC which was used to determine Curve Number for each sub-catchment. Curve Number helped in calculating runoff value for each sub-catchment using the model's equation shown below.

$$\text{Runoff} = \frac{(\text{Rainfall} - \text{Ia})\text{^}2}{(\text{Rainfall} - \text{Ia}) + S}$$

Where:

Ia = Initial Abstraction; 0.05 * S (this being the most appropriate value for urban watershed)

S = Potential Maximum retention after runoff begins; (1000/CN) – 10

Travel time (Tt) is the time that water takes to travel from one location to another in a catchment and was calculated using the formula below;

$$\text{Tt}= \frac{L}{3600V} \quad , \qquad \text{V}= \frac{1.49}{n} r^{2/3} S^{0.5}$$

Where L= Flow length

V= Average Velocity

r= Hydraulic radius

S= Slope of hydraulic grade line

n= Manning Roughness coefficient for open channel flow.

For unpaved areas; n is 0.05, r is 0.4, Paved areas; n is 0.025, r is 0.2

Time of Concentration (Tc), is the time of runoff to travel from the hydraulic most distance point of the watershed to the point of interest within the catchment. It was calculated by summing all the travel times of the consecutive components of the conveyance system;

$$Tc = Tt_1 + Tt_2 + Tt_3 + \ldots\ldots\ldots + Tt_m$$

Unit Peak discharge was determined by SCS TR 55 graphical method and the value used to calculate the peak discharge.

$$q_p = q_u\, A_m\, Q\, F_p$$

where q_p = peak discharge (cfs)

q_u = unit peak discharge (csm/in)

$A_{m=}$ drainage area (mi_2)

Q= Runoff (in) (Flood depth)

F_p= Pond and swamp adjustment factor

Peak discharge was calculated by multiplying unit peak discharge (csm/in) by drainage area (mi_2) by Runoff (in) and by the Pond and swamp adjustment factor.

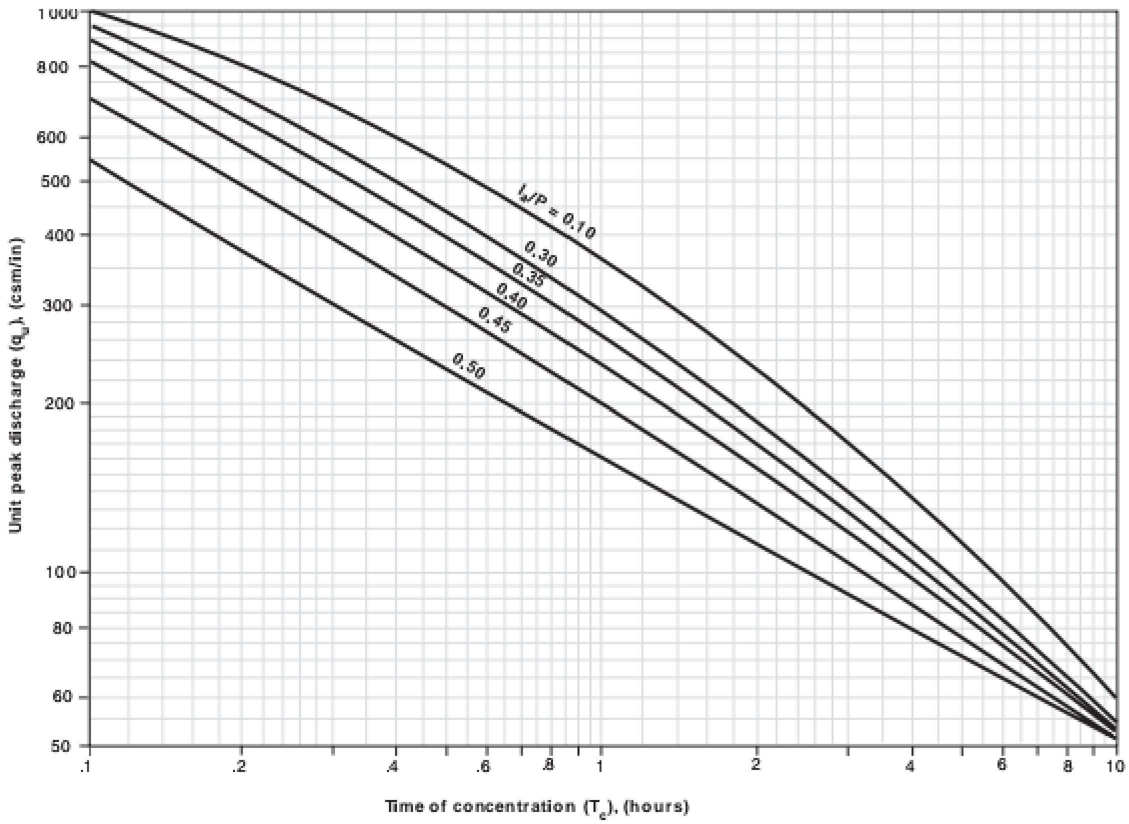

Figure 3.5: Unit peak discharge for SCS type II rainfall (USDA 1986)

Table 3.3: Adjustment factor F_p for pond and swamp areas that are spread throughout the catchment (USDA 1986)

Percentage of pond and swamp areas	F_p
0	1.00
0.2	0.97
1.0	0.87
3.0	0.75
5.0	0.72

3.7.4. Development of Flood Hazard Map

The flow chart for flood hazard mapping is lustrated in figure 3.6 presented below.

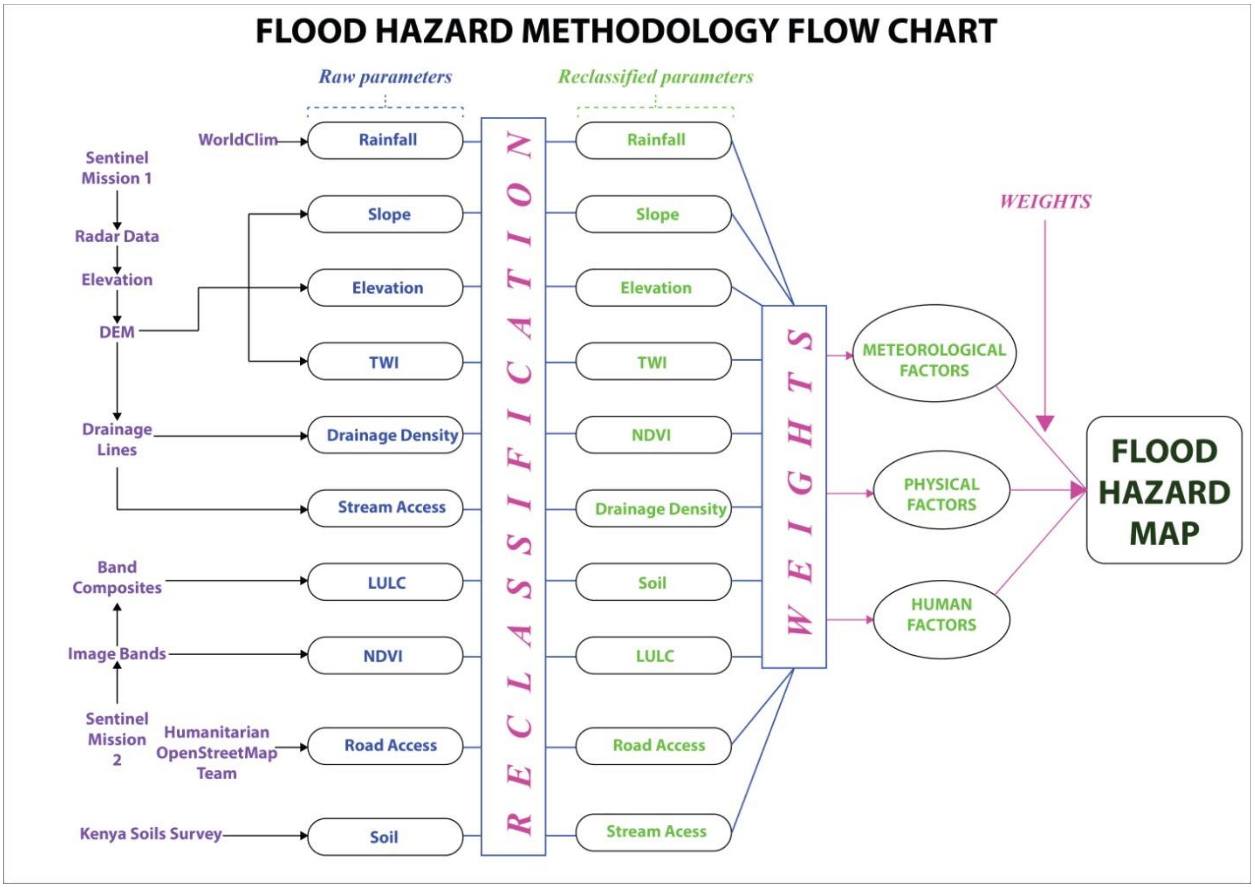

Figure 3.6: Flood Hazard Methodology Flow Chart

Overall maps showing flood zone areas and flood depths in the study area was produced using analyst tools in ArcGIS software.

The Flood Hazard Map was created by overlay analysis. The parameters were evaluated as physical and human parameters first, and then used together with the rainfall data to obtain the Flood Hazard Map. Editing of the spatial data was done to produce a high-resolution flood map shown in figure 4.15.

A map showing flood depths in the study area was also obtained using analyst tools in ArcGIS software by computing the runoff values obtained from the SCS TR 55 model into the software and is shown in figure 4.16.

3.7.5. Validation of the Flood Depth Map

The results of the map were validated using overlay analysis. Analytical Hierarchy Process (AHP) method of Multi Criteria Evaluation Analysis (MCEA) was used to perform the overlay analysis. The parameters were evaluated as physical and human parameters first then used together with the rainfall data to obtain the final overlay analysis as shown in the flow chart in figure below;

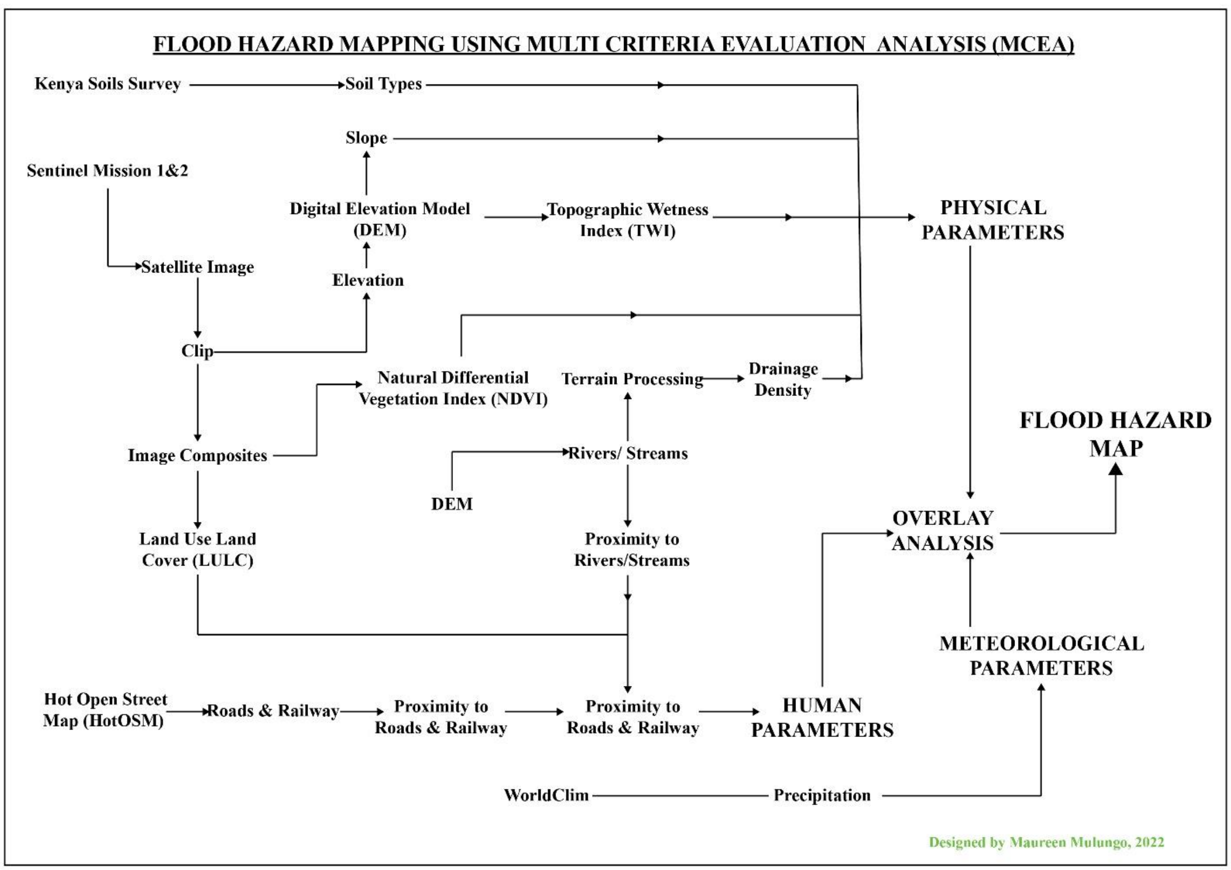

Figure 3.7: Multi Criteria Evaluation Analysis

The weights used were developed by obtaining experts opinions from five respondents on how the parameters affect flood susceptibility in the study area. This was done through questionnaires and the results used to create pairwise comparison tables. Each respondent's evaluation was then used to develop the final weighting for the parameters as shown in the appendix on table A6. The weights for each parameter were eventually computed for the overlay analysis.

Overlay analysis uses harmonized data and is for this reason that all the data are standardized using the Reclassify tool in ArcGIS.

Reclassification was done into the following classes of flooding conditions;

1. Very low floods
2. Low floods
3. Moderate floods
4. High floods
5. Very high floods

Flood hazard map formed as shown in figure 4.15.

The table showing the criteria for standardization is presented in the appendix on table A5.

Through observation, the flood hazard map from overlay analysis results show a close resemblance with the simulated flood map shown in figure 4.16. The areas that show high risk from the hazard map from the overlay analysis has high flood depth as can be seen in the flood depth risk map from simulation. Alternatively, Kappa Coefficient, Producer and user accuracy etc., can be used to assess semblance between observed and simulated maps.

There are no maps done previously to show the state of flooding in the areas.

CHAPTER 4

4.0. RESULTS AND DISCUSSION

4.1. Results

4.1.1. Factors affecting flood risk in the study area

A. Meteorological factor

Rainfall

As mentioned in the methodology, rainfall distribution was one of the factors considered in the analysis of flood risk in the study area. When there is heavy rainfall, there is less chance of it being infiltrated into the soil, therefore it runs off into the river. The faster it reaches the river, the more likely it will flood.

The map shown below was created using rainfall data that shows the wettest month of the year (June 2021). It shows that the western part of the study area experiences very heavy rainfall.

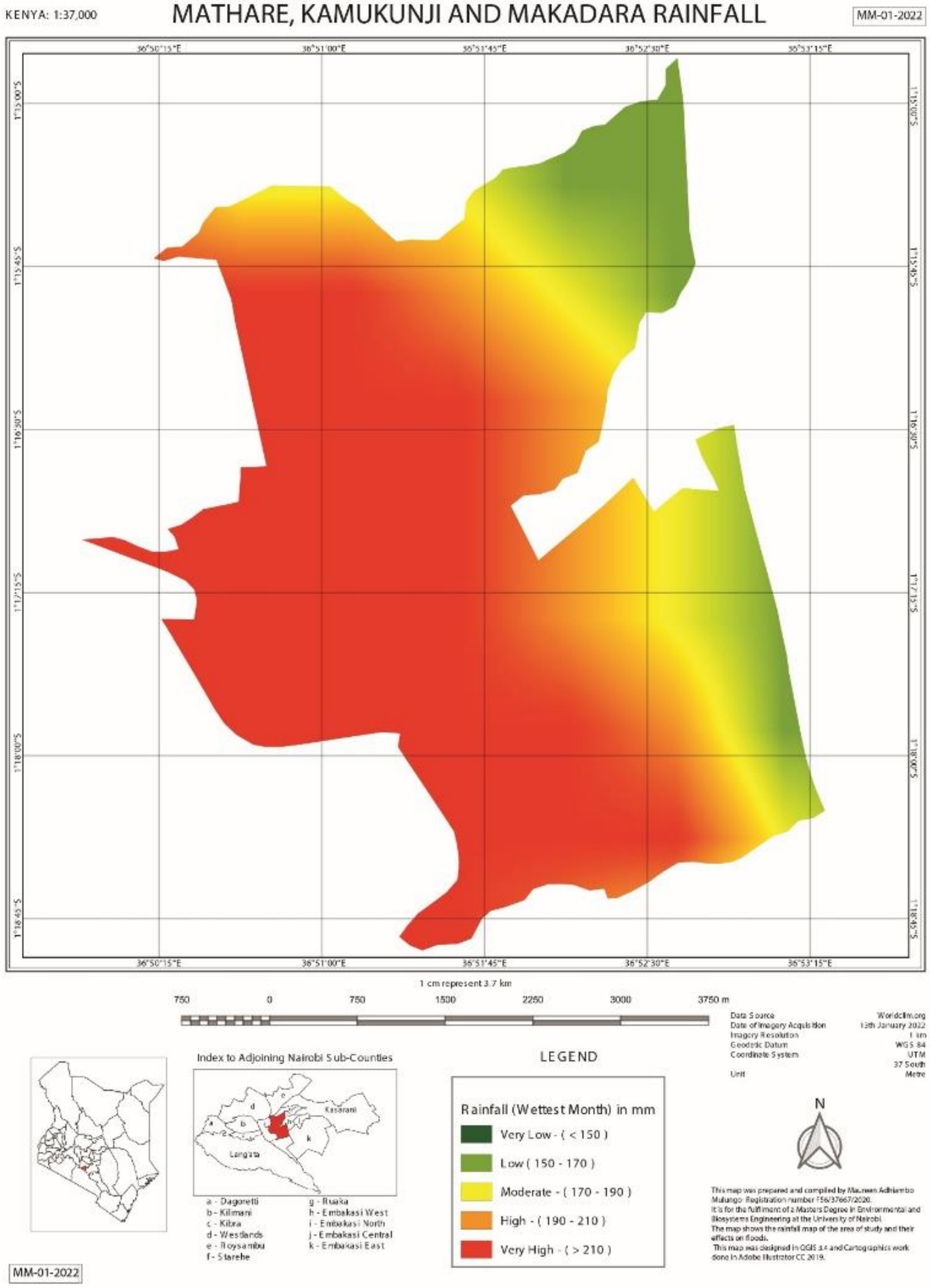

Figure 4.1: Rainfall Distribution Map in the Study Area

B. Physical Factors

Drainage Density

Flow velocity is higher in the river network. Drainage density significantly affects the concentration time and therefore the peak flow magnitude. Increase in drainage density leads to increase in flood peaks. Moreover, a long concentration of time implies more opportunity for water to infiltrate. The map below shows that very high drainage density is experienced in areas surrounding the river channels. Very low drainage density is in areas where there are no water bodies.

Flow length

The results show that extensive flow length led to decreased flood risk in the area. From figure 3.3, Sub catchment 3 (A3) which had highest flow length had low flood depth and therefore not prone to flooding. In contrast, sub catchment 17 (D6) with the lowest flow length of 4956ft (shown in table 4.3) had high flood depth hence prone to flooding.

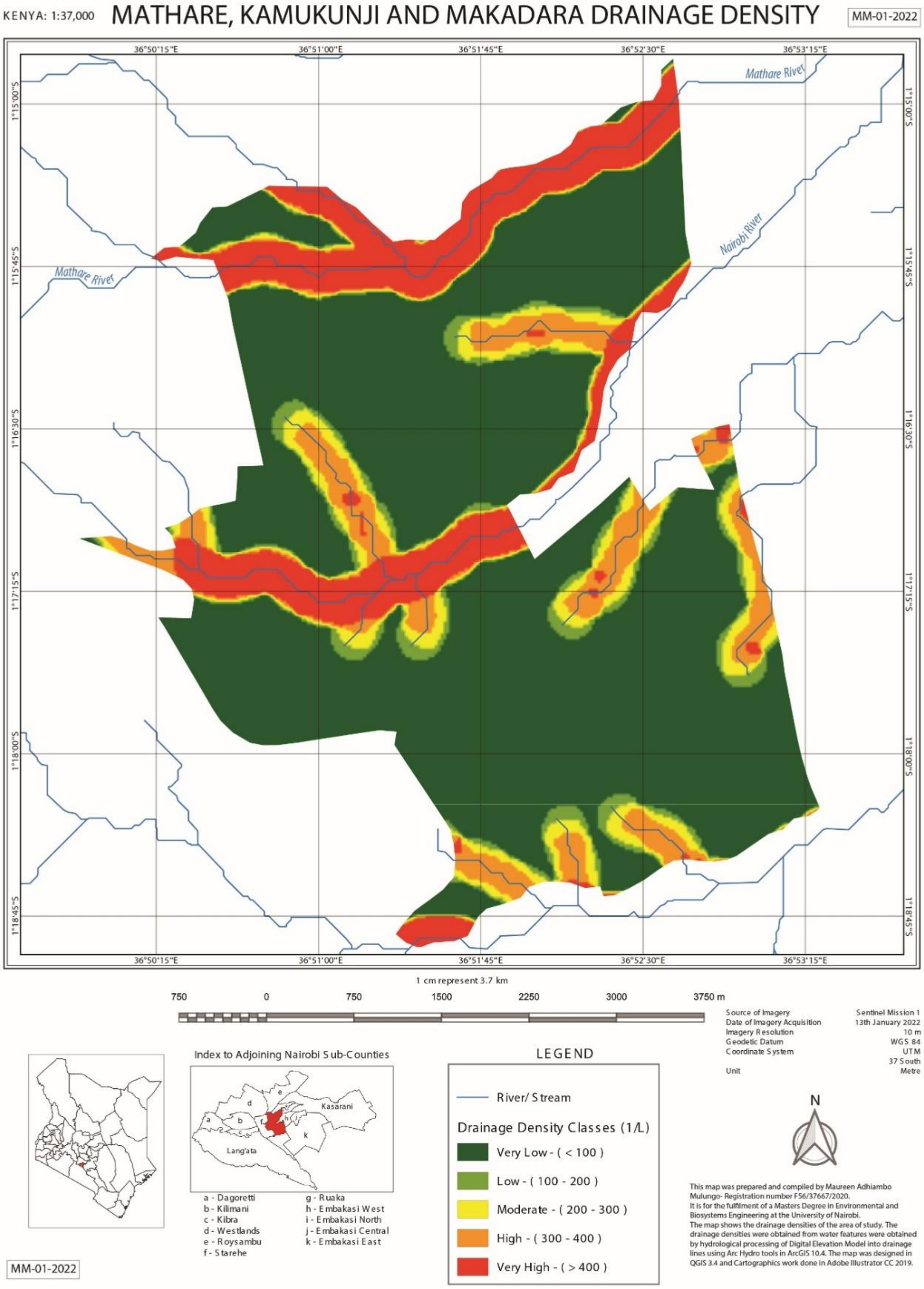

Figure 4.2: Drainage Densities Map in the Study Area

Elevation

Elevation is the altitude of a given area. Generally, areas with low topographic elevation have gentle slope therefore less prone to floods. Very high elevation of above 1640m is experienced in the north eastern part of the study area, that is, parts of Mathare and Kamukunji sub-counties as shown in the map below. Very low elevation of below 1580m was experienced in the western part of the study area.

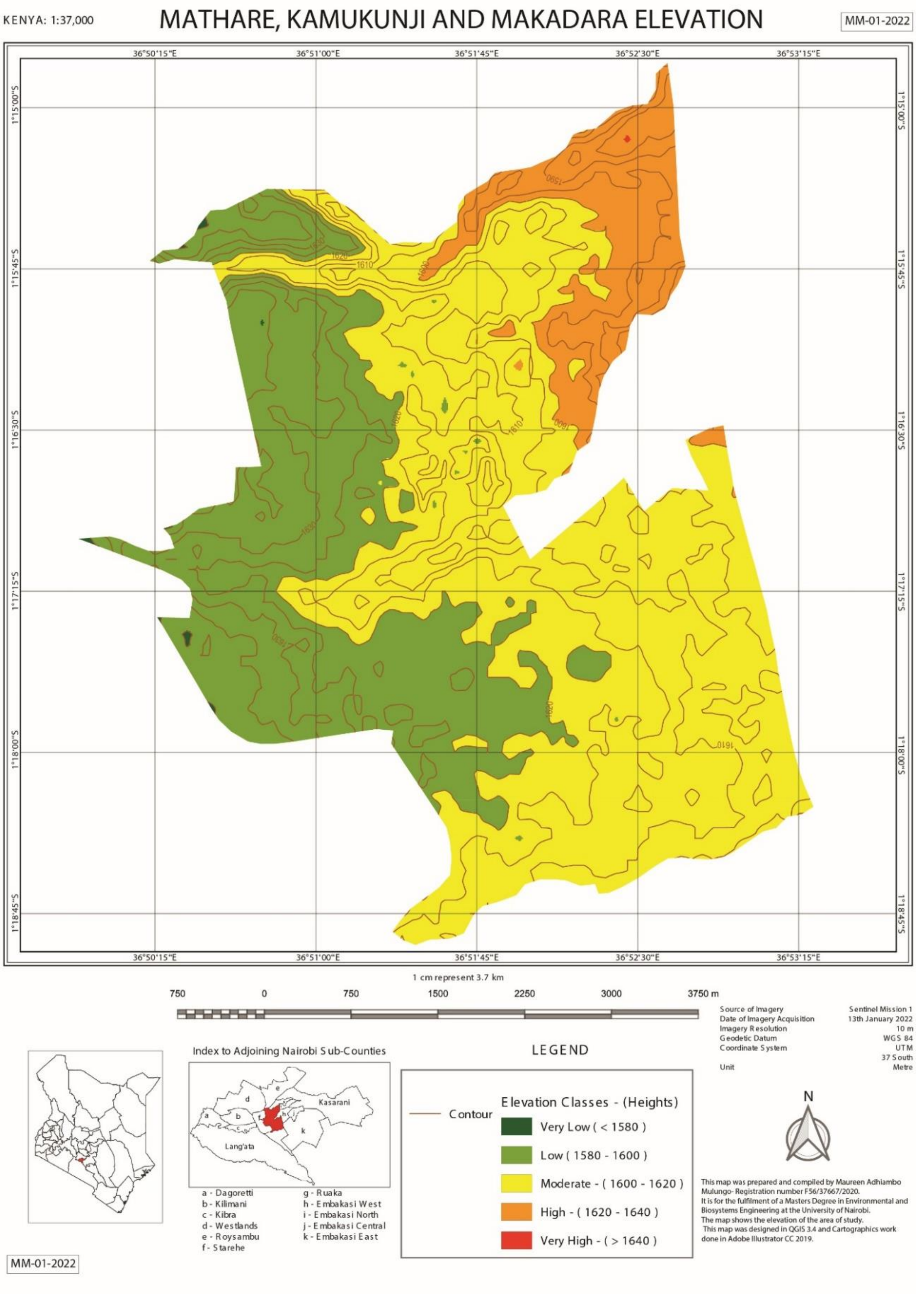

Figure 4.3: Elevation Map in the Study Area

Normalized Differences Vegetation Index (NDVI)

NDVI was used to map and identify the likely flood events in the area. The lower the NDVI the more likely it is to flood. Little vegetation means less water is being intercepted and stored by the trees and grass. The map below shows that most of the areas have very low NDVI. This can be attributed to the fact that the area is urbanized and therefore little vegetation.

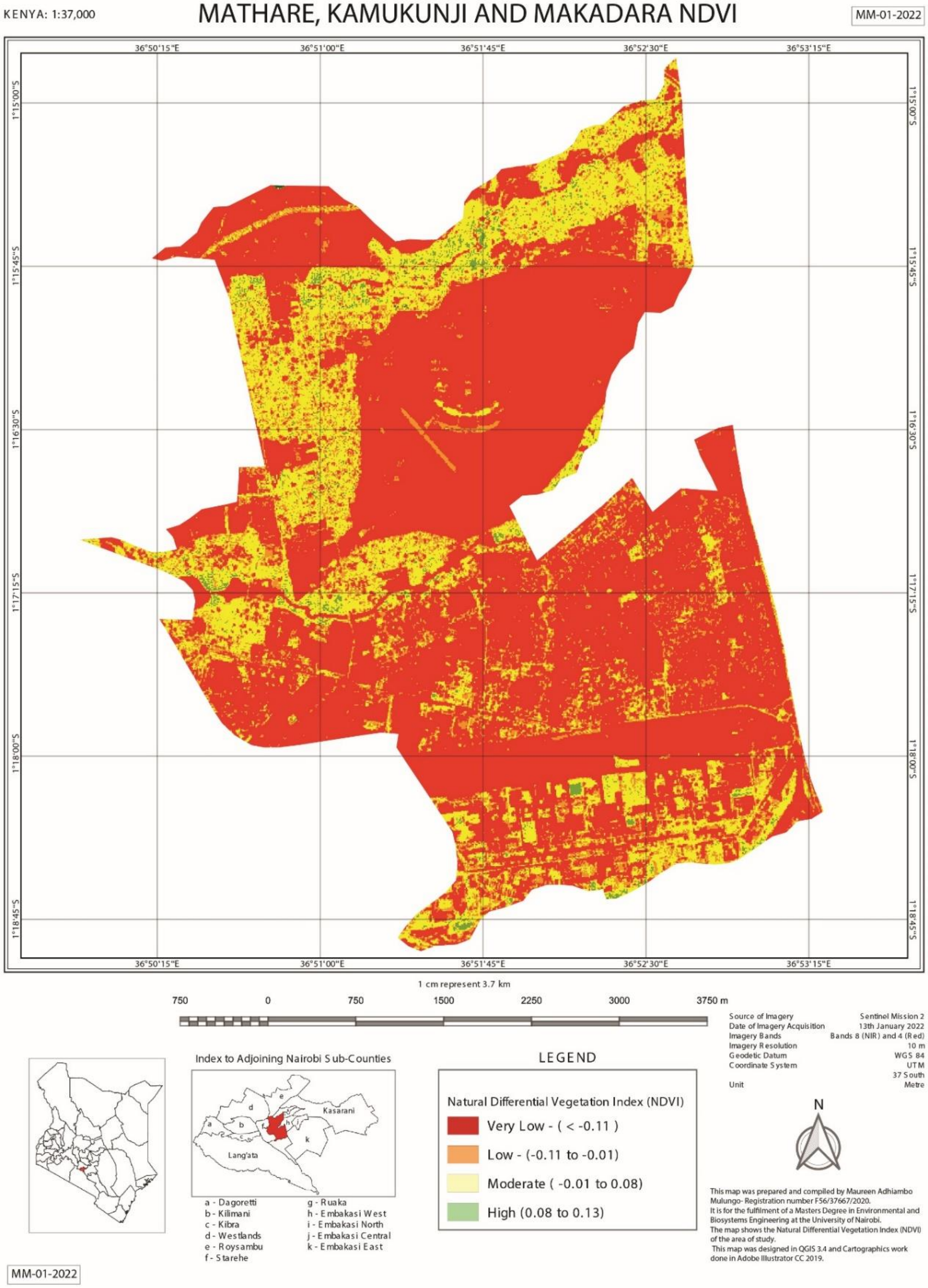

Figure 4.4: Natural Differential Vegetation Index Map in the Study Area

Slope

Slope is the measure of steepness of a ground measured in degree or in percentage. The longer the slope length, the greater the volume of water, flow speed and inertia force. This means that the further the distance from the watershed line, the greater the kinetic energy of flow and the higher the velocity of flow leading to an increase in flood risk. The steeper the more water will run via overland flow quickly into the rivers and also because of the steep angles of slopes, rain is less likely to infiltrate into the ground in these areas. With more overland flow and a quicker overland flow rate, the end result is flooding.

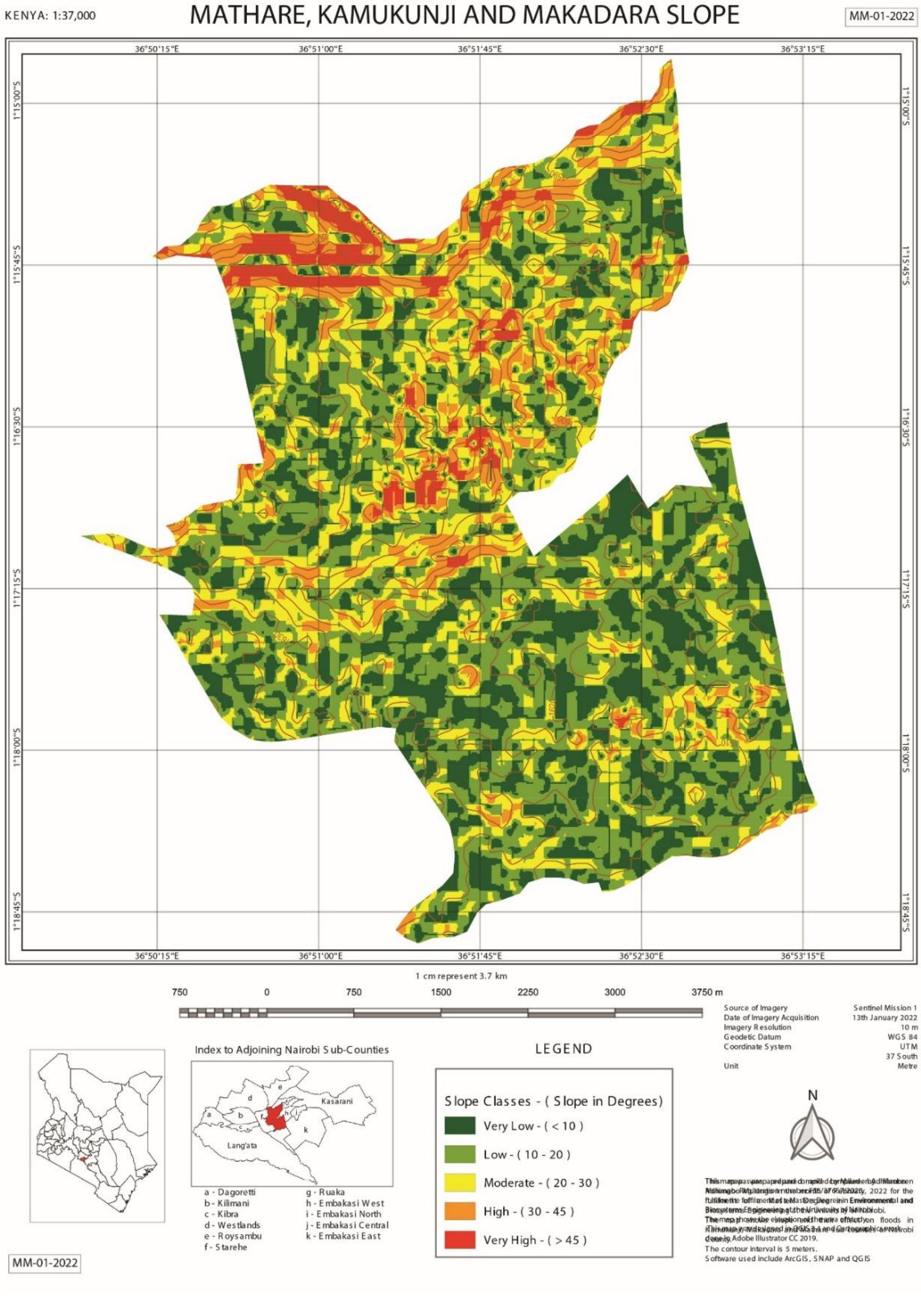

Figure 4.5: Slope Map in the Study Area

Soils

The factor determining soil structural behavior is the quality of flooding water which depends on the soil profile characteristics. Soils without a tough horizon have no limitations for free down and upward water movements throughout the profile. The soils in the area are a mixture of red clay, black cotton and alluvium soil which makes most sections of the area slightly unstable in regard to the bearing capacity of the soil, making the area prone to waterlogging. This is because the soils are soft, thick and they absorb rainfall like a sponge and release it slowly into streams and rivers. Therefore, when water is added to them, it infiltrates less hence high floods.

The area was found to have hydrological soil group D with urbanized area covering 70% of it especially on the western part of the study area.

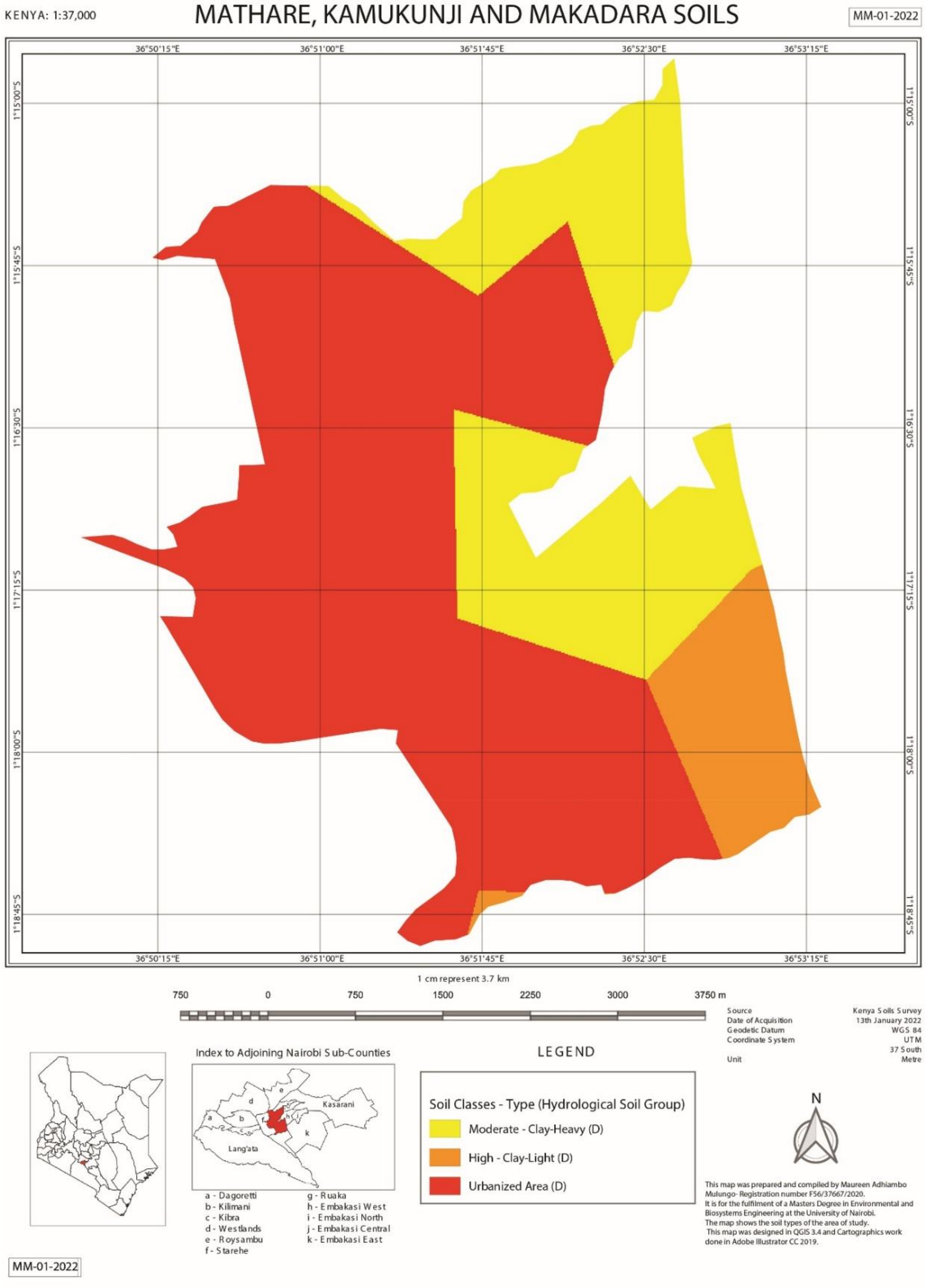

Figure 4.6: Soil Map in the Study Area

Topographic Wetness Index (TWI)

TWI is a physical indicator of the effect of topography of runoff flow direction and accumulation. It helps identify rainfall runoff patterns, areas of potential increased moisture and ponding areas. Smaller values of TWI indicate less potential for ponding while larger values occur where greater upslope areas are drained and the slope is gentle. This shows that the larger the TWI, the more prone the area is to flooding and vise vasa.

The map below shows that about 80% of the area is covered by low and very low TWI.

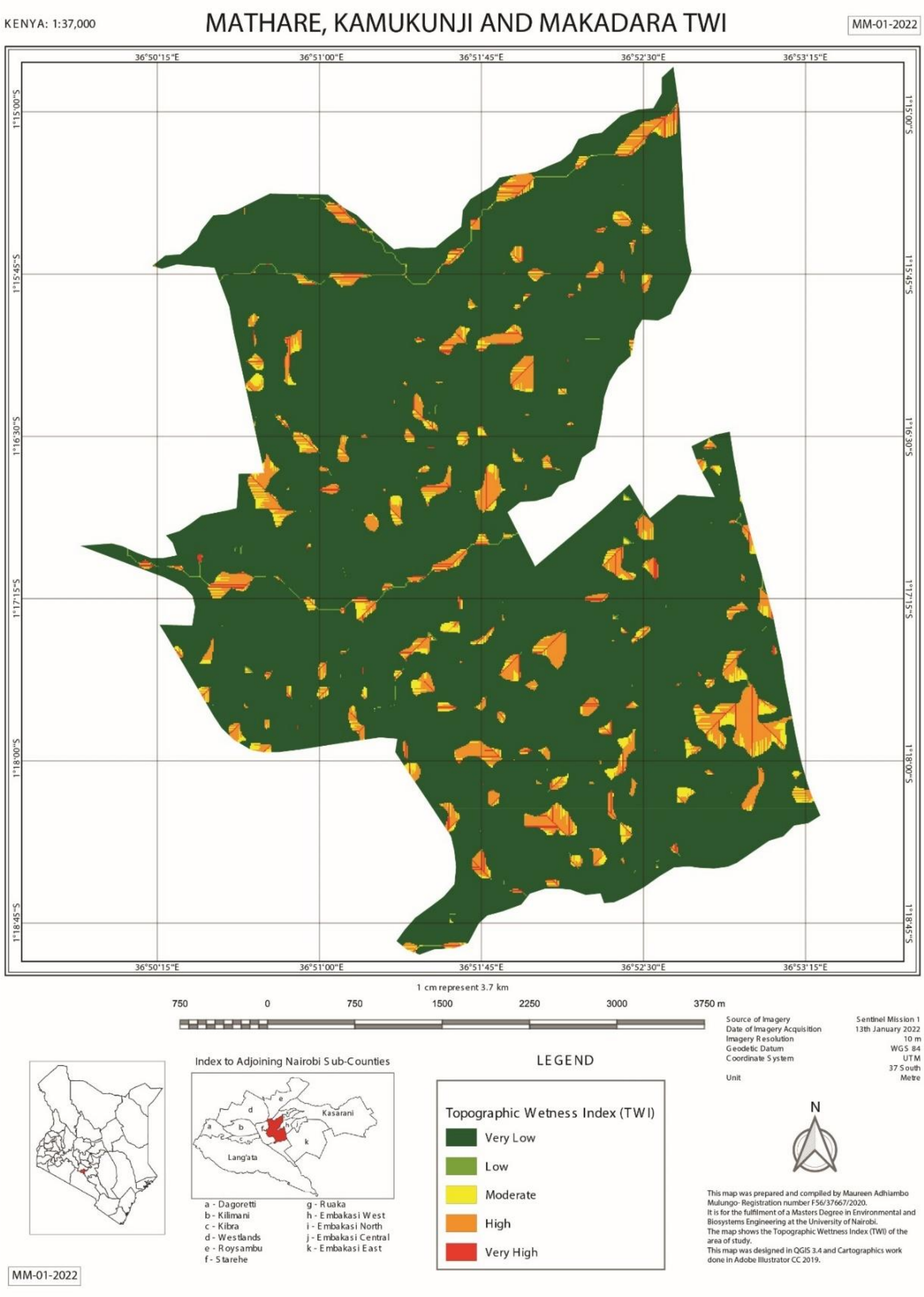

Figure 4.7: Topographic Wetness Index Map in the Study Area

Overall Physical Parameter Map

All the physical parameter maps were overlaid in ArcGIS to give the overall physical parameter map below.

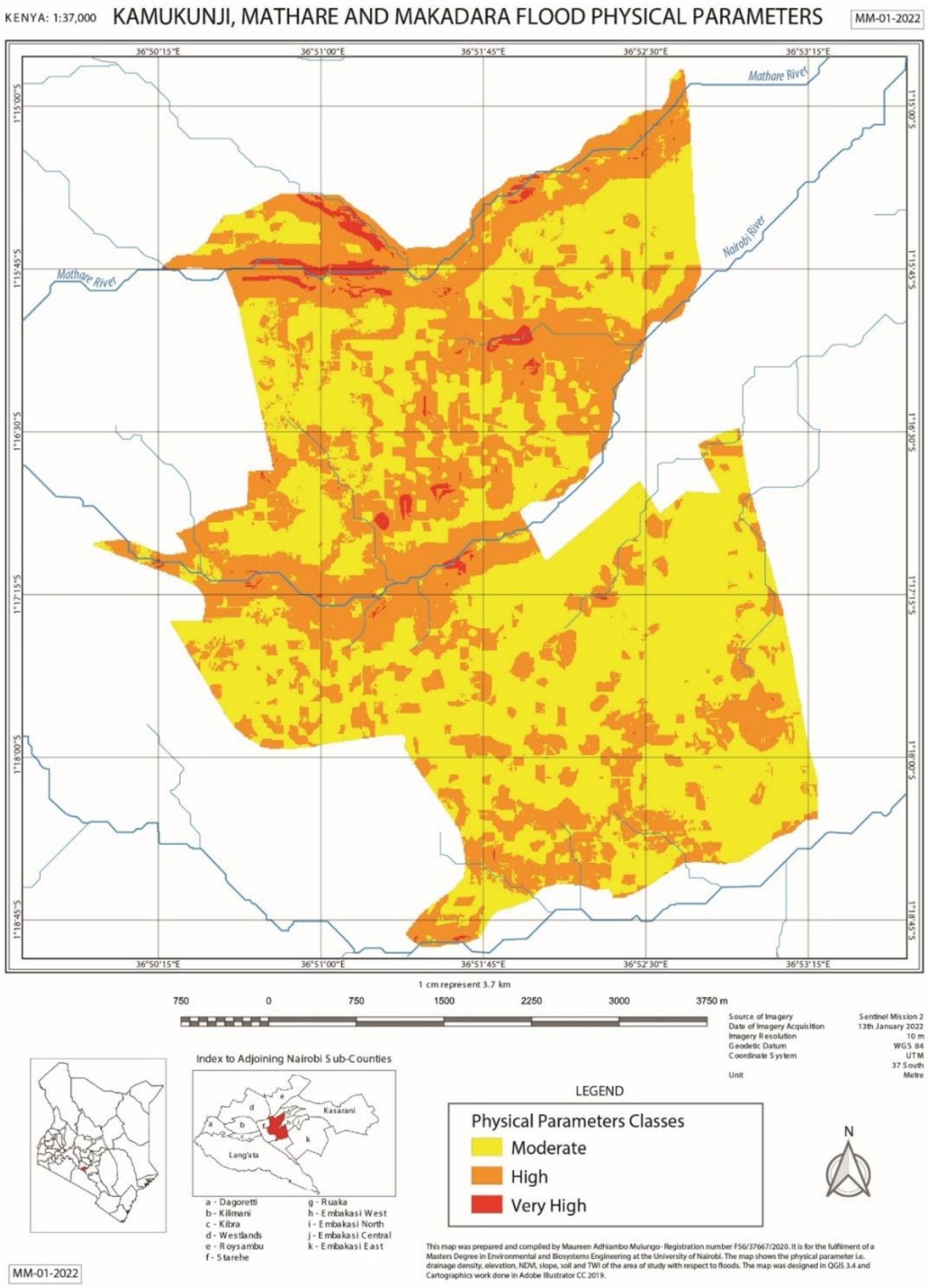

Figure 4.8: Overall Physical Parameters Map

C. Human Factors

Land Use/ Land Cover Map (LULC)

Land cover changes caused by urbanization, deforestation and cultivation have led to increase in floods after precipitation events. LULC changes alter the natural drainage systems, impact on surface run off and affect infiltration capacities which contribute to flooding.

Figure 4.11 shows the different land use/ land cover found in the study area. The most dominant land use being the residential permanent.

The results from figure 4.11 show that sub catchment 17 (D6), 12 (D1) and 10 (C4) which are composed of 100, 80 and 100% of impervious areas had high CN values (95, 92 and 91), and high runoff (195 and 172 mm) compared to other sub catchments. This shows that there's a strong relation between runoff and CN.

The results revealed that the impervious areas greatly affected the flood phenomenon. Sub catchments with more than 70% impervious areas generally have runoff depth ranging between 13.6 and 19.5 cm. Sub catchment 17 (D6) consists of 100% impervious areas and the highest runoff depth of 19.5 cm.

In contrast, sub catchment 1 (A1) and 5 (B2) had the lowest runoff value of 136mm with 20 and 10% impervious area and therefore the areas were not susceptible to high rate of flooding.

This shows that sub catchments with high runoff values and more impervious areas are vulnerable to flooding. Therefore, increase in impervious areas leads to high flood risk.

Table 4.1: Land Use/ Land Cover and their areas' computations.

Land Use/ Land Cover	**Area**	**%**
Concrete	72600	0.3
Low Density Vegetation	3418100	14.2
Bare Ground	2851425	11.85
Residential- Permanent	11110625	46.17
Tarmac	1642825	6.84
Medium Density Vegetation	979525	4.07
High Density Vegetation	70575	0.29
Water Body	3600	0.01
Residential- Slums	1012750	4.21
Industrial & Commercial	2901575	12.06
Total	**24063600**	

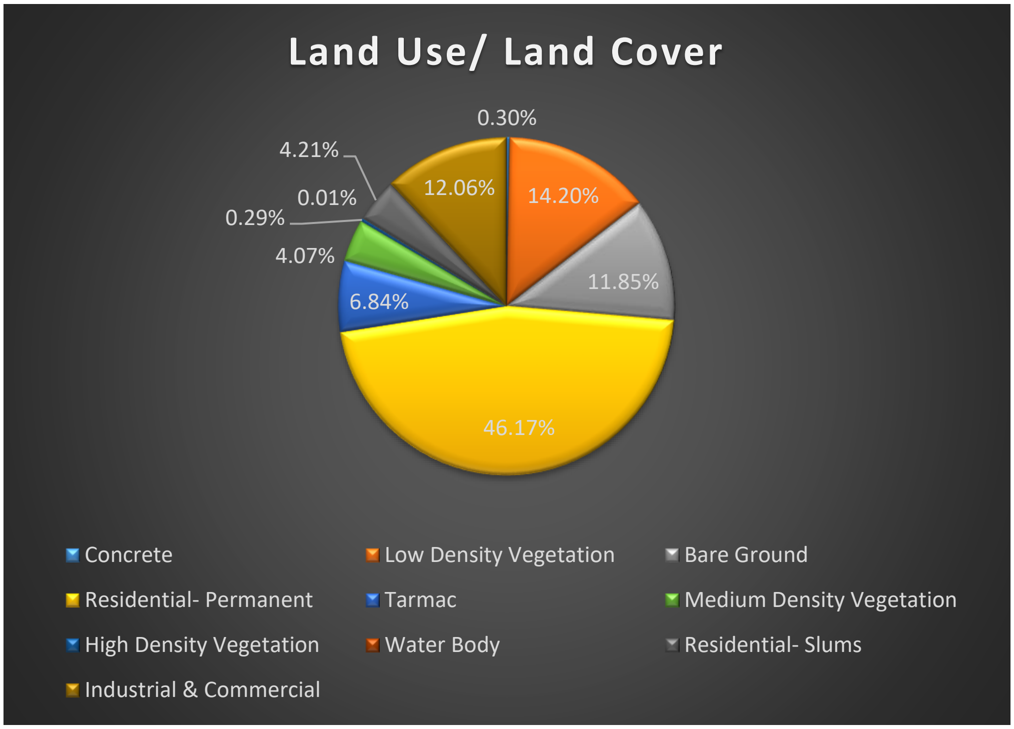

Figure 4.9: The visual representation of LULC in the study area

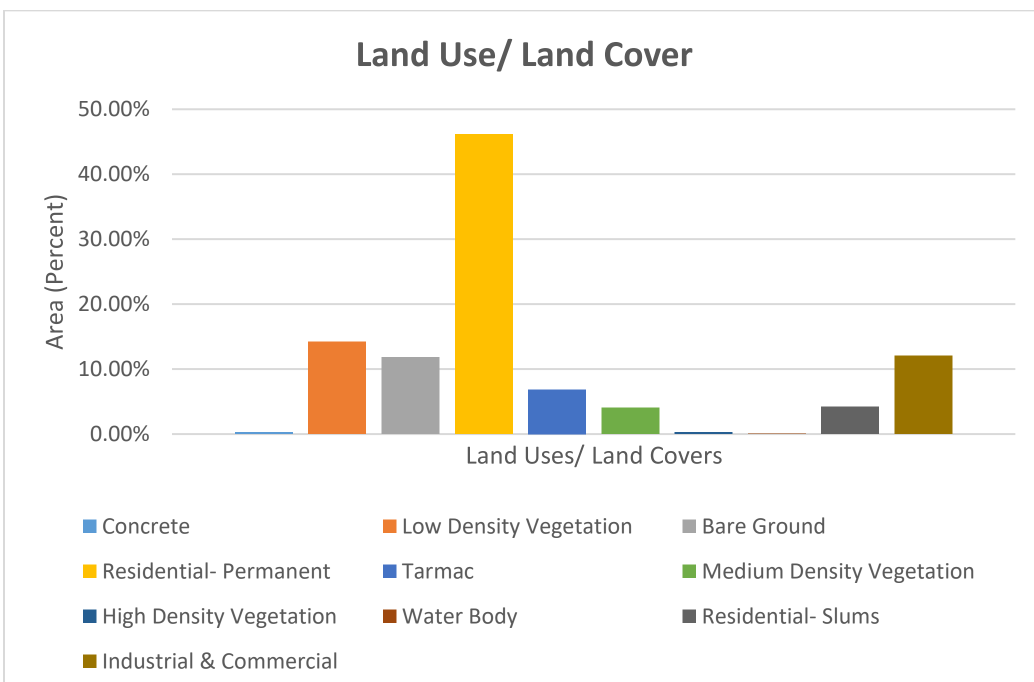

Figure 4.10: Graphical presentation of LULC in the study area

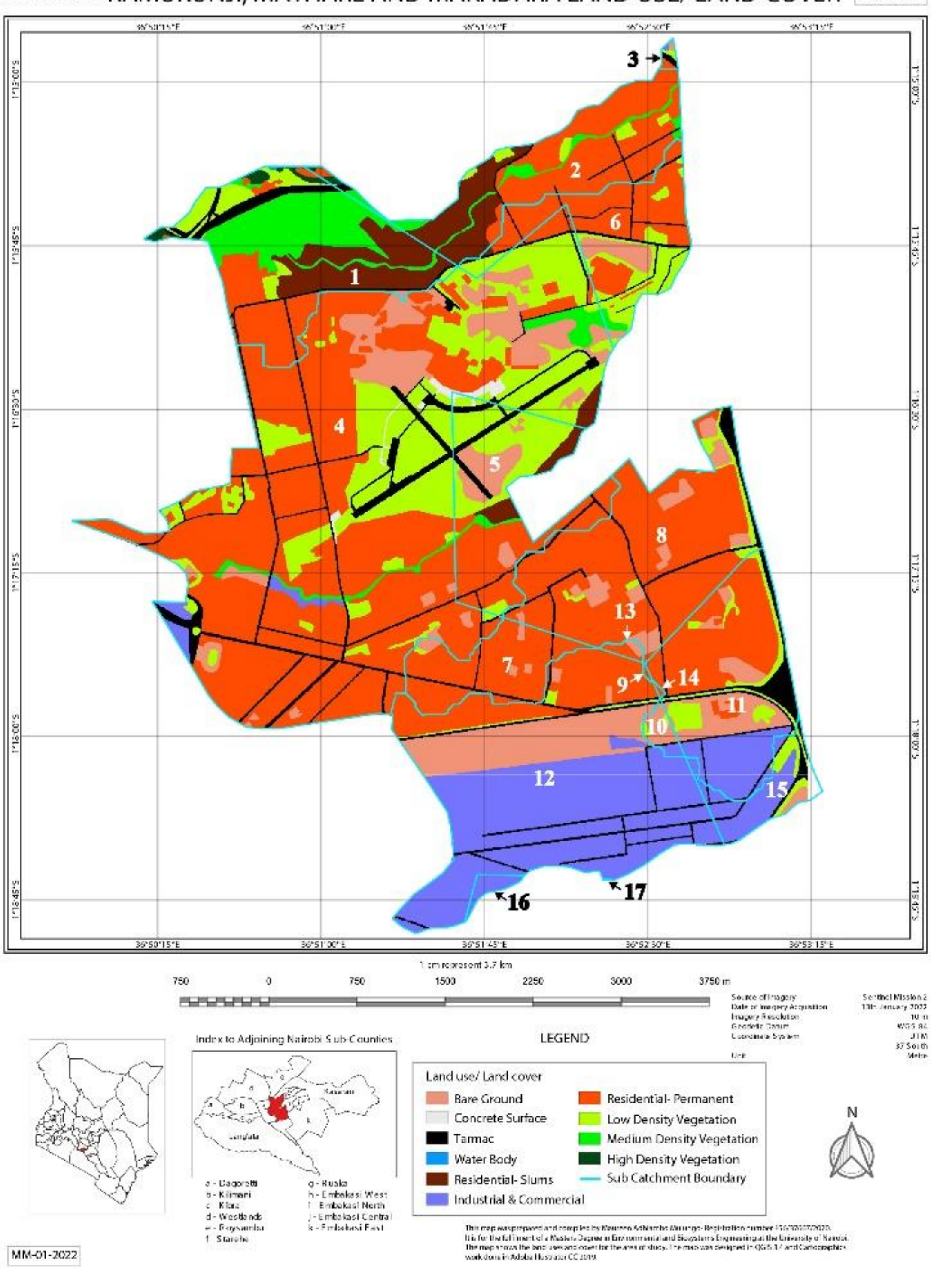

Figure 4.11: Land use/ Land cover Map in the Study Area

Rivers

Rivers flood when pulses of rainfall move downstream. This causes water to overtop the channel's banks and spill onto the neighboring flood plains.

The map below shows the vulnerability of the areas prone to flooding in relation to their distance from the rivers or streams. Very high chances of flooding will occur at a distance between 300-600m.

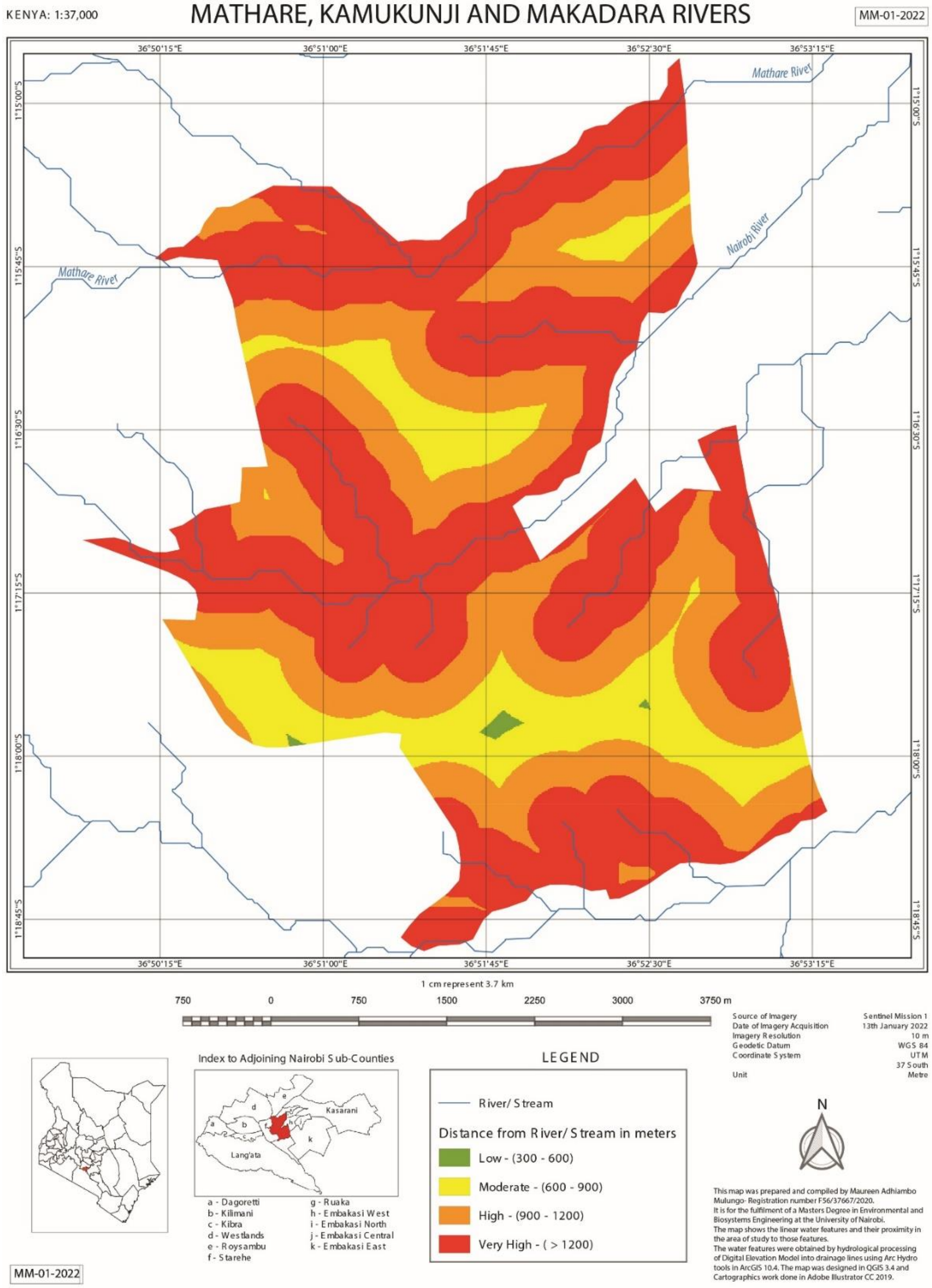

Figure 4.12: Proximity to Rivers Map in the Study Area

Roads and Railways

Transport network supports economic activities by enabling movement of goods and people. During extreme weather events, transport infrastructure can be directly or indirectly damaged posing threat to human safety. Intense precipitation causes flooding which disrupt the transport sector. Existing approaches to assess the disruptive impact of floods on roads fail to capture the interaction between flood water and transport system typically assuming that roads are fully operational.

The map below shows that areas surrounding the roads have very high chances of flooding with a distance of below 30m from the road.

Figure 4.13: Proximity to Roads and Railways Map in the Study Area

Overall Human Parameter Map

All the human parameters maps were overlaid in ArcGIS to give the overall human parameter map below.

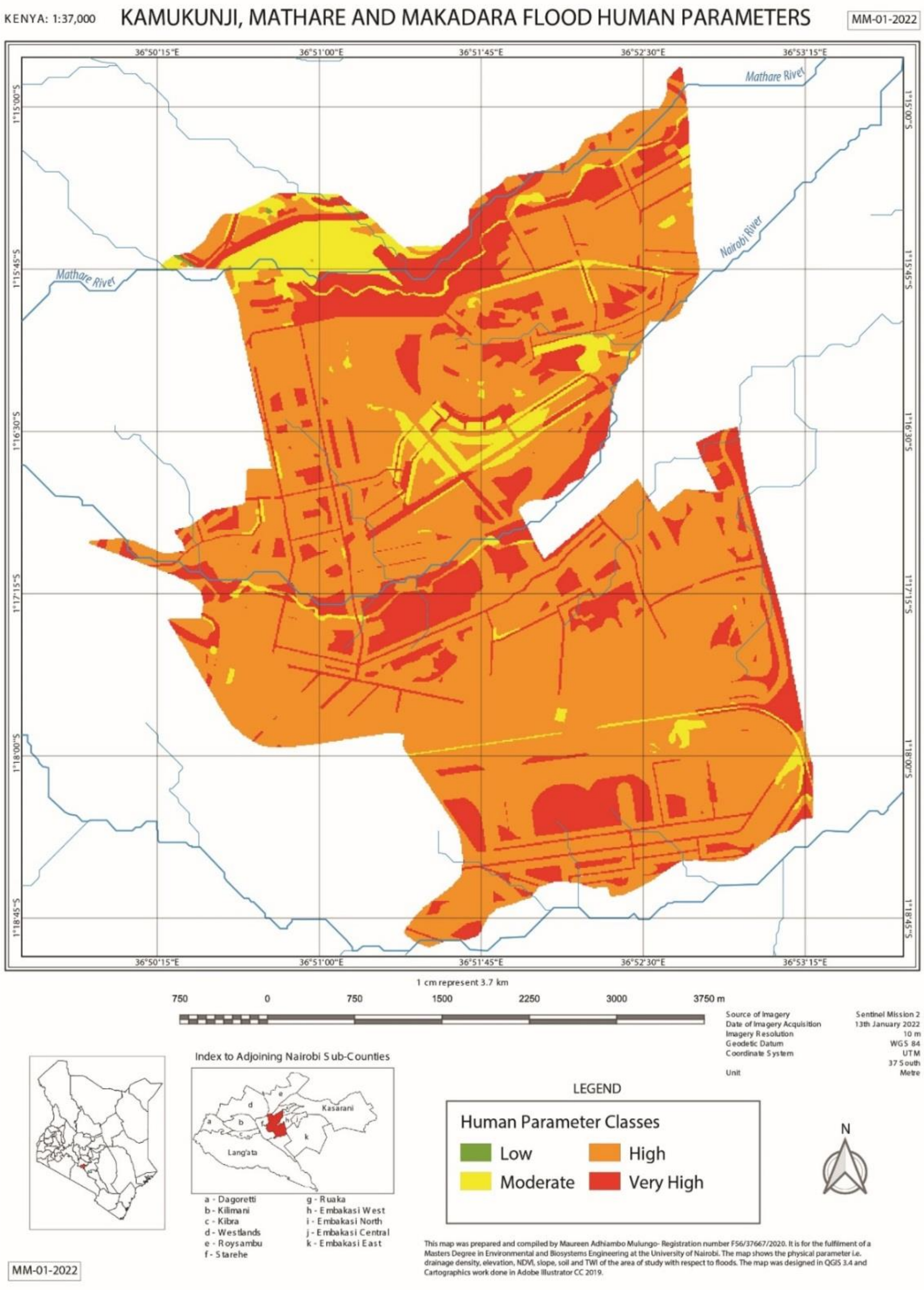

Figure 4.14: Overall Human Parameters Map

4.1.2. Flood Hazard Map

The overall physical parameter map, human parameter map and the meteorological map were overlaid in ArcGIS to produce the flood hazard map shown below.

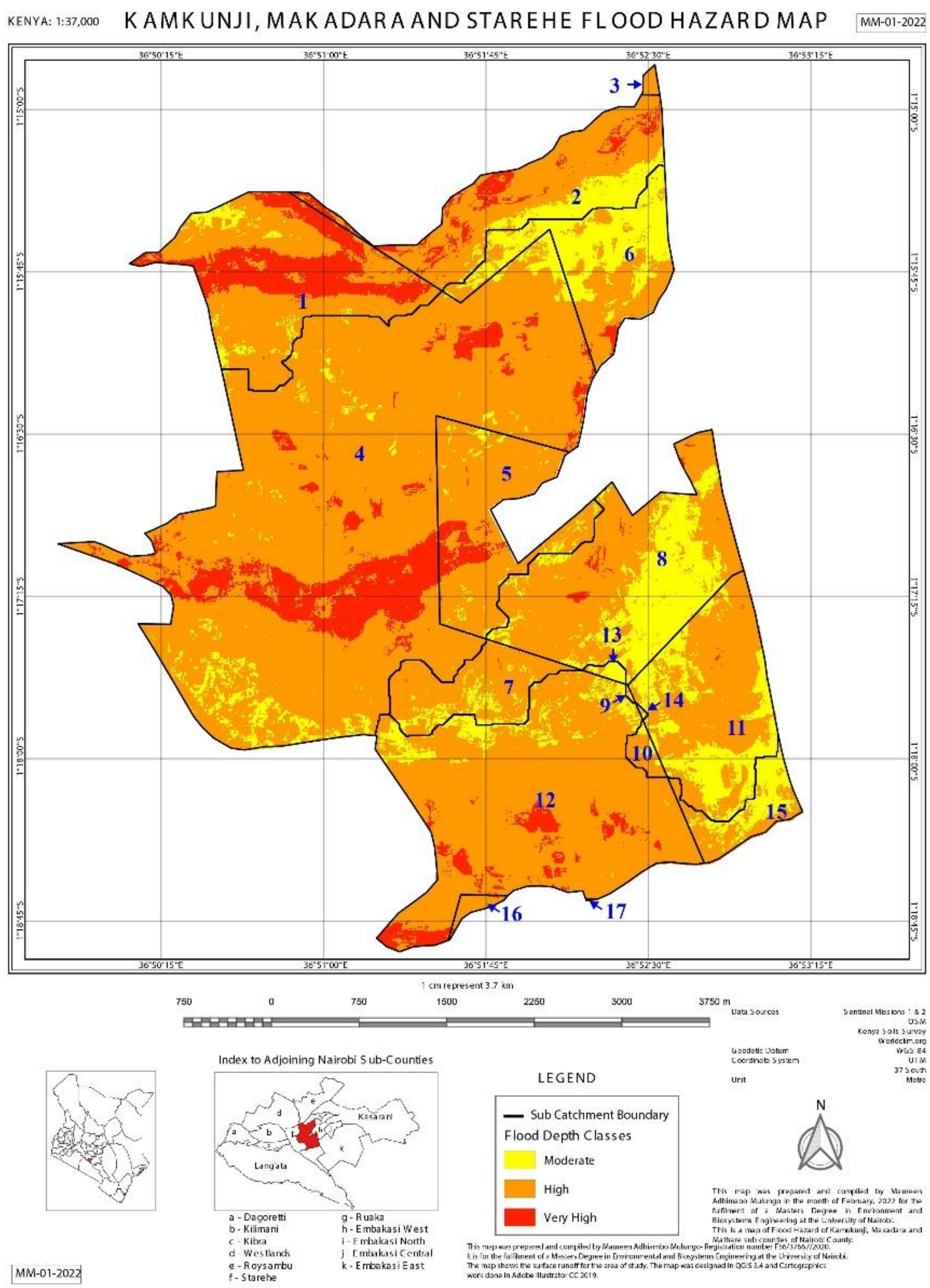

Figure 4.15: Flood Hazard map

4.1.2. Modeling of Flood risk depth map

Table 4.2 shows runoff computations and table 4.4 shows peak discharge computations for the sub catchments in the study area. The results show a number of sub catchments with high peak discharge and high runoff depth indicating the area is prone to flooding. The runoff and peak discharge values generated from SCS TR-55 model represents the hydrological response of the catchment. Runoff depth risk map generated and illustrated in Figure 4.16 shows the areas of the study that are vulnerable to floods and also the level of flooding based on the calculations in table 4.2. This was done using rainfall intensity of the month of June 2021.

Table 4.2: Runoff computations

Catchment	Sub Catchment	Total Area (m^2)	Ultimate Curve Number	CN	Conditional CN	Runoff
A	A_1	2,014,425	83.387	83	68	136
	A_2	1,458,525	86.042	86	72	146
	A_3	24,825	81.541	82	66	130
B	B_1	8,901,300	84.240	84	68	136
	B_2	1,187,525	83.786	84	68	136
	B_3	1,352,950	84.107	84	68	136
C	C_1	719,675	85.149	85	68	136
	C_2	2,313,025	85.351	85	68	136
	C_3	5,550	85.000	85	68	136
	C_4	90,275	91.731	92	81	172
	C_5	1,661,400	87.122	87	75	155
D	D_1	3,670,150	92.170	92	81	172
	D_2	41,200	87.545	88	75	136
	D_3	5,800	84.392	84	68	136
	D_4	399,725	89.604	90	78	146
	D_5	53,350	95.000	95	89	163
	D_6	675	95.000	95	89	195

Table 4.3: Flow Length Computation

Sub Catchment	Area (mi^2)	Runoff, Q (m)	Flow Length, L (ft)	Flow Length, L (m)
A_1	0.777769493	0.136	6214.062	20387.34252
A_2	0.563136503	0.146	5200.431	17061.7815
A_3	0.009584933	0.13	7434	24389.76378
B_1	3.43679193	0.136	6615.3846	21704.01772
B_2	0.458503403	0.136	5209	17089.89501
B_3	0.522373995	0.136	5565.969	18261.05315
C_1	0.277866518	0.136	5909.077	19386.73556
C_2	0.893058953	0.136	5560	18241.46982
C_3	0.002142855	0.136	6557.169	21513.02165
C_4	0.034855178	0.172	5191.015	17030.88911
C_5	0.64146654	0.155	5197.292	17051.48294
D_1	1.417044915	0.172	5184.738	17010.29528
D_2	0.01590732	0.136	5206.708	17082.37533
D_3	0.00223938	0.136	5230.769	17161.31562
D_4	0.154333823	0.146	5218.215	17120.12795
D_5	0.020598435	0.163	5194.154	17041.18766
D_6	0.000260618	0.195	4956	16259.84252

Travel Time Computation

Sub Catchment	**Slope (%)**	**Velocity (m/s)**	**Travel time(paved), Tt (hours)**	**Velocity (m/s)**	**Travel time(unpaved), Tt (hours)**
A_1	12.6964	72.62872207	0.077973982	57.64546268	0.098241049
A_2	9.7152	63.53221212	0.074598123	50.42555697	0.093987732
A_3	5.6751	48.55733731	0.139524421	38.53998935	0.175789732
B_1	11.8889	70.28116333	0.085782499	55.78220381	0.108079161
B_2	10.1042	64.7916547	0.073268588	51.42517734	0.092312624
B_3	9.4584	62.68692153	0.08091823	49.75464929	0.101950568
C_1	5.707	48.69361759	0.110593638	38.6481551	0.139339234
C_2	4.2524	42.03249396	0.120551375	33.36121706	0.151885195
C_3	1.2342	22.64440301	0.263899178	17.972877	0.332492085
C_4	3.7946	70.28116333	0.067312525	31.51431214	0.150116002
C_5	6.2795	64.7916547	0.073103906	40.54033783	0.116834819
D_1	8	62.68692153	0.075375882	45.75829402	0.103261761
D_2	2.715	48.69361759	0.097448177	26.65690646	0.178006561
D_3	2.255	42.03249396	0.113413021	24.29394837	0.196223028
D_4	5.7291	22.64440301	0.210011767	38.72291407	0.122810775
D_5	2.5295	39.70553989	0.119219214	25.7301414	0.183973464
D_6	2.3253	51.07761813	0.088426655	24.66972605	0.183083627

Table 4.4: Peak Discharge Computation

Sub Catchment	Time of Concentration, tc (hours)	Unit Peak Discharge (csm/in)	Unit Peak Discharge (csm/m)	Peak Discharge, qp
A_1	0.176215031	740	18.79603759	1.988181908
A_2	0.168585855	650	16.51003302	1.357420729
A_3	0.315314153	575	14.60502921	0.018198468
B_1	0.19386166	725	18.41503683	8.607256396
B_2	0.165581212	750	19.0500381	1.187892991
B_3	0.182868799	735	18.66903734	1.326301868
C_1	0.249932872	640	16.25603251	0.614312971
C_2	0.27243657	610	15.49403099	1.881843299
C_3	0.596391263	400	10.16002032	0.002960917
C_4	0.217428526	350	8.89001778	0.053296461
C_5	0.189938725	590	14.98602997	1.490020703
D_1	0.178637643	375	9.52501905	2.321549327
D_2	0.275454738	650	16.51003302	0.035717731
D_3	0.309636049	580	14.73202946	0.004486723
D_4	0.332822543	450	11.43002286	0.257549711
D_5	0.303192677	300	7.62001524	0.025584543
D_6	0.271510282	725	18.41503683	0.00093586

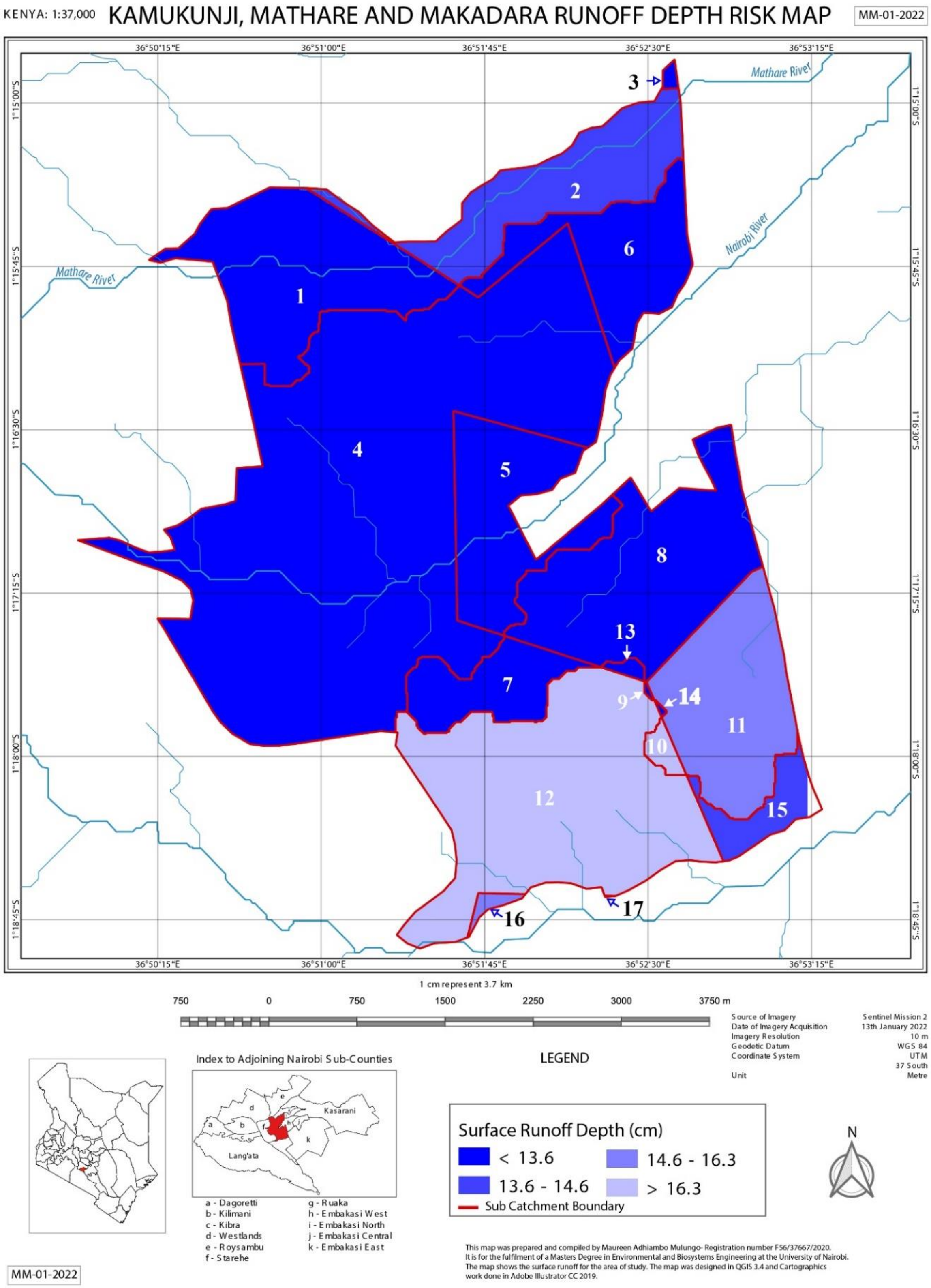

Figure 4.16: Flood Depth Risk Map

4.2. Discussion

The results show that approximately 100% of the area of study can be subjected to flooding caused by rainfall. The threshold for floods is a depth that is >9cm and the flood depth in the study area ranged from 13-19.5cm showing that the area is vulnerable to flooding. Around 60% of the flooded area had <13.6cm depth, 10 % of flooded area had a depth of 13.6-14.6 cm, 10% with a depth of 14.7-16.3 cm and the remaining 20% flooded to a depth of 16.4-19.5 cm.

The areas of high risk of floods with flood depth of above 16.3 cm and were located in the Southern part of the study area, Makadara Sub- County. This area had a high proportion of permanent resident, industrial and commercial land use.

For SCS method of flood prediction, CN values are obtained from LULC features and they vary with the type of LULC. This therefore means that LULC plays an important role in determining and affecting the runoff volume for the sub catchments. The results show that the sub catchments with high CN values have high runoff values therefore serious flooding risk in those areas. These results support the findings of Daword et.al (2011) and Dang and Kumar (2017), who concluded that the higher the CN value the higher the runoff hence flood hazard.

From the LULC created, a number of impervious areas were noted i.e. Tarmac, concrete, residential, industrial and commercial etc. as shown in figure 4.11. The results imply that increase in impervious areas increases the volume of runoff thereby increasing the risk of floods. These results support the findings of Dang and Kumar (2017), Gholami et.al (2010), Brilly et.al (2006), Camorani et.al (2005) and Shuster et.al (2005). The researchers concluded that the growth of impervious areas due urbanization affects the hydrological cycle which causes increased volume of runoff thereby increasing flood risks. According the flood map shown in figure 4.16, highly developed areas which were characterized by high proportion of residential, industrial and commercial land uses, were graced with high risk of flooding. This is because the areas are impervious and thus accelerate the risk of floods in the area.

Some areas with few impervious areas were flooded e.g. areas in sub catchment 1 (A1) and 5 (B2). This was because the areas had water bodies e.g. rivers and also had high elevation which contributed to the flood phenomena in those areas.

High values of both runoff and peak discharge in urban areas normally lead to increase in the magnitude and occurrence of flooding. Dawod et.al (2011) concluded that one of the main factors affecting flood risk is the flow length. The results show that a decrease in peak discharge leads to an increase in the flow length therefore reduction in flood risk. This explains why some sub catchments with a lot of impervious areas were not heavily flooded e.g. sub catchment 3 (A3), 4 (B1), 7 (C1), 8 (C2), 9 (C3), 13(D2) and 15 (D4). Long et.al 2007 explains that the drainage area and the drainage capacities of the existing rivers are decreased due to rapid urbanization leading to decrease in the flow length of the urban areas therefore increasing flood risks.

Different from the other researches in the study area, this research points out the leading underlying factors of floods which increase flood risks. They included; reduced flow length and increased number of impervious areas. These factors are due to the rapid growth of urbanization in the area.

To improve on the accuracy of the results, SAR, from sentinel mission 1, was used to create the 10m scale of DEM. The use of 10m resolution DEM enabled successful delineation of the sub catchments and was reliable for extracting information supporting the hydrological models for flood risk analysis. This was simple and straightforward due to the use of ArcGIS analyst tools. SAR data provides the opportunity to create high quality DEM with improved vertical accuracy.

In this research, the reliability of the data collected and the use of 10m resolution DEM enabled high accurate results.

The findings corresponded to the documentations and the observed records verifying the accuracy of the method developed in the study. Almost 100% of the areas are susceptible to floods due to increased number of residential, industrial and commercial land use as confirmed by Kinyua (2018).

The results of the study were validated using the results from the MCE analysis as shown in chapter 3 and table A5 in the appendix.

There are no maps previously done to show the state of flooding in the area.

CHAPTER 5

5.0. CONCLUSION AND RECOMMENDATION

5.1. Conclusion

The study used effective techniques for predicting flood hazard in the study area. The RS techniques used were effective in supporting the GIS based hydrological models. Flooded areas and levels of floods caused by rainfall were projected based on the current infrastructure which is frequently updated from the RS data since the data used was of the year 2021. These techniques helped in updating important variables like LULC, extracted from the sentinel imagery, for flood risk analysis especially the impervious areas. Climatic data such as rainfall were as well updated. This was not considered in the other studies hence the research contributed to solving the issue of shortage of up-to-date information on infrastructure and climatic conditions for use in flood forecasting so as to enable flood phenomena to be predicted more accurately.

The maps of flood zone areas and flood depth caused by rainfall provide information on the areas in the three sub counties that are subject to flooding so that the County Government of Nairobi can work on preventing and reducing the floods in the area. Their primary objective should be to manage floods by using effective and efficient methods such as storm water drainages. The Flood hazard and flood depth risk maps produced information that can be used for identifying locations that are at high risk of flooding in order to prevent loss of life, minimize damage to property and support planning.

Growing urbanization increases the number of impervious surfaces in the study area, as shown in the LULC map in figure 4.11. This factor contributes to an increase in flood risk hence there is need to come up with projects that aim at managing the urbanization processes that involves utilization of appropriate infrastructure to minimize the risk of flooding.

Increased flow length of the catchment reduces runoff volume thereby reducing flood risk. There is need to improve the infiltration capacity and reduce water overflow in the urban landscape with optimized drainage system to reduce the risk of floods in the urban area.

The methods used in this study are precise and the outputs are in digital form. LULC, rainfall and topographical values have the ability to be reused across the world.

Despite getting accurate results from the hydrological model, calibration and validation of the models also need to be done. This will entail adjusting SCS TR-55 model's parameters and input data to match observed or measured data from the study area.

5.2. Recommendations

SCS TR 55 models needs to be calibrated and validated for use in all the parts of the world. This is because the model is based on equations and variables developed using data from US and some of the parameters of soil and LULC may not be transferable to Kenya and other parts of the world and that is why we employed other models and software to support it. There is still the need for further research on the hydrological models used especially on calibration for their application in flood risk analysis.

Bankful discharge is also an important factor to be considered in the study of floods but this factor was not considered in this study due to lack of the data in Kenya. Also, we did not believe it will make a significant difference since there are a few rivers and canals therefore it would impact negligibly on the results. This should however be taken into considerations in future with further developments since the hydrological model considers this parameter of flooding.

The County Government of Kenya should implement the use of flood control structures and also limit the use of impermeable surfaces like concrete and pavement in developed areas and practice the use of green infrastructure that reduces runoff during flood events.

This research significantly contributed to flood risk management by identifying specific flood prone areas and flood depths, which were not undertaken in the previous studies done in the study area. The findings of this research came in handy, thus, need to be considered for informed decision making and planning in flood risk prevention and management.

6.0. REFERENCES

Anees, M. T., Abdullah, K., Nawawi, M. N. M., Ab Rahman, N. N. N., Piah, A. R. M., Zakaria, N. A., & Omar, A. M. (2016). Numerical modeling techniques for flood analysis. Journal of African Earth Sciences, 124, 478-486. z.

Bayazıt, Y., Koç, C., & Bakış, R. (2021). Urbanization impacts on flash urban floods in Bodrum Province, Turkey. Hydrological Sciences Journal, 66(1), 118-133.

Brilly M, Rusjan S, Vidmar A. (2006). Monitoring the impact of urbanization on the Glinscica stream. Phys Chem Earth Parts A/B/C. 31:1089–1096.

Burges, S. J. (1986). Trends and directions in hydrology. Water Resources Research, 22(9S), 1S-5S.

Camorani G, Castellarin A, Brath A. (2005). Effects of land-use changes on the hydrologic response of reclamation systems. Phys Chem Earth Parts A/B/C. 30:561–574.

Cheseto, M. N. (2013). Challenges in planning for electricity infrastructure in informal settlements: Case of Kosovo village, Mathare valley–Nairobi (Doctoral dissertation, University of Nairobi).

Craig, J. R., Brown, G., Chlumsky, R., Jenkinson, R. W., Jost, G., Lee, K., ... & Tolson, B. A. (2020). Flexible watershed simulation with the Raven hydrological modelling framework. Environmental Modelling & Software, 129, 104728.

Dang, A. N. T & Kumar, L (2017) Application of remote sensing and GIS-based hydrological modelling for flood risk analysis: a case study of District 8, Ho Chi Minh city, Vietnam, Geomatics, Natural Hazards and Risk, 8:2, 1792-1811, DOI: 10.1080/19475705.2017.1388853.

Dawod GM, Mirza MN, Al-Ghamdi KA. (2011). GIS-based spatial mapping of flash flood hazard in Makkah City, Saudi Arabia. JGIS. 03:225–230.

Fan, F., Deng, Y., Hu, X., & Weng, Q. (2013). Estimating composite curve number using an improved SCS-CN method with remotely sensed variables in Guangzhou, China. Remote Sensing, 5(3), 1425-1438.

Fleming M, Doan J. (2009). HEC-GeoHMS geospatial hydrologic modelling extension: user's manual version 4.2. California: US Army Corps of Engineers, Institute for Water Resources, Hydrologic Engineering Centre.

Gajbhiye S, Mishra S. (2012). Application of NRSC-SCS curve number model in runoff estimation using RS & GIS. Proceedings of the 2012 International Conference on Advances in Engineering, Science and Management; Mar 30–31; Tamil Nadu, India. IEEE.

Gallegos HA, Schubert JE, Sanders BF. (2009). Two-dimensional, high-resolution modeling of urban dam-break flooding: a case study of Baldwin Hills, California. Adv Water Resource. 32:1323–1335.

Gholami V, Mohseni Saravi M, Ahmadi H. (2010). Effects of impervious surfaces and urban development on runoff generation and flood hazard in the Hajighoshan watershed. Caspian J Environ Sci. 8:1–12.

Ho LP. (2008). Impacts of climate changes and urbanization on urban inundation in Ho Chi Minh City. Proceedings of the 11th International Conference on Urban Drainage; 31 Aug–5 Sep; Scotland (UK). IAHR/IWA.

Jones, P. Formalizing the informal, (2017): Understanding the position of informal settlements and slums in sustainable urbanization policies and strategies in Bandung, Indonesia. Sustainability 2017, 9, 1436. [CrossRef].

Kenya: Floods –ReliefWeb. (April 2012). https://reliefweb.int/disaster/ff-2012-000062-ken.

Kenya National Bureau of Statistics – Economic Survey 2019 (2019, May 2). The Elephant. https://www.theelephant.info/documents/kenya-national-bureau-of-statistics-economic-survey-2019/.

Kenya National Bureau of Statistics, (2019). Kenya Population and Housing Census; Kenya National Bureau of Statistics: Nairobi, Kenya, 2019; Volume I, report.

Kim NW, Lee JW, Lee J, Lee JE. (2010). SWAT application to estimate design runoff curve number for South Korean conditions. Hydrol Process. 24:2156–2170.

Kinyua, G. J. (2018). Flood risk analyses using the risk curves in Mathare valley Nairobi Kenya.

Kinyua, G. J., & Fujimi, T. (2018). Risk Analysis of Flood Physical Vulnerability in Residential areas of Mathare Nairobi Kenya.

K. Smith and R. Ward, (1998) floods physical processes and human impacts on chi Chester, Volume 24, issue 13.

Lempert R, Kalra N, Peyraud S, Mao Z, Tan SB, Cira D, Lotsch A. (2013). Ensuring robust flood risk management in Ho Chi Minh city. World Bank Policy Res Working Paper. 6465:1–63.

Limited, A. (2022). Mathare River, Mathare, Nairobi, Kenya. The Mathare River which is one of tributaries of the Nairobi River basin is extremely polluted with human, Ani Stock Photo. Alamy.https://www.alamy.com/mathare-river-mathare-nairobi-kenya-the-mathare-river-which-is-one-of-tributaries-of-the-nairobi-river-basin-is-extremely-polluted-with-human-ani-image349242074.html.

Long PH. (2007). Climate change and urban flooding in Ho Chi Minh City. Proceedings of 3rd International Conference on Climate and Water; Sep 3–6; Helsinki (Finland).

Mbaria, J. (2006). Linking research to extension for watershed management: The Nyando experience, Nairobi: World Agroforestry Centre (ICRAF). 62 p. [also available at http://worldagroforestrycentre. org/water/downloads/publications/Nyandobook.pdf].

Merwade V, Cook A, Coonrod J. (2008). GIS techniques for creating river terrain models for hydrodynamic modelling and flood inundation mapping. Environ Modelling Softw. 23:1300–1311.

Mwaniki, D. M. (2012). Mapping pollution in the Mathare River: An analysis of waste disposal patterns and river pollution in an informal settlement (Doctoral dissertation, University of Nairobi, Kenya).

Nelson, S. Tulane Univ:http://www.tulane.edu/sanelson/Natural_Disasters/riverflooding.htm. (Updated on 13 July 2012).

Nicandrou A. (2011). Hydrological assessment and modelling of the River Fani Catchment, Albania [dissertation]. London (UK): University of Glamorgan.

Nicandrou A, Mofor LA, Delpak R, Robinson RB. (2004). Hydrological assessment and modeling of the River Fani catchment in Albania using GIS and remote sensing. Remote Sens Agric Ecosyst Hydrol V. 5232:340–350.

Ongor, D. (2007). Integrating water resource management and flood management: A community participatory approach. A case study of the Nyando river watershed in Kenya. Catchment and Lake Research, 6:50-55.

Piers Blaikie and others, (1994). Risk of Natural hazards, people's vulnerability and disasters first edition.

Programme, U. N. E., & Columbia University, S. C. for C. C. L. (2017, May 1). The status of Climate Change Litigation: A Global Review. UN Environment Document Repository Home. https://wedocs.unep.org/handle/20.500.11822/20767.

Ramana GV. (2014). Rainfall runoff modeling between TR-55 hydrologic watershed model and overland time of concentration model. Int J. 3:220–241.

Rai, H. (1974). 'Limnological studies on the river yamuna at Delhi, India. part I relation between the chemistry and the state of pollution in the river yamuna', Archiv für Hydrobiologie, 73(3), pp. 369–393. doi:10.1127/archiv-hydrobiol/73/1974/369.

Ramiaramanana, F. N., & Teller, J. (2021). Urbanization and Floods in Sub-Saharan Africa: Spatiotemporal Study and Analysis of Vulnerability Factors—Case of Antananarivo Agglomeration (Madagascar). Water, 13(2), 149.

Rafiq, F., Ahmed, S., Ahmad, S., & Khan, A. A. (2016). Urban floods in India. International Journal of Scientific & Engineering Research, 7(1), 721-734.

Reliefweb, (2013): http://reliefweb.int/disaster/fl-2013-000038-ken. (Accessed on 6th December 2016).

Samarasinghea S, Nandalalb H, Weliwitiyac D, Fowzed J, Hazarikad M, Samarakoond L. (2010). Application of remote sensing and GIS for flood risk analysis: a case study at Kalu-Ganga River, Sri Lanka. Int Arch Photogramm RemoteSens Spatial Inform Sci. 38:110–115.

Sarker MZ, Sivertun A. (2011). GIS and RS combined analysis for flood prediction mapping – a case study of Dhaka City Corporation, Bangladesh. J Electro Control Eng. 1:250–257.

Seeni M. I, Mansor MA. (2000). Application of remote sensing and hydrological modelling in flood prediction studies. Malaysian J Remote Sens GIS. 1:91–98.

Shadeed S, Almasri M. (2010). Application of GIS-based SCS-CN method in West Bank catchments, Palestine. Water Sci Eng. 3:1–13.

Shuster W, Bonta J, Thurston H, Warnemuende E, Smith D. (2005). Impacts of impervious surface on watershed hydrology: a review. Urban Water J. 2:263–275.

Smith, H. M., Wall, G., & Blackstock, K. L. (2013). The role of map-based environmental information in supporting integration between river basin planning and spatial planning. Environmental Science & Policy, 30, 81–89.

Sivertun A, Prange L. (2003). Non-point source critical area analysis in the Gisseleo watershed using GIS. EnvironModelling Softw. 18:887–898.

Soulis K, Valiantzas J. (2011). SCS-CN parameter determination using rainfall-runoff data in heterogeneous watersheds– the two-CN system approach. Hydrol Earth Syst Sci Discuss. 8:8963–9004.

UN Habitat, (2018). The challenge of slums: Global report on human settlements. Manag. Environ. Qual. 2004, 15, 337–338.

UN Habitat, (2003). The challenge of slums: Global report on human settlements. Manag. Environ. Qual. 2004, 15, 337–338.

United Nations. Sustainable development goals report (2020). United Nations. https://www.un.org/en/desa/sustainable-development-goals-report-2020.

Vitvar, t., Gurtz, j., & Lang, h. (1999). Application of GIS-based distributed hydrological modelling for estimation of water residence times. In Integrated Methods in Catchment Hydrology: Tracer, Remote Sensing and New Hydrometric Techniques: Proceedings of an International Symposium Held During IUGG 99, the XXII General Assembly of the International Union of Geodesy and Geophysics, at Birmingham, UK 18-30 July 1999 (Vol. 22, p. 241).

Wangara, A. A. (2017). Disaster response coordination among disaster management organizations in modern cities: The case of Nairobi County, Kenya. Prehospital and Disaster Medicine, 32(S1). https://doi.org/10.1017/s1049023x17000747.

Wikimedia Foundation. (2022, June 21). Kamukunji constituency. Wikipedia. https://en.wikipedia.org/wiki/Kamukunji_Constituency.

World Health Organization, (2013); Guidelines for Drinking Water Quality, Vol.1, Recommendations, 4th ed.; World Health Organization: Geneva, Switzerland.

World Health Organization, (2013); Health topic/ Floods Article. https://www.who.int/health-topics/floods.

Xu, Z., Xu, J., Yin, H., Jin, W., Li, H., & He, Z. (2019). Urban river pollution control in developing countries. Nature Sustainability, 2(3), 158-160.

7.0. APPENDICES

7.1. Sub Catchment calculations

Table A1: Calculations for Catchment A.

Sub Catchment A_1							
Day	**P**	**AMC**	**$P_{AMC\ I}$**	**$CN_{AMC\ I}$**	**S**	**Ia**	**Runoff (Q)**
27	2		0	68	4.705882353	0.235294118	
28	1.8		0	68	4.705882353	0.235294118	
29	1.2		0	68	4.705882353	0.235294118	
30	1.3		0	68	4.705882353	0.235294118	
31	0.7		0	68	4.705882353	0.235294118	
1	1.3	I	8.3	68	4.705882353	0.235294118	5.092911914
2	1.3	I	7.6	68	4.705882353	0.235294118	4.493475519
3	2.2	I	8	68	4.705882353	0.235294118	4.834628191
4	2.8	I	9.6	68	4.705882353	0.235294118	6.232697226
5	0.9	I	9.2	68	4.705882353	0.235294118	5.878748608
6	1.1	I	9.6	68	4.705882353	0.235294118	6.232697226
7	1.1	I	9.4	68	4.705882353	0.235294118	6.05539091
8	0.8	I	8.9	68	4.705882353	0.235294118	5.615095365
9	0.7	I	7.4	68	4.705882353	0.235294118	4.324386405
10	0.6	I	5.2	68	4.705882353	0.235294118	2.548790611
11	1	I	5.3	68	4.705882353	0.235294118	2.62535326

12	1.2	I	5.4	68	4.705882353	0.235294118	2.702390801
13	1.8	I	6.1	68	4.705882353	0.235294118	3.253818456
14	1.6	I	6.9	68	4.705882353	0.235294118	3.906420985
15	2.4	I	8.6	68	4.705882353	0.235294118	5.353110605
16	1.7	I	9.7	68	4.705882353	0.235294118	6.321590604
17	1.1	I	9.8	68	4.705882353	0.235294118	6.410639639
18	1.7	I	10.3	68	4.705882353	0.235294118	6.858109026
19	1.1	I	9.6	68	4.705882353	0.235294118	6.232697226
20	1.6	I	9.6	68	4.705882353	0.235294118	6.232697226
21	0.7	I	7.9	68	4.705882353	0.235294118	4.748983245
22	0.6	I	6.8	68	4.705882353	0.235294118	3.823701339
23	1	I	6.7	68	4.705882353	0.235294118	3.741291082
24	0.8	I	5.8	68	4.705882353	0.235294118	3.015012465
25	1.1	I	5.8	68	4.705882353	0.235294118	3.015012465
26	0.9	I	5.1	68	4.705882353	0.235294118	2.472717741
27	0.6	I	5	68	4.705882353	0.235294118	2.397150164
28	0.8	I	5.2	68	4.705882353	0.235294118	2.548790611
29	1.6	I	5.8	68	4.705882353	0.235294118	3.015012465
30	1	I	6	68	4.705882353	0.235294118	3.173826834
31	0.7	I	5.6	68	4.705882353	0.235294118	2.857833975
Sum of Runoff							**136.0149822**

Sub Catchment A_2 Area = CN =							
Day	**P**	**AMC**	**$P_{AMC\ I}$**	**CN (AMC I)**	**S**	**Ia**	**Q**
27	2		0	72	3.888888889	0.194444444	
28	1.8		0	72	3.888888889	0.194444444	
29	1.2		0	72	3.888888889	0.194444444	
30	1.3		0	72	3.888888889	0.194444444	
31	0.7		0	72	3.888888889	0.194444444	
1	1.3	I	8.3	72	3.888888889	0.194444444	5.477538469
2	1.3	I	7.6	72	3.888888889	0.194444444	4.855683992
3	2.2	I	8	72	3.888888889	0.194444444	5.209883874
4	2.8	I	9.6	72	3.888888889	0.194444444	6.654243859
5	0.9	I	9.2	72	3.888888889	0.194444444	6.289532768
6	1.1	I	9.6	72	3.888888889	0.194444444	6.654243859
7	1.1	I	9.4	72	3.888888889	0.194444444	6.471618819
8	0.8	I	8.9	72	3.888888889	0.194444444	6.01747047
9	0.7	I	7.4	72	3.888888889	0.194444444	4.679822512
10	0.6	I	5.2	72	3.888888889	0.194444444	2.816992852
11	1	I	5.3	72	3.888888889	0.194444444	2.898088669
12	1.2	I	5.4	72	3.888888889	0.194444444	2.979600217

13	1.8	I	6.1	72	3.888888889	0.194444444	3.560751875
14	1.6	I	6.9	72	3.888888889	0.194444444	4.244156033
15	2.4	I	8.6	72	3.888888889	0.194444444	5.746771602
16	1.7	I	9.7	72	3.888888889	0.194444444	6.745750956
17	1.1	I	9.8	72	3.888888889	0.194444444	6.837383926
18	1.7	I	10.3	72	3.888888889	0.194444444	7.29734242
19	1.1	I	9.6	72	3.888888889	0.194444444	6.654243859
20	1.6	I	9.6	72	3.888888889	0.194444444	6.654243859
21	0.7	I	7.9	72	3.888888889	0.194444444	5.12103764
22	0.6	I	6.8	72	3.888888889	0.194444444	4.157758367
23	1	I	6.7	72	3.888888889	0.194444444	4.071622424
24	0.8	I	5.8	72	3.888888889	0.194444444	3.309540992
25	1.1	I	5.8	72	3.888888889	0.194444444	3.309540992
26	0.9	I	5.1	72	3.888888889	0.194444444	2.736326946
27	0.6	I	5	72	3.888888889	0.194444444	2.656105786
28	0.8	I	5.2	72	3.888888889	0.194444444	2.816992852
29	1.6	I	5.8	72	3.888888889	0.194444444	3.309540992
30	1	I	6	72	3.888888889	0.194444444	3.476679401
31	0.7	I	5.6	72	3.888888889	0.194444444	3.143816829
Sum of Runoff							**146.8543281**

Sub Catchment A_3

Area =

CN =

Day	P	AMC	P(AMC)	CN (AMC I)	S	Ia	Q
27	2		0	66	5.151515152	0.257575758	
28	1.8		0	66	5.151515152	0.257575758	
29	1.2		0	66	5.151515152	0.257575758	
30	1.3		0	66	5.151515152	0.257575758	
31	0.7		0	66	5.151515152	0.257575758	
1	1.3	I	8.3	66	5.151515152	0.257575758	4.902295347
2	1.3	I	7.6	66	5.151515152	0.257575758	4.314987616
3	2.2	I	8	66	5.151515152	0.257575758	4.649093758
4	2.8	I	9.6	66	5.151515152	0.257575758	6.02188876
5	0.9	I	9.2	66	5.151515152	0.257575758	5.673853782
6	1.1	I	9.6	66	5.151515152	0.257575758	6.02188876
7	1.1	I	9.4	66	5.151515152	0.257575758	5.847507725
8	0.8	I	8.9	66	5.151515152	0.257575758	5.414805347
9	0.7	I	7.4	66	5.151515152	0.257575758	4.149542504
10	0.6	I	5.2	66	5.151515152	0.257575758	2.420022197
11	1	I	5.3	66	5.151515152	0.257575758	2.494231254
12	1.2	I	5.4	66	5.151515152	0.257575758	2.568941401
13	1.8	I	6.1	66	5.151515152	0.257575758	3.10479436

14	1.6	I	6.9	66	5.151515152	0.257575758	3.741057025
15	2.4	I	8.6	66	5.151515152	0.257575758	5.157577799
16	1.7	I	9.7	66	5.151515152	0.257575758	6.109342595
17	1.1	I	9.8	66	5.151515152	0.257575758	6.196967197
18	1.7	I	10.3	66	5.151515152	0.257575758	6.637533694
19	1.1	I	9.6	66	5.151515152	0.257575758	6.02188876
20	1.6	I	9.6	66	5.151515152	0.257575758	6.02188876
21	0.7	I	7.9	66	5.151515152	0.257575758	4.565180943
22	0.6	I	6.8	66	5.151515152	0.257575758	3.660299025
23	1	I	6.7	66	5.151515152	0.257575758	3.579872959
24	0.8	I	5.8	66	5.151515152	0.257575758	2.872511743
25	1.1	I	5.8	66	5.151515152	0.257575758	2.872511743
26	0.9	I	5.1	66	5.151515152	0.257575758	2.346329272
27	0.6	I	5	66	5.151515152	0.257575758	2.273168128
28	0.8	I	5.2	66	5.151515152	0.257575758	2.420022197
29	1.6	I	5.8	66	5.151515152	0.257575758	2.872511743
30	1	I	6	66	5.151515152	0.257575758	3.026952417
31	0.7	I	5.6	66	5.151515152	0.257575758	2.719807664
Sum of Runoff							**130.6792765**

Table A2: Calculations for Catchment B

Sub Catchment B_1

Day	P	AMC	P(AMC)	CN (AMC I)	S	Ia	Runoff (Q)
27	2		0	68	4.705882353	0.235294118	
28	1.8		0	68	4.705882353	0.235294118	
29	1.2		0	68	4.705882353	0.235294118	
30	1.3		0	68	4.705882353	0.235294118	
31	0.7		0	68	4.705882353	0.235294118	
1	1.3	I	8.3	68	4.705882353	0.235294118	5.092911914
2	1.3	I	7.6	68	4.705882353	0.235294118	4.493475519
3	2.2	I	8	68	4.705882353	0.235294118	4.834628191
4	2.8	I	9.6	68	4.705882353	0.235294118	6.232697226
5	0.9	I	9.2	68	4.705882353	0.235294118	5.878748608
6	1.1	I	9.6	68	4.705882353	0.235294118	6.232697226
7	1.1	I	9.4	68	4.705882353	0.235294118	6.05539091
8	0.8	I	8.9	68	4.705882353	0.235294118	5.615095365
9	0.7	I	7.4	68	4.705882353	0.235294118	4.324386405
10	0.6	I	5.2	68	4.705882353	0.235294118	2.548790611
11	1	I	5.3	68	4.705882353	0.235294118	2.62535326
12	1.2	I	5.4	68	4.705882353	0.235294118	2.702390801
13	1.8	I	6.1	68	4.705882353	0.235294118	3.253818456

14	1.6	I	6.9	68	4.705882353	0.235294118	3.906420985
15	2.4	I	8.6	68	4.705882353	0.235294118	5.353110605
16	1.7	I	9.7	68	4.705882353	0.235294118	6.321590604
17	1.1	I	9.8	68	4.705882353	0.235294118	6.410639639
18	1.7	I	10.3	68	4.705882353	0.235294118	6.858109026
19	1.1	I	9.6	68	4.705882353	0.235294118	6.232697226
20	1.6	I	9.6	68	4.705882353	0.235294118	6.232697226
21	0.7	I	7.9	68	4.705882353	0.235294118	4.748983245
22	0.6	I	6.8	68	4.705882353	0.235294118	3.823701339
23	1	I	6.7	68	4.705882353	0.235294118	3.741291082
24	0.8	I	5.8	68	4.705882353	0.235294118	3.015012465
25	1.1	I	5.8	68	4.705882353	0.235294118	3.015012465
26	0.9	I	5.1	68	4.705882353	0.235294118	2.472717741
27	0.6	I	5	68	4.705882353	0.235294118	2.397150164
28	0.8	I	5.2	68	4.705882353	0.235294118	2.548790611
29	1.6	I	5.8	68	4.705882353	0.235294118	3.015012465
30	1	I	6	68	4.705882353	0.235294118	3.173826834
31	0.7	I	5.6	68	4.705882353	0.235294118	2.857833975
Sum of Runoff							**136.0149822**

Sub Catchment B_2

Area =

CN =							
Day	**P**	**AMC**	**P(AMC)**	**CN (AMC I)**	**S**	**Ia**	**Q**
27	2		0	68	4.705882353	0.235294118	
28	1.8		0	68	4.705882353	0.235294118	
29	1.2		0	68	4.705882353	0.235294118	
30	1.3		0	68	4.705882353	0.235294118	
31	0.7		0	68	4.705882353	0.235294118	
1	1.3	I	8.3	68	4.705882353	0.235294118	5.092911914
2	1.3	I	7.6	68	4.705882353	0.235294118	4.493475519
3	2.2	I	8	68	4.705882353	0.235294118	4.834628191
4	2.8	I	9.6	68	4.705882353	0.235294118	6.232697226
5	0.9	I	9.2	68	4.705882353	0.235294118	5.878748608
6	1.1	I	9.6	68	4.705882353	0.235294118	6.232697226
7	1.1	I	9.4	68	4.705882353	0.235294118	6.05539091
8	0.8	I	8.9	68	4.705882353	0.235294118	5.615095365
9	0.7	I	7.4	68	4.705882353	0.235294118	4.324386405
10	0.6	I	5.2	68	4.705882353	0.235294118	2.548790611
11	1	I	5.3	68	4.705882353	0.235294118	2.62535326
12	1.2	I	5.4	68	4.705882353	0.235294118	2.702390801
13	1.8	I	6.1	68	4.705882353	0.235294118	3.253818456
14	1.6	I	6.9	68	4.705882353	0.235294118	3.906420985

15	2.4	I	8.6	68	4.705882353	0.235294118	5.353110605
16	1.7	I	9.7	68	4.705882353	0.235294118	6.321590604
17	1.1	I	9.8	68	4.705882353	0.235294118	6.410639639
18	1.7	I	10.3	68	4.705882353	0.235294118	6.858109026
19	1.1	I	9.6	68	4.705882353	0.235294118	6.232697226
20	1.6	I	9.6	68	4.705882353	0.235294118	6.232697226
21	0.7	I	7.9	68	4.705882353	0.235294118	4.748983245
22	0.6	I	6.8	68	4.705882353	0.235294118	3.823701339
23	1	I	6.7	68	4.705882353	0.235294118	3.741291082
24	0.8	I	5.8	68	4.705882353	0.235294118	3.015012465
25	1.1	I	5.8	68	4.705882353	0.235294118	3.015012465
26	0.9	I	5.1	68	4.705882353	0.235294118	2.472717741
27	0.6	I	5	68	4.705882353	0.235294118	2.397150164
28	0.8	I	5.2	68	4.705882353	0.235294118	2.548790611
29	1.6	I	5.8	68	4.705882353	0.235294118	3.015012465
30	1	I	6	68	4.705882353	0.235294118	3.173826834
31	0.7	I	5.6	68	4.705882353	0.235294118	2.857833975
Sum of Runoff							**136.0149822**

Sub Catchment B_3

Area =							
CN =							
Day	**P**	**AMC**	**P(AMC)**	**CN (AMC I)**	**S**	**Ia**	**Q**
27	2		0	68	4.705882353	0.235294118	
28	1.8		0	68	4.705882353	0.235294118	
29	1.2		0	68	4.705882353	0.235294118	
30	1.3		0	68	4.705882353	0.235294118	
31	0.7		0	68	4.705882353	0.235294118	
1	1.3	I	8.3	68	4.705882353	0.235294118	5.092911914
2	1.3	I	7.6	68	4.705882353	0.235294118	4.493475519
3	2.2	I	8	68	4.705882353	0.235294118	4.834628191
4	2.8	I	9.6	68	4.705882353	0.235294118	6.232697226
5	0.9	I	9.2	68	4.705882353	0.235294118	5.878748608
6	1.1	I	9.6	68	4.705882353	0.235294118	6.232697226
7	1.1	I	9.4	68	4.705882353	0.235294118	6.05539091
8	0.8	I	8.9	68	4.705882353	0.235294118	5.615095365
9	0.7	I	7.4	68	4.705882353	0.235294118	4.324386405
10	0.6	I	5.2	68	4.705882353	0.235294118	2.548790611
11	1	I	5.3	68	4.705882353	0.235294118	2.62535326
12	1.2	I	5.4	68	4.705882353	0.235294118	2.702390801
13	1.8	I	6.1	68	4.705882353	0.235294118	3.253818456

14	1.6	I	6.9	68	4.705882353	0.235294118	3.906420985
15	2.4	I	8.6	68	4.705882353	0.235294118	5.353110605
16	1.7	I	9.7	68	4.705882353	0.235294118	6.321590604
17	1.1	I	9.8	68	4.705882353	0.235294118	6.410639639
18	1.7	I	10.3	68	4.705882353	0.235294118	6.858109026
19	1.1	I	9.6	68	4.705882353	0.235294118	6.232697226
20	1.6	I	9.6	68	4.705882353	0.235294118	6.232697226
21	0.7	I	7.9	68	4.705882353	0.235294118	4.748983245
22	0.6	I	6.8	68	4.705882353	0.235294118	3.823701339
23	1	I	6.7	68	4.705882353	0.235294118	3.741291082
24	0.8	I	5.8	68	4.705882353	0.235294118	3.015012465
25	1.1	I	5.8	68	4.705882353	0.235294118	3.015012465
26	0.9	I	5.1	68	4.705882353	0.235294118	2.472717741
27	0.6	I	5	68	4.705882353	0.235294118	2.397150164
28	0.8	I	5.2	68	4.705882353	0.235294118	2.548790611
29	1.6	I	5.8	68	4.705882353	0.235294118	3.015012465
30	1	I	6	68	4.705882353	0.235294118	3.173826834
31	0.7	I	5.6	68	4.705882353	0.235294118	2.857833975
Sum of Runoff							**136.0149822**

Table A3: Calculations for Catchment C

Sub Catchment C_1							
Day	**P**	**AMC**	**P(AMC)**	**CN (AMC I)**	**S**	**Ia**	**Runoff (Q)**
27	2		0	68	4.705882353	0.235294118	
28	1.8		0	68	4.705882353	0.235294118	
29	1.2		0	68	4.705882353	0.235294118	
30	1.3		0	68	4.705882353	0.235294118	
31	0.7		0	68	4.705882353	0.235294118	
1	1.3	I	8.3	68	4.705882353	0.235294118	5.092911914
2	1.3	I	7.6	68	4.705882353	0.235294118	4.493475519
3	2.2	I	8	68	4.705882353	0.235294118	4.834628191
4	2.8	I	9.6	68	4.705882353	0.235294118	6.232697226
5	0.9	I	9.2	68	4.705882353	0.235294118	5.878748608
6	1.1	I	9.6	68	4.705882353	0.235294118	6.232697226
7	1.1	I	9.4	68	4.705882353	0.235294118	6.05539091
8	0.8	I	8.9	68	4.705882353	0.235294118	5.615095365
9	0.7	I	7.4	68	4.705882353	0.235294118	4.324386405
10	0.6	I	5.2	68	4.705882353	0.235294118	2.548790611
11	1	I	5.3	68	4.705882353	0.235294118	2.62535326
12	1.2	I	5.4	68	4.705882353	0.235294118	2.702390801
13	1.8	I	6.1	68	4.705882353	0.235294118	3.253818456

14	1.6	I	6.9	68	4.705882353	0.235294118	3.906420985
15	2.4	I	8.6	68	4.705882353	0.235294118	5.353110605
16	1.7	I	9.7	68	4.705882353	0.235294118	6.321590604
17	1.1	I	9.8	68	4.705882353	0.235294118	6.410639639
18	1.7	I	10.3	68	4.705882353	0.235294118	6.858109026
19	1.1	I	9.6	68	4.705882353	0.235294118	6.232697226
20	1.6	I	9.6	68	4.705882353	0.235294118	6.232697226
21	0.7	I	7.9	68	4.705882353	0.235294118	4.748983245
22	0.6	I	6.8	68	4.705882353	0.235294118	3.823701339
23	1	I	6.7	68	4.705882353	0.235294118	3.741291082
24	0.8	I	5.8	68	4.705882353	0.235294118	3.015012465
25	1.1	I	5.8	68	4.705882353	0.235294118	3.015012465
26	0.9	I	5.1	68	4.705882353	0.235294118	2.472717741
27	0.6	I	5	68	4.705882353	0.235294118	2.397150164
28	0.8	I	5.2	68	4.705882353	0.235294118	2.548790611
29	1.6	I	5.8	68	4.705882353	0.235294118	3.015012465
30	1	I	6	68	4.705882353	0.235294118	3.173826834
31	0.7	I	5.6	68	4.705882353	0.235294118	2.857833975
Sum of Runoff							**136.0149822**

Sub Catchment C_2

Area =

CN =

Day	P	AMC	P(AMC)	CN (AMC I)	S	Ia	Q
27	2		0	68	4.705882353	0.235294118	
28	1.8		0	68	4.705882353	0.235294118	
29	1.2		0	68	4.705882353	0.235294118	
30	1.3		0	68	4.705882353	0.235294118	
31	0.7		0	68	4.705882353	0.235294118	
1	1.3	I	8.3	68	4.705882353	0.235294118	5.092911914
2	1.3	I	7.6	68	4.705882353	0.235294118	4.493475519
3	2.2	I	8	68	4.705882353	0.235294118	4.834628191
4	2.8	I	9.6	68	4.705882353	0.235294118	6.232697226
5	0.9	I	9.2	68	4.705882353	0.235294118	5.878748608
6	1.1	I	9.6	68	4.705882353	0.235294118	6.232697226
7	1.1	I	9.4	68	4.705882353	0.235294118	6.05539091
8	0.8	I	8.9	68	4.705882353	0.235294118	5.615095365
9	0.7	I	7.4	68	4.705882353	0.235294118	4.324386405
10	0.6	I	5.2	68	4.705882353	0.235294118	2.548790611
11	1	I	5.3	68	4.705882353	0.235294118	2.62535326
12	1.2	I	5.4	68	4.705882353	0.235294118	2.702390801
13	1.8	I	6.1	68	4.705882353	0.235294118	3.253818456

14	1.6	I	6.9	68	4.705882353	0.235294118	3.906420985
15	2.4	I	8.6	68	4.705882353	0.235294118	5.353110605
16	1.7	I	9.7	68	4.705882353	0.235294118	6.321590604
17	1.1	I	9.8	68	4.705882353	0.235294118	6.410639639
18	1.7	I	10.3	68	4.705882353	0.235294118	6.858109026
19	1.1	I	9.6	68	4.705882353	0.235294118	6.232697226
20	1.6	I	9.6	68	4.705882353	0.235294118	6.232697226
21	0.7	I	7.9	68	4.705882353	0.235294118	4.748983245
22	0.6	I	6.8	68	4.705882353	0.235294118	3.823701339
23	1	I	6.7	68	4.705882353	0.235294118	3.741291082
24	0.8	I	5.8	68	4.705882353	0.235294118	3.015012465
25	1.1	I	5.8	68	4.705882353	0.235294118	3.015012465
26	0.9	I	5.1	68	4.705882353	0.235294118	2.472717741
27	0.6	I	5	68	4.705882353	0.235294118	2.397150164
28	0.8	I	5.2	68	4.705882353	0.235294118	2.548790611
29	1.6	I	5.8	68	4.705882353	0.235294118	3.015012465
30	1	I	6	68	4.705882353	0.235294118	3.173826834
31	0.7	I	5.6	68	4.705882353	0.235294118	2.857833975
Sum of Runoff							**136.0149822**

Sub Catchment C_3

Area =

CN =

Day	P	AMC	P(AMC)	CN (AMC I)	S	Ia	Q
27	2		0	68	4.705882353	0.235294118	
28	1.8		0	68	4.705882353	0.235294118	
29	1.2		0	68	4.705882353	0.235294118	
30	1.3		0	68	4.705882353	0.235294118	
31	0.7		0	68	4.705882353	0.235294118	
1	1.3	I	8.3	68	4.705882353	0.235294118	5.092911914
2	1.3	I	7.6	68	4.705882353	0.235294118	4.493475519
3	2.2	I	8	68	4.705882353	0.235294118	4.834628191
4	2.8	I	9.6	68	4.705882353	0.235294118	6.232697226
5	0.9	I	9.2	68	4.705882353	0.235294118	5.878748608
6	1.1	I	9.6	68	4.705882353	0.235294118	6.232697226
7	1.1	I	9.4	68	4.705882353	0.235294118	6.05539091
8	0.8	I	8.9	68	4.705882353	0.235294118	5.615095365
9	0.7	I	7.4	68	4.705882353	0.235294118	4.324386405
10	0.6	I	5.2	68	4.705882353	0.235294118	2.548790611
11	1	I	5.3	68	4.705882353	0.235294118	2.62535326
12	1.2	I	5.4	68	4.705882353	0.235294118	2.702390801
13	1.8	I	6.1	68	4.705882353	0.235294118	3.253818456

14	1.6	I	6.9	68	4.705882353	0.235294118	3.906420985
15	2.4	I	8.6	68	4.705882353	0.235294118	5.353110605
16	1.7	I	9.7	68	4.705882353	0.235294118	6.321590604
17	1.1	I	9.8	68	4.705882353	0.235294118	6.410639639
18	1.7	I	10.3	68	4.705882353	0.235294118	6.858109026
19	1.1	I	9.6	68	4.705882353	0.235294118	6.232697226
20	1.6	I	9.6	68	4.705882353	0.235294118	6.232697226
21	0.7	I	7.9	68	4.705882353	0.235294118	4.748983245
22	0.6	I	6.8	68	4.705882353	0.235294118	3.823701339
23	1	I	6.7	68	4.705882353	0.235294118	3.741291082
24	0.8	I	5.8	68	4.705882353	0.235294118	3.015012465
25	1.1	I	5.8	68	4.705882353	0.235294118	3.015012465
26	0.9	I	5.1	68	4.705882353	0.235294118	2.472717741
27	0.6	I	5	68	4.705882353	0.235294118	2.397150164
28	0.8	I	5.2	68	4.705882353	0.235294118	2.548790611
29	1.6	I	5.8	68	4.705882353	0.235294118	3.015012465
30	1	I	6	68	4.705882353	0.235294118	3.173826834
31	0.7	I	5.6	68	4.705882353	0.235294118	2.857833975
Sum of Runoff							**136.0149822**

Sub Catchment C_4

Area =

CN =

Day	P	AMC	P(AMC)	CN (AMC I)	S	Ia	Q
27	2		0	81	2.345679012	0.117283951	
28	1.8		0	81	2.345679012	0.117283951	
29	1.2		0	81	2.345679012	0.117283951	
30	1.3		0	81	2.345679012	0.117283951	
31	0.7		0	81	2.345679012	0.117283951	
1	1.3	I	8.3	81	2.345679012	0.117283951	6.359643759
2	1.3	I	7.6	81	2.345679012	0.117283951	5.696864964
3	2.2	I	8	81	2.345679012	0.117283951	6.074971874
4	2.8	I	9.6	81	2.345679012	0.117283951	7.602206656
5	0.9	I	9.2	81	2.345679012	0.117283951	7.218487844
6	1.1	I	9.6	81	2.345679012	0.117283951	7.602206656
7	1.1	I	9.4	81	2.345679012	0.117283951	7.410207238
8	0.8	I	8.9	81	2.345679012	0.117283951	6.931466827
9	0.7	I	7.4	81	2.345679012	0.117283951	5.50849365
10	0.6	I	5.2	81	2.345679012	0.117283951	3.477736742
11	1	I	5.3	81	2.345679012	0.117283951	3.567897995
12	1.2	I	5.4	81	2.345679012	0.117283951	3.658317199
13	1.8	I	6.1	81	2.345679012	0.117283951	4.297693741
14	1.6	I	6.9	81	2.345679012	0.117283951	5.039794695

15	2.4	I	8.6	81	2.345679012	0.117283951	6.645164973
16	1.7	I	9.7	81	2.345679012	0.117283951	7.698306973
17	1.1	I	9.8	81	2.345679012	0.117283951	7.794472131
18	1.7	I	10.3	81	2.345679012	0.117283951	8.276216198
19	1.1	I	9.6	81	2.345679012	0.117283951	7.602206656
20	1.6	I	9.6	81	2.345679012	0.117283951	7.602206656
21	0.7	I	7.9	81	2.345679012	0.117283951	5.98028303
22	0.6	I	6.8	81	2.345679012	0.117283951	4.946470939
23	1	I	6.7	81	2.345679012	0.117283951	4.853296733
24	0.8	I	5.8	81	2.345679012	0.117283951	4.022380744
25	1.1	I	5.8	81	2.345679012	0.117283951	4.022380744
26	0.9	I	5.1	81	2.345679012	0.117283951	3.387843999
27	0.6	I	5	81	2.345679012	0.117283951	3.29823091
28	0.8	I	5.2	81	2.345679012	0.117283951	3.477736742
29	1.6	I	5.8	81	2.345679012	0.117283951	4.022380744
30	1	I	6	81	2.345679012	0.117283951	4.205722727
31	0.7	I	5.6	81	2.345679012	0.117283951	3.839889919
Sum of Runoff							**172.1211807**

Sub Catchment C_5

Area =

CN =							
Day	**P**	**AMC**	**P(AMC)**	**CN (AMC I)**	**S**	**Ia**	**Q**
27	2		0	75	3.333333333	0.166666667	
28	1.8		0	75	3.333333333	0.166666667	
29	1.2		0	75	3.333333333	0.166666667	
30	1.3		0	75	3.333333333	0.166666667	
31	0.7		0	75	3.333333333	0.166666667	
1	1.3	I	8.3	75	3.333333333	0.166666667	5.768992248
2	1.3	I	7.6	75	3.333333333	0.166666667	5.131991744
3	2.2	I	8	75	3.333333333	0.166666667	5.495024876
4	2.8	I	9.6	75	3.333333333	0.166666667	6.970322019
5	0.9	I	9.2	75	3.333333333	0.166666667	6.598472597
6	1.1	I	9.6	75	3.333333333	0.166666667	6.970322019
7	1.1	I	9.4	75	3.333333333	0.166666667	6.784173298
8	0.8	I	8.9	75	3.333333333	0.166666667	6.320810313
9	0.7	I	7.4	75	3.333333333	0.166666667	4.951524711
10	0.6	I	5.2	75	3.333333333	0.166666667	3.028021248
11	1	I	5.3	75	3.333333333	0.166666667	3.112335958
12	1.2	I	5.4	75	3.333333333	0.166666667	3.197016861
13	1.8	I	6.1	75	3.333333333	0.166666667	3.799040767
14	1.6	I	6.9	75	3.333333333	0.166666667	4.503752759

15	2.4	I	8.6	75	3.333333333	0.166666667	6.044287063
16	1.7	I	9.7	75	3.333333333	0.166666667	7.063557858
17	1.1	I	9.8	75	3.333333333	0.166666667	7.156898029
18	1.7	I	10.3	75	3.333333333	0.166666667	7.625082508
19	1.1	I	9.6	75	3.333333333	0.166666667	6.970322019
20	1.6	I	9.6	75	3.333333333	0.166666667	6.970322019
21	0.7	I	7.9	75	3.333333333	0.166666667	5.404016064
22	0.6	I	6.8	75	3.333333333	0.166666667	4.414827202
23	1	I	6.7	75	3.333333333	0.166666667	4.326126126
24	0.8	I	5.8	75	3.333333333	0.166666667	3.539157373
25	1.1	I	5.8	75	3.333333333	0.166666667	3.539157373
26	0.9	I	5.1	75	3.333333333	0.166666667	2.944086022
27	0.6	I	5	75	3.333333333	0.166666667	2.860544218
28	0.8	I	5.2	75	3.333333333	0.166666667	3.028021248
29	1.6	I	5.8	75	3.333333333	0.166666667	3.539157373
30	1	I	6	75	3.333333333	0.166666667	3.712121212
31	0.7	I	5.6	75	3.333333333	0.166666667	3.367427123
Sum of Runoff							**155.1369122**

Table A4: Calculations for Catchment *D*

Sub Catchment D_1

Area =

CN =

Day	P	AMC	P(AMC)	CN (AMC I)	S	Ia	Runoff (Q)
27	2		0	81	2.345679012	0.117283951	
28	1.8		0	81	2.345679012	0.117283951	
29	1.2		0	81	2.345679012	0.117283951	
30	1.3		0	81	2.345679012	0.117283951	
31	0.7		0	81	2.345679012	0.117283951	
1	1.3	I	8.3	81	2.345679012	0.117283951	6.359643759
2	1.3	I	7.6	81	2.345679012	0.117283951	5.696864964
3	2.2	I	8	81	2.345679012	0.117283951	6.074971874
4	2.8	I	9.6	81	2.345679012	0.117283951	7.602206656
5	0.9	I	9.2	81	2.345679012	0.117283951	7.218487844
6	1.1	I	9.6	81	2.345679012	0.117283951	7.602206656
7	1.1	I	9.4	81	2.345679012	0.117283951	7.410207238
8	0.8	I	8.9	81	2.345679012	0.117283951	6.931466827
9	0.7	I	7.4	81	2.345679012	0.117283951	5.50849365
10	0.6	I	5.2	81	2.345679012	0.117283951	3.477736742
11	1	I	5.3	81	2.345679012	0.117283951	3.567897995
12	1.2	I	5.4	81	2.345679012	0.117283951	3.658317199
13	1.8	I	6.1	81	2.345679012	0.117283951	4.297693741

14	1.6	I	6.9	81	2.345679012	0.117283951	5.039794695
15	2.4	I	8.6	81	2.345679012	0.117283951	6.645164973
16	1.7	I	9.7	81	2.345679012	0.117283951	7.698306973
17	1.1	I	9.8	81	2.345679012	0.117283951	7.794472131
18	1.7	I	10.3	81	2.345679012	0.117283951	8.276216198
19	1.1	I	9.6	81	2.345679012	0.117283951	7.602206656
20	1.6	I	9.6	81	2.345679012	0.117283951	7.602206656
21	0.7	I	7.9	81	2.345679012	0.117283951	5.98028303
22	0.6	I	6.8	81	2.345679012	0.117283951	4.946470939
23	1	I	6.7	81	2.345679012	0.117283951	4.853296733
24	0.8	I	5.8	81	2.345679012	0.117283951	4.022380744
25	1.1	I	5.8	81	2.345679012	0.117283951	4.022380744
26	0.9	I	5.1	81	2.345679012	0.117283951	3.387843999
27	0.6	I	5	81	2.345679012	0.117283951	3.29823091
28	0.8	I	5.2	81	2.345679012	0.117283951	3.477736742
29	1.6	I	5.8	81	2.345679012	0.117283951	4.022380744
30	1	I	6	81	2.345679012	0.117283951	4.205722727
31	0.7	I	5.6	81	2.345679012	0.117283951	3.839889919
Sum of Runoff							**172.1211807**

Sub Catchment D_2

Area =

CN =							
Day	**P**	**AMC**	**P(AMC)**	**CN (AMC I)**	**S**	**Ia**	**Q**
27	2		0	68	4.705882353	0.235294118	
28	1.8		0	68	4.705882353	0.235294118	
29	1.2		0	68	4.705882353	0.235294118	
30	1.3		0	68	4.705882353	0.235294118	
31	0.7		0	68	4.705882353	0.235294118	
1	1.3	I	8.3	68	4.705882353	0.235294118	5.092911914
2	1.3	I	7.6	68	4.705882353	0.235294118	4.493475519
3	2.2	I	8	68	4.705882353	0.235294118	4.834628191
4	2.8	I	9.6	68	4.705882353	0.235294118	6.232697226
5	0.9	I	9.2	68	4.705882353	0.235294118	5.878748608
6	1.1	I	9.6	68	4.705882353	0.235294118	6.232697226
7	1.1	I	9.4	68	4.705882353	0.235294118	6.05539091
8	0.8	I	8.9	68	4.705882353	0.235294118	5.615095365
9	0.7	I	7.4	68	4.705882353	0.235294118	4.324386405
10	0.6	I	5.2	68	4.705882353	0.235294118	2.548790611
11	1	I	5.3	68	4.705882353	0.235294118	2.62535326
12	1.2	I	5.4	68	4.705882353	0.235294118	2.702390801
13	1.8	I	6.1	68	4.705882353	0.235294118	3.253818456
14	1.6	I	6.9	68	4.705882353	0.235294118	3.906420985

15	2.4	I	8.6	68	4.705882353	0.235294118	5.353110605
16	1.7	I	9.7	68	4.705882353	0.235294118	6.321590604
17	1.1	I	9.8	68	4.705882353	0.235294118	6.410639639
18	1.7	I	10.3	68	4.705882353	0.235294118	6.858109026
19	1.1	I	9.6	68	4.705882353	0.235294118	6.232697226
20	1.6	I	9.6	68	4.705882353	0.235294118	6.232697226
21	0.7	I	7.9	68	4.705882353	0.235294118	4.748983245
22	0.6	I	6.8	68	4.705882353	0.235294118	3.823701339
23	1	I	6.7	68	4.705882353	0.235294118	3.741291082
24	0.8	I	5.8	68	4.705882353	0.235294118	3.015012465
25	1.1	I	5.8	68	4.705882353	0.235294118	3.015012465
26	0.9	I	5.1	68	4.705882353	0.235294118	2.472717741
27	0.6	I	5	68	4.705882353	0.235294118	2.397150164
28	0.8	I	5.2	68	4.705882353	0.235294118	2.548790611
29	1.6	I	5.8	68	4.705882353	0.235294118	3.015012465
30	1	I	6	68	4.705882353	0.235294118	3.173826834
31	0.7	I	5.6	68	4.705882353	0.235294118	2.857833975
Sum of Runoff							**136.0149822**

Sub Catchment D_3

Area =

CN =							
Day	**P**	**AMC**	**P(AMC)**	**CN (AMC I)**	**S**	**Ia**	**Q**
27	2		0	68	4.705882353	0.235294118	
28	1.8		0	68	4.705882353	0.235294118	
29	1.2		0	68	4.705882353	0.235294118	
30	1.3		0	68	4.705882353	0.235294118	
31	0.7		0	68	4.705882353	0.235294118	
1	1.3	I	8.3	68	4.705882353	0.235294118	5.092911914
2	1.3	I	7.6	68	4.705882353	0.235294118	4.493475519
3	2.2	I	8	68	4.705882353	0.235294118	4.834628191
4	2.8	I	9.6	68	4.705882353	0.235294118	6.232697226
5	0.9	I	9.2	68	4.705882353	0.235294118	5.878748608
6	1.1	I	9.6	68	4.705882353	0.235294118	6.232697226
7	1.1	I	9.4	68	4.705882353	0.235294118	6.05539091
8	0.8	I	8.9	68	4.705882353	0.235294118	5.615095365
9	0.7	I	7.4	68	4.705882353	0.235294118	4.324386405
10	0.6	I	5.2	68	4.705882353	0.235294118	2.548790611
11	1	I	5.3	68	4.705882353	0.235294118	2.62535326
12	1.2	I	5.4	68	4.705882353	0.235294118	2.702390801
13	1.8	I	6.1	68	4.705882353	0.235294118	3.253818456
14	1.6	I	6.9	68	4.705882353	0.235294118	3.906420985

15	2.4	I	8.6	68	4.705882353	0.235294118	5.353110605
16	1.7	I	9.7	68	4.705882353	0.235294118	6.321590604
17	1.1	I	9.8	68	4.705882353	0.235294118	6.410639639
18	1.7	I	10.3	68	4.705882353	0.235294118	6.858109026
19	1.1	I	9.6	68	4.705882353	0.235294118	6.232697226
20	1.6	I	9.6	68	4.705882353	0.235294118	6.232697226
21	0.7	I	7.9	68	4.705882353	0.235294118	4.748983245
22	0.6	I	6.8	68	4.705882353	0.235294118	3.823701339
23	1	I	6.7	68	4.705882353	0.235294118	3.741291082
24	0.8	I	5.8	68	4.705882353	0.235294118	3.015012465
25	1.1	I	5.8	68	4.705882353	0.235294118	3.015012465
26	0.9	I	5.1	68	4.705882353	0.235294118	2.472717741
27	0.6	I	5	68	4.705882353	0.235294118	2.397150164
28	0.8	I	5.2	68	4.705882353	0.235294118	2.548790611
29	1.6	I	5.8	68	4.705882353	0.235294118	3.015012465
30	1	I	6	68	4.705882353	0.235294118	3.173826834
31	0.7	I	5.6	68	4.705882353	0.235294118	2.857833975
Sum of Runoff							**136.0149822**

Sub Catchment D_4

Area =

CN =							
Day	**P**	**AMC**	**P(AMC)**	**CN (AMC I)**	**S**	**Ia**	**Q**
27	2		0	72	3.888888889	0.194444444	
28	1.8		0	72	3.888888889	0.194444444	
29	1.2		0	72	3.888888889	0.194444444	
30	1.3		0	72	3.888888889	0.194444444	
31	0.7		0	72	3.888888889	0.194444444	
1	1.3	I	8.3	72	3.888888889	0.194444444	5.477538469
2	1.3	I	7.6	72	3.888888889	0.194444444	4.855683992
3	2.2	I	8	72	3.888888889	0.194444444	5.209883874
4	2.8	I	9.6	72	3.888888889	0.194444444	6.654243859
5	0.9	I	9.2	72	3.888888889	0.194444444	6.289532768
6	1.1	I	9.6	72	3.888888889	0.194444444	6.654243859
7	1.1	I	9.4	72	3.888888889	0.194444444	6.471618819
8	0.8	I	8.9	72	3.888888889	0.194444444	6.01747047
9	0.7	I	7.4	72	3.888888889	0.194444444	4.679822512
10	0.6	I	5.2	72	3.888888889	0.194444444	2.816992852
11	1	I	5.3	72	3.888888889	0.194444444	2.898088669
12	1.2	I	5.4	72	3.888888889	0.194444444	2.979600217
13	1.8	I	6.1	72	3.888888889	0.194444444	3.560751875
14	1.6	I	6.9	72	3.888888889	0.194444444	4.244156033

15	2.4	I	8.6	72	3.888888889	0.194444444	5.746771602
16	1.7	I	9.7	72	3.888888889	0.194444444	6.745750956
17	1.1	I	9.8	72	3.888888889	0.194444444	6.837383926
18	1.7	I	10.3	72	3.888888889	0.194444444	7.29734242
19	1.1	I	9.6	72	3.888888889	0.194444444	6.654243859
20	1.6	I	9.6	72	3.888888889	0.194444444	6.654243859
21	0.7	I	7.9	72	3.888888889	0.194444444	5.12103764
22	0.6	I	6.8	72	3.888888889	0.194444444	4.157758367
23	1	I	6.7	72	3.888888889	0.194444444	4.071622424
24	0.8	I	5.8	72	3.888888889	0.194444444	3.309540992
25	1.1	I	5.8	72	3.888888889	0.194444444	3.309540992
26	0.9	I	5.1	72	3.888888889	0.194444444	2.736326946
27	0.6	I	5	72	3.888888889	0.194444444	2.656105786
28	0.8	I	5.2	72	3.888888889	0.194444444	2.816992852
29	1.6	I	5.8	72	3.888888889	0.194444444	3.309540992
30	1	I	6	72	3.888888889	0.194444444	3.476679401
31	0.7	I	5.6	72	3.888888889	0.194444444	3.143816829
Sum of Runoff							**146.8543281**

Sub Catchment D_5

Area =

CN =							
Day	**P**	**AMC**	**P(AMC)**	**CN (AMC I)**	**S**	**Ia**	**Q**
27	2		0	78	2.820512821	0.141025641	
28	1.8		0	78	2.820512821	0.141025641	
29	1.2		0	78	2.820512821	0.141025641	
30	1.3		0	78	2.820512821	0.141025641	
31	0.7		0	78	2.820512821	0.141025641	
1	1.3	I	8.3	78	2.820512821	0.141025641	6.063021114
2	1.3	I	7.6	78	2.820512821	0.141025641	5.41236129
3	2.2	I	8	78	2.820512821	0.141025641	5.783374888
4	2.8	I	9.6	78	2.820512821	0.141025641	7.286313721
5	0.9	I	9.2	78	2.820512821	0.141025641	6.908127868
6	1.1	I	9.6	78	2.820512821	0.141025641	7.286313721
7	1.1	I	9.4	78	2.820512821	0.141025641	7.097040206
8	0.8	I	8.9	78	2.820512821	0.141025641	6.625477504
9	0.7	I	7.4	78	2.820512821	0.141025641	5.227717225
10	0.6	I	5.2	78	2.820512821	0.141025641	3.248082138
11	1	I	5.3	78	2.820512821	0.141025641	3.335429438
12	1.2	I	5.4	78	2.820512821	0.141025641	3.423089943
13	1.8	I	6.1	78	2.820512821	0.141025641	4.044584232
14	1.6	I	6.9	78	2.820512821	0.141025641	4.768912315

15	2.4	I	8.6	78	2.820512821	0.141025641	6.343750036
16	1.7	I	9.7	78	2.820512821	0.141025641	7.38108045
17	1.1	I	9.8	78	2.820512821	0.141025641	7.475931048
18	1.7	I	10.3	78	2.820512821	0.141025641	7.951374241
19	1.1	I	9.6	78	2.820512821	0.141025641	7.286313721
20	1.6	I	9.6	78	2.820512821	0.141025641	7.286313721
21	0.7	I	7.9	78	2.820512821	0.141025641	5.690415999
22	0.6	I	6.8	78	2.820512821	0.141025641	4.677672819
23	1	I	6.7	78	2.820512821	0.141025641	4.586620123
24	0.8	I	5.8	78	2.820512821	0.141025641	3.776642398
25	1.1	I	5.8	78	2.820512821	0.141025641	3.776642398
26	0.9	I	5.1	78	2.820512821	0.141025641	3.161060122
27	0.6	I	5	78	2.820512821	0.141025641	3.074376097
28	0.8	I	5.2	78	2.820512821	0.141025641	3.248082138
29	1.6	I	5.8	78	2.820512821	0.141025641	3.776642398
30	1	I	6	78	2.820512821	0.141025641	3.95502405
31	0.7	I	5.6	78	2.820512821	0.141025641	3.599305175
Sum of Runoff							**163.5570925**

Sub Catchment D6

Area =

CN =							
Day	**P**	**AMC**	**P(AMC)**	**CN (AMC I)**	**S**	**Ia**	**Q**
27	2		0	89	1.235955056	0.061797753	
28	1.8		0	89	1.235955056	0.061797753	
29	1.2		0	89	1.235955056	0.061797753	
30	1.3		0	89	1.235955056	0.061797753	
31	0.7		0	89	1.235955056	0.061797753	
1	1.3	I	8.3	89	1.235955056	0.061797753	7.163484212
2	1.3	I	7.6	89	1.235955056	0.061797753	6.47634766
3	2.2	I	8	89	1.235955056	0.061797753	6.868756752
4	2.8	I	9.6	89	1.235955056	0.061797753	8.4440295
5	0.9	I	9.2	89	1.235955056	0.061797753	8.04949625
6	1.1	I	9.6	89	1.235955056	0.061797753	8.4440295
7	1.1	I	9.4	89	1.235955056	0.061797753	8.246711176
8	0.8	I	8.9	89	1.235955056	0.061797753	7.753881204
9	0.7	I	7.4	89	1.235955056	0.061797753	6.280408711
10	0.6	I	5.2	89	1.235955056	0.061797753	4.141900031
11	1	I	5.3	89	1.235955056	0.061797753	4.238198347
12	1.2	I	5.4	89	1.235955056	0.061797753	4.334609276
13	1.8	I	6.1	89	1.235955056	0.061797753	5.012248822
14	1.6	I	6.9	89	1.235955056	0.061797753	5.791441536

15	2.4	I	8.6	89	1.235955056	0.061797753	7.458535335
16	1.7	I	9.7	89	1.235955056	0.061797753	8.542725654
17	1.1	I	9.8	89	1.235955056	0.061797753	8.641445569
18	1.7	I	10.3	89	1.235955056	0.061797753	9.135379835
19	1.1	I	9.6	89	1.235955056	0.061797753	8.4440295
20	1.6	I	9.6	89	1.235955056	0.061797753	8.4440295
21	0.7	I	7.9	89	1.235955056	0.061797753	6.770591738
22	0.6	I	6.8	89	1.235955056	0.061797753	5.693814129
23	1	I	6.7	89	1.235955056	0.061797753	5.596246986
24	0.8	I	5.8	89	1.235955056	0.061797753	4.721282242
25	1.1	I	5.8	89	1.235955056	0.061797753	4.721282242
26	0.9	I	5.1	89	1.235955056	0.061797753	4.045719713
27	0.6	I	5	89	1.235955056	0.061797753	3.949663126
28	0.8	I	5.2	89	1.235955056	0.061797753	4.141900031
29	1.6	I	5.8	89	1.235955056	0.061797753	4.721282242
30	1	I	6	89	1.235955056	0.061797753	4.915176018
31	0.7	I	5.6	89	1.235955056	0.061797753	4.527749026
Sum of Runoff							**195.7163959**

7.2. Overlay Analysis

7.2.1. Criteria for Reclassification

Table A5: Reclassification criterion

Parameter	Unit	Range	Class Rating	Class Rating Value
Drainage Density	m^-1	< 100	Very Low	1
		100 – 200	Low	2
		200 – 300	Moderate	3
		300 – 400	High	4
		> 400	Very High	5
Elevation	M	< 1580	Very Low	1
		1580 – 1600	Low	2
		1600 – 1620	Moderate	3
		1620 – 1640	High	4
		> 1640	Very High	5
Land use/ Land cover	Classes	Bare Ground	High	4
		Concrete Surfaces	Very High	5
		High Density Vegetation	Very Low	1
		Industrial & Commercial	High	4
		Low Density Vegetation	Moderate	3
		Medium Density Vegetation	Low	2

		Residential-Permanent	High	4
		Residential- Slums	Very High	5
		Tarmac	Very High	5
		Water Body	Very High	5
Natural Differential Vegetation Index	Absolute (-1 to 1)	< -0.11	Very Low	1
		-0.11 - -0.01	Low	2
		-0.01 – 0.08	Moderate	3
		0.08 - 0.13	High	4
Precipitation	Mm	< 150	Very Low	1
		150 – 170	Low	2
		170 – 190	Moderate	3
		190 – 210	High	4
		> 210	Very High	5
Proximity to River	M	< 300	Very High	5
		300 – 600	High	4
		600 – 900	Moderate	3
		900 – 1200	Low	2
		> 1200	Very Low	1
Proximity to Road & Railway	M	< 30	Very High	5
		30 – 60	High	4

		60 – 100	Moderate	3
		100 – 150	Low	2
		> 150	Very Low	1
Slope	Degrees	< 10	Very Low	1
		10 20	Low	2
		20 – 30	Moderate	3
		30 – 45	High	4
		> 45	Very High	5
Soil	HSG	D	High	4
Topographic Wetness Index	Absolute	-13.1 - -6.9	Very Low	1
		-6.9 - -3.5	Low	2
		-3.5 – 0.16	Moderate	3
		0.16 - 2.6	High	4
		> 2.6	Very High	5

7.2.2. Computation of weights for overlay analysis

Table A6: Computation of weights

RESPONDENT 1

PHYSICAL PARAMETERS

	D Densities	Elevation	NDVI	Slope	Soil	TWI	Sum	Weights
D Densities	1	0.5	3	0.3333333	0.5	0.25	5.58333	10.3812
Elevation	2	1	3	0.5	0.3333333	0.3333333	7.16667	13.3251
NDVI	0.33333333	0.3333333	1	0.3333333	0.5	0.2	2.7	5.02014
Slope	3	2	3	1	0.3333333	0.5	9.83333	18.2832
Soil	2	3	2	3	1	2	13	24.1711
TWI	4	3	5	2	0.5	1	15.5	28.8193
					Σ Sum		**53.7833**	

HUMAN PARAMETERS

	LULC	Prox River	Prox Road	Sum	Weights
LULC	1	3	4	8	61.776062
Prox River	0.25	1	2	3.25	25.096525
Prox Road	0.2	0.5	1	1.7	13.127413
		Σ Sum		12.95	

TOTAL

	Precipitation	Physical	Human	Sum	Weights
Precipitation	1	0.2	0.3333333	1.5333333	10.926366
Physical	5	1	2	8	57.007126
Human	3	0.5	1	4.5	32.066508
		Σ Sum		14.033333	

PARAMETERS	WEIGHTS

Physical Parameters	D Densities	10
	Elevation	13
	NDVI	5
	Slope	18
	Soil	24
	TWI	29
Human Parameters	LULC	61
	Prox River	25
	Prox Road	13
Meteorological + Physical + Human	Precipitation	11
	Physical	57
	Human	32

RESPONDENT 2

PHYSICAL PARAMETERS

	D Densities	Elevation	NDVI	Slope	Soil	TWI	Sum	Weights
D Densities	1	4	6	0.1666667	0.1428571	0.2	11.5095	13.4832
Elevation	0.25	1	0.1666667	0.1428571	0.3333333	0.1666667	2.05952	2.4127
NDVI	0.16666667	6	1	0.2	0.1428571	0.2	7.70952	9.03157
Slope	6	7	5	1	0.3333333	0.5	19.8333	23.2344
Soil	7	3	7	3	1	4	25	29.2871
TWI	5	6	5	2	0.25	1	19.25	22.551
					Σ Sum		**85.3619**	

HUMAN PARAMETERS

	LULC	Prox River	Prox Road	Sum	Weights
LULC	1	7	6	14	67.63285
Prox River	0.25	1	0.25	1.5	7.2463768
Prox Road	0.2	4	1	5.2	25.120773
		Σ Sum		20.7	

TOTAL

	Precipitation	Physical	Human	Sum	Weights
Precipitation	1	4	5	10	59.88024
Physical	0.25	1	4	5.25	31.437126
Human	0.2	0.25	1	1.45	8.6826347
		Σ Sum		16.7	

PARAMETERS	WEIGHTS

Physical Parameters	D Densities	13
	Elevation	2
	NDVI	9
	Slope	23
	Soil	29
	TWI	23
Human Parameters	LULC	68
	Prox River	7
	Prox Road	25
Meteorological + Physical + Human	Precipitation	60
	Physical	31
	Human	9

RESPONDENT 3

PHYSICAL PARAMETERS

	D Densities	Elevation	NDVI	Slope	Soil	TWI	Sum	Weights
D Densities	1	3	4	0.2	0.14286	0.33333	8.67619	11.2685
Elevation	0.33333	1	0.16667	0.14286	0.33333	0.14286	2.11905	2.75218
NDVI	0.25	6	1	0.2	0.33333	0.5	8.28333	10.7582
Slope	5	7	5	1	0.25	0.5	18.75	24.3522
Soil	7	3	3	4	1	6	24	31.1708
TWI	3	7	2	2	0.16667	1	15.1667	19.6982
					Σ Sum		**76.9952**	

HUMAN PARAMETERS

	LULC	Prox River	Prox Road	Sum	Weights
LULC	1	5	7	13	69.6073
Prox River	0.2	1	0.33333	1.53333	8.2101
Prox Road	0.14286	3	1	4.14286	22.1826
		Σ Sum		18.6762	

TOTAL

	Precipitation	Physical	Human	Sum	Weights
Precipitation	1	0.33333	5	6.33333	35.7815
Physical	3	1	6	10	56.4972
Human	0.2	0.16667	1	1.36667	7.72128
		Σ Sum		17.7	

PARAMETERS		WEIGHTS
Physical Parameters	D Densities	11
	Elevation	3
	NDVI	11
	Slope	24
	Soil	31
	TWI	20
Human Parameters	LULC	70
	Prox River	8
	Prox Road	22
Meteorological + Physical + Human	Precipitation	36
	Physical	56
	Human	8

RESPONDENT 4

PHYSICAL PARAMETERS

	D Densities	Elevation	NDVI	Slope	Soil	TWI	Sum	Weights
D Densities	1	0.5	3	0.2	0.2	0.33333	5.23333	8.34884
Elevation	2	1	3	0.25	0.25	3	9.5	15.1555
NDVI	0.33333	0.33333	1	0.25	0.2	2	4.11667	6.5674
Slope	5	4	4	1	0.33333	3	17.3333	27.6522
Soil	5	4	5	3	1	3	21	33.5017
TWI	3	0.33333	0.5	0.33333	0.33333	1	5.5	8.77426
					Σ Sum		**62.6833**	

HUMAN PARAMETERS

	LULC	Prox River	Prox Road	Sum	Weights
LULC	1	0.33333	3	4.33333	33.3333
Prox River	3	1	3	7	53.8462
Prox Road	0.33333	0.33333	1	1.66667	12.8205
		Σ Sum		13	

TOTAL

	Precipitation	Physical	Human	Sum	Weights
Precipitation	1	0.25	0.2	1.45	9.18691
Physical	4	1	3	8	50.6864
Human	5	0.33333	1	6.33333	40.1267
		Σ Sum		15.7833	

PARAMETERS		WEIGHTS
Physical Parameters	D Densities	8
	Elevation	15
	NDVI	7
	Slope	28
	Soil	34
	TWI	6
Human Parameters	LULC	33
	Prox River	54
	Prox Road	13
Meteorological + Physical + Human	Precipitation	9
	Physical	51
	Human	40

RESPONDENT 5

PHYSICAL PARAMETERS

	D Densities	Elevation	NDVI	Slope	Soil	TWI	Sum	Weights
D Densities	1	0.25	4	0.25	0.14286	0.33333	5.97619	8.74016
Elevation	4	1	0.16667	0.33333	0.33333	0.2	6.03333	8.82373
NDVI	0.25	6	1	0.2	0.33333	0.5	8.28333	12.1144
Slope	4	3	5	1	0.33333	0.5	13.8333	20.2312
Soil	7	3	3	3	1	4	21	30.7124
TWI	3	5	2	2	0.25	1	13.25	19.3781
					Σ Sum		**68.3762**	

HUMAN PARAMETERS

	LULC	Prox River	Prox Road	Sum	Weights
LULC	1	4	7	12	67.6964
Prox River	0.25	1	3	4.25	23.9758
Prox Road	0.14286	0.33333	1	1.47619	8.32774
		Σ Sum		17.7262	

TOTAL

	Precipitation	**Physical**	**Human**	**Sum**	**Weights**
Precipitation	1	0.2	4	5.2	32.9461
Physical	5	1	3	9	57.0222
Human	0.25	0.33333	1	1.58333	10.0317
		Σ Sum		15.7833	

PARAMETERS		**WEIGHTS**
Physical Parameters	D Densities	9
	Elevation	9
	NDVI	12
	Slope	20
	Soil	31
	TWI	19
Human Parameters	LULC	68
	Prox River	24
	Prox Road	8
Meteorological + Physical + Human	Precipitation	33
	Physical	57
	Human	10

SUMMARY

PARAMETERS		RESPONDENTS 1	2	3	4	5	Sum	Average	Approx. Weight
Physical Parameters	D Densities	10	13	11	8	9	51	10.2	10
	Elevation	13	3	3	15	9	43	8.6	9
	NDVI	5	9	11	7	12	44	8.8	9
	Slope	18	23	24	28	20	113	22.6	23
	Soil	24	29	31	34	31	149	29.8	30
	TWI	29	23	20	6	19	97	19.4	19
Human Parameters	LULC	61	68	70	33	68	300	60	60
	Proximity to River	25	7	8	54	24	118	23.6	24
	Proximity to Road	13	25	22	13	8	81	16.2	16
Meteorological + Physical + Human	Precipitation	11	60	36	9	33	149	29.8	30
	Physical	57	31	56	51	57	252	50.4	50
	Human	32	9	8	40	10	99	19.8	20